NEW ROLES FOR METABOTROPIC GLUTAMATE RECEPTOR SIGNALING IN THE PHYSIOLOGY AND PATHOLOGY OF DOPAMINE NEURONS

by

Paul F. Kramer

A DISSERTATION

presented to THE NEUROSCIENCE GRADUATE PROGRAM

at the VOLLUM INSTITUTE

and the OREGON HEALTH & SCIENCE UNIVERSITY

SCHOOL OF MEDICINE

in partial fulfillment of

the requirements for the degree of

DOCTOR OF PHILOSOPHY

December 16, 2016

School of Medicine

Oregon Health & Science University

CERTIFICATE OF APPROVAL

This is to certify that the Ph.D. dissertation of

Paul Frederick Kramer

has been approved on December 16, 2016

_____

John T. Williams, Ph.D., Advisor

_____

Tianyi Mao, Ph.D., Chair

_____

John Adelman, Ph.D.

_____

David Farrens, Ph.D.

_____

Laurence Trussell, Ph.D.

_____

Matt Whorton, Ph.D.

Table of Contents

List of Figures

List of Diagrams

Abbreviations

AMPA	α-amino-3-hydroxyl-5-methyl-4-isoxazolepropionic acid
BAPTA	1,2-Bis(2-aminophenoxy)ethane-N,N,N',N',-tetraacetic acid
CHPG	(*RS*)-2-Chloro-5-hydroxyphenylglycine
CICR	calcium-induced calcium release
CPA	cyclopiazonic acid
DA	dopamine
DAG	1,2-diacylglycerol
DHPG	*(S)*-3,5-Dihydoxyphenylglycine
DMNPE-4	dimethoxynitrophenyl-EGTA-4
EGTA	ethylene glycol tetraacetic acid
GABA	gamma-aminobutyric acid
GIRK	G protein-coupled inwardly rectifying potassium channel
GPCR	G protein-coupled receptor
GppNHp	guanosine-5'-[(β,γ)-imido]triphosphate
GTP	guanosine 5'-triphosphate
IP_3	inositol 1,4,5-trisphosphate
IPSC	inhibitory postsynaptic current
LED	light-emitting diode
LTD	long-term depression
LTP	long-term potentiation
mGluR	metabotropic glutamate receptor
MSN	medium spiny neuron
NAc	nucleus accumbens
NAM	negative allosteric modulator
NMDA	*N*-methyl-D-aspartate
PAM	positive allosteric modulator
PIP_2	phosphatidylinositol 4,5-bisphosphate
PLA_2	cytosolic phospholipase A2
PLC	phospholipase C
PKA	protein kinase A
PKC	protein kinase C
SERCA	sarco/endoplasmic reticulum calcium-ATPase
SNc	Substantia nigra *pars compacta*
TRP	transient receptor potential (channel)
VTA	ventral tegmental area
WT	wild type

Acknowledgements

The support of my mentor, John Williams, has been invaluable. John supported my research both financially and philosophically. He allowed me the freedom to come up with my own ideas, and was patient as I figured out how to be an independent scientist. He is an ongoing role model and inspiration for how to be successful while still enjoying the work.

In addition to John, the other members of the Williams Lab have helped me in the day-to-day tasks involved in the scientific method. From learning how to patch, to writing a manuscript and thinking of new experiments, to forgetting a difficult day by going to the bar and having a few pints. Everyone in the Williams Lab has helped me get here today. I could not have asked for better colleagues and friends.

I would like to thank my committee members, Drs. Tianyi Mao, John Adelman, Dave Farrens, Larry Trussell, and Matt Whorton, for making time for my questions and meetings, and for their technical and academic advice.

The Kramer family has been an unending fountain of support throughout my entire life. My sisters, my brothers-in-law, and my parents have helped me achieve my goals. Their moral support and guidance has shaped me into the person I am today, and their financial support has set me up for success.

Kacey Lundgren has given me unconditional and unending encouragement and dedication throughout my schooling. She has fought for us, and been resilient throughout this journey. I am lucky to have her as my partner.

Finally I would like to acknowledge the support of the Neuroscience Graduate Program, for advocating for us as graduate students, and supporting us financially through NIH training grants. Furthermore, the financial support from the ARCS Portland Chapter, and the Oregon Brain Institute Neurobiology of Disease fellowship have been two sources of security that allowed me to focus on my studies.

Abstract

G protein-coupled receptors (GPCRs) modulate the activity of neurons in many ways on both short and long timescales. These receptors initiate intracellular signaling cascades that can activate ion channels, suppress neurotransmitter release, mobilize calcium release from stores, promote gene transcription, increase or decrease adenylyl cyclase activity, and perform many other functions. Therefore the comprehensive result of activating a single GPCR is not straightforward, and will depend on the context in which that receptor was stimulated.

Dopamine neurons synthesize and release dopamine throughout the brain, and contribute to behaviors like movement, learning, and reward; as well as many diseases of the central nervous system such as addiction and Parkinson's Disease. These neurons express a wide variety of diverse GPCRs that couple to different intracellular signaling networks. Group I metabotropic glutamate receptors, expressed by dopamine neurons, couple to G_q and mediate acute inhibition through activation of the calcium-sensitive potassium channel SK, though they also activate a non-selective cation conductance. These receptors modulate the development of cellular changes induced by systemic *in vivo* cocaine exposure, but it is not known if or how the receptors are modulated by that same treatment. Moreover, other GPCRs on dopamine neurons, such as $GABA_B$ receptors, have altered signaling properties following cocaine

administration, but the upstream mediators of these changes are not well understood.

The goal of the work presented here was to gain a better understanding of how the intracellular signaling cascade generated by group I metabotropic glutamate receptors functions physiologically and pathologically within dopamine neurons. Physiologically, the interaction between the mGluR signaling pathway and G_i-coupled GPCRs was tested. Pathologically, the effect of a single injection of cocaine on the signaling of mGluRs on dopamine neurons was tested. For the course of this dissertation, electrophysiological recordings were made from dopamine neurons in acutely prepared brain slices. Through the use of pharmacological tools such as specific agonists, antagonists, and multiple caged compounds, data were gathered on isolated GPCR signaling. These data included coupling to ion channels, functional intracellular interactions, and activation of relevant downstream signaling molecules.

Physiologically, activation of Group I metabotropic receptors produced an unexpected rapid, and reversible, inhibition of the inwardly rectifying potassium current mediated by $GABA_B$ receptors. This inhibition of GIRK was mediated by calcium release from stores. Pathologically, a single injection of cocaine reduced mGlu1 receptor signaling in dopamine neurons. The reduction in mGluR1 signaling was prevented by injecting the animal with an mGlu5 receptor negative allosteric modulator, MPEP, prior to cocaine.

The investigation of the signaling cascades generated by metabotropic glutamate receptor activation in dopamine neurons has furthered our understanding of how these receptors affect the balance of neuronal inhibition and excitation. Not only do mGluRs directly activate both excitatory and inhibitory channels, they also mediate a secondary disinhibition of the neuron by transiently inhibiting GIRK. These results offer new insights for predicting how mGluR activation will alter dopamine neuron output within the context of synaptic transmission and modulation by cocaine.

Chapter 1 Introduction

The brain receives information through sensory inputs, processes and transforms that information, then outputs relevant behaviors. Networks within the brain have been described that are integral for the range of voluntary and involuntary behaviors for which the brain is responsible. In these networks, neurons are the basic unit of computation. They receive input, modulate and integrate the information, and produce outputs. One way that neurons process information is through the use of intracellular signaling pathways built upon molecular components. These subcellular molecular networks can increase or decrease the output activity of the neuron, and their function can be altered through experience. By affecting the output of individual neurons, intracellular molecular networks impact the processing within the larger neuronal network, which ultimately affects the behavior of an organism.

Neurons receive most of their inputs through chemical synaptic transmission. This form of neurotransmission has both a pre and postsynaptic component that are in close apposition. Briefly, a chemical signal is released from the presynaptic neuron following an action potential, and is received by the postsynaptic neuron through the activation of receptors. These receptors can be grouped into two major families, ionotropic and metabotropic. The ionotropic family is defined by receptors that function also as channels. Within this family, the primary receptors are those that are activated by glutamate and GABA but

there are also receptors that respond selectively to acetylcholine, serotonin, and other neurotransmitters.

Metabotropic receptors, such as G protein-coupled receptors (GPCRs), form a large family of diverse receptors that transduce the signal of ligand binding into an intracellular signaling cascade that activates a combination of channels, enzymes, transcription factors, and/or other signaling targets. This is accomplished through the exchange of GTP for GDP in the α subunit of an associated heterotrimeric G protein complex, subsequently releasing the α and the βγ G proteins from the receptor. GPCRs fall into three major subfamilies defined by the subtype of their α subunit; these are broadly known as $G\alpha_{q/11}$, $G\alpha_{i/o}$, and $G\alpha_{s}$.

GPCRs are also subdivided by the ligands to which they respond. These receptors form a large family that respond to diverse neurotransmitters such as signaling peptides, the biogenic amines, GABA, and glutamate. Glutamate sensing GPCRs, the metabotropic glutamate receptors (mGluRs), are divided into three subclasses based on sequence homology, pharmacology and associated G proteins: the G_q-coupled Group I (mGlu1 and mGlu5), and the G_i-coupled Group II (mGlu2 and mGlu3) and Group III (mGlu4, mGlu6, mGlu7, mGlu8). All mGlu receptors form obligate homodimers, though there is evidence they can form heterodimers. However, these heterodimer combinations are restricted by the class of the associated α subunit (Doumazane et al. 2011).

Group II/III mGlu receptors are expressed throughout the brain, and are typically located in the presynaptic compartment on terminal boutons. Activation of these receptors inhibits neurotransmitter release, often, but not exclusively, functioning as an autoreceptor. An example of this occurs in the rat SNc, where endogenous glutamate release acts on presynaptic group II mGlu receptors to inhibit further glutamate release (Wang, Kitai, and Xiang 2005).

Group II/II mGluRs, like many G_i-coupled GPCRs, can also activate the inwardly rectifying potassium channel GIRK (Diagram 1; Saugstad, Segerson, and Westbrook 1996). This channel is stabilized in the open position by the binding of βγ G proteins, but also requires the phospholipid PIP_2 (Huang, Fend, and Hilgemann 1998). This potassium channel mediates inhibition of firing in many different neurons, including dopamine neurons. The GIRK channel is modulated post-synaptically by the depletion of PIP_2 following G_q receptor activation (Sohn, Lee, Cho, Lim, Shin, Lee, and Ho 2007a), and by the activation of PKC (Mao et al. 2004). What's more, acute cocaine expsoure been shown to modulate the activity of GIRK channels in dopamine neurons (Arora et al. 2011). Thus GIRK channels mediate inhibition in a dynamic fashion that is modulated by the activity of other receptors or through events like drug exposure.

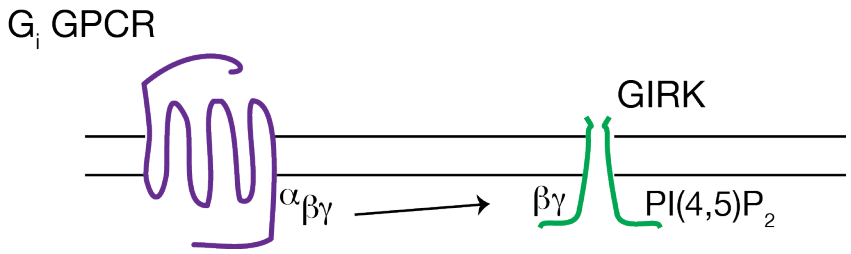

Diagram 1. Gi-coupled GPCRs activate GIRK

The activation of GIRK requires both the βγ proteins as well as the binding of the PIP_2.

One family of G_q GPCRs that modulate GIRK are the Group I mGlu receptors. These receptors are expressed throughout the brain, but are most often located in the postsynaptic compartment on dendrites and spines. These receptors have diverse cellular functions. Classically, when mGlu1 or mGlu5 receptors bind glutamate, the G_q G protein is activated. The α subunit activates PLC (typically PLCβ), which hydrolyses PIP_2 into its metabolites IP_3 and DAG. The most prominent role for DAG is to activate PKC. DAG may also activate or potentiate a TRP conductance (for a review on TRP channels see Venkatachalam and Montell 2007). The other metabolite of PLC-mediated PIP_2 hydrolysis, IP_3, binds to the IP_3 receptor located on the smooth endoplasmic reticulum and releases calcium from internal stores.

Depending on the cell type being examined, and the particular receptor being studied, activation of Group I mGlu receptors can have a variety of functional outcomes. For example, in dopaminergic neurons of the olfactory bulb, mGluR1 activation causes an inward current through release of calcium from stores and stimulation of the Na^+/Ca^{2+} exchanger, whereas mGluR5 opens a K^+ conductance (Jian et al. 2010). In cerebellar Purkinje neurons, mGluR1 activation

produces an inward current through the activation of a TRP channel (Kim et al. 2003), but in CA3 pyramidal neurons mGluR1 initiates an inward current through block of a potassium leak conductance (Guerineau, Gähwiler, and Gerber 1994). Finally, in type II neurons of the globus pallidus, activation of mGluR1 causes a depolarization of the neuron (unknown mechanism); whereas mGluR5 activation decreases the activity of mGluR1 through PKC-dependent phosphorylation, without inducing any current (Poisik et al. 2003). Therefore, understanding the context in which mGluR is being studied is critical to predicting the physiological impact of the receptors.

Acutely following Group I mGluR activation in dopamine neurons of the ventral midbrain, there is a non-selective cation conductance that is not part of the IP_3 cascade. Some evidence indicates that this inward current is mediated by TRP channels, possibly from a heteromer composed of a few different TRPC channel subunits (Tozzi et al. 2003). Immunohistochemical labeling and structural data show the presence of TRPC1 protein in nigral dendritic processes, and the co-expression of mGluR1 and TRPC1 in the same dopaminergic neurons (Martorana et al. 2006). However the exact nature of this current, and the identity of the channel, is still under investigation.

Group I mGluR activation in dopamine neurons also induces an outward current that is part of the IP_3 cascade. IP_3 liberation by hydrolysis of PIP_2 and subsequent activation of the IP_3 receptor releases calcium from internal stores, which often results in a calcium wave in the neuron (Morikawa et al. 2000). This

release of calcium from stores activates the calcium-sensitive small conductance potassium channel SK, which produces an outward current that hyperpolarizes the neuron and pauses action potential generation. The SK current is not dependent only on PLC-mediated liberation of IP_3. Block of the IP_3 receptor only partially inhibits the mGlu receptor-mediated SK current. In order to completely block the mobilization of calcium from stores and the resulting SK current, both ryanodine and IP_3 receptors must be inhibited. Furthermore, mGlu receptor activation in dopamine neurons activates cyclic ADP-ribose, which in turn activates the ryanodine receptor and releases calcium from stores (Morikawa, Khodakhah, and Williams 2003). Thus, in dopamine neurons, there are two parallel pathways that mobilize calcium release from internal stores and activate SK (Diagram 2).

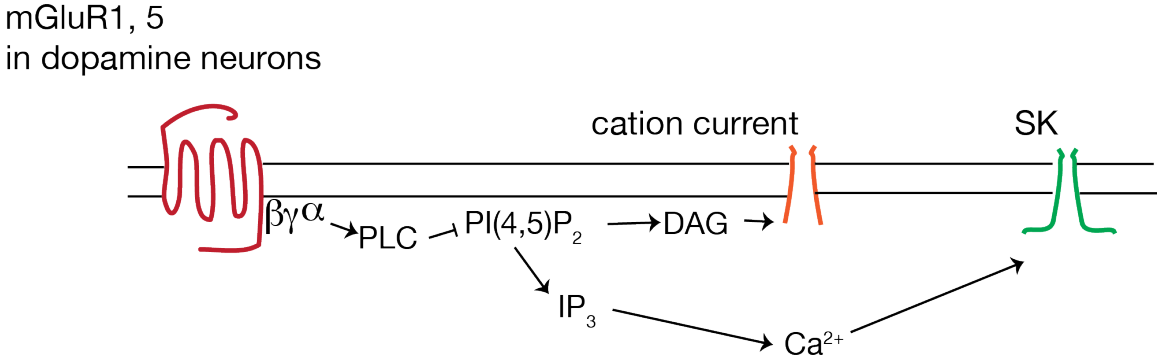

Diagram 2. Schema of mGluR activation in dopamine neurons

mGluR1 and mGluR5 are both Gq coupled GPCRs that, in dopamine neurons, lead to the activation of two distinct currents.

Taken together, when mGlu receptors are activated in dopamine neurons, two distinct currents of opposing sign are produced: an outward current mediated

by SK and an inward current through a non-selective cation conductance that is revealed upon block of the SK channel with apamin (Diagram 3).

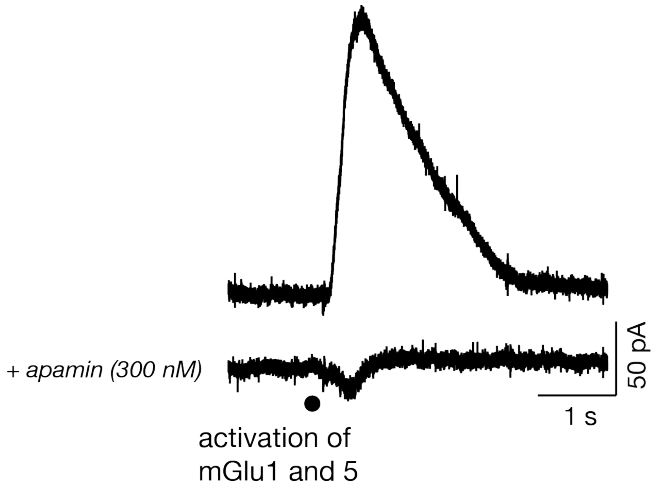

Diagram 3. Group I mGluR mediated currents

Example traces of the two currents mediated by mGluR1 and mGluR5 activation in dopamine neurons. The top trace is what is typically seen following receptor activation. The bottom trace is only seen following the application of apamin to block the SK channel.

Local electrical stimulation produces an mGluR-mediated IPSC that is inhibited by mGluR1-specific antagonists (Fiorillo and Williams 1998). This IPSC is mimicked by a short duration application of agonist within close proximity to the neuron being recorded from, often using iontophoresis of L-aspartate or pressure ejection of DHPG. However, bath perfusion of an agonist, such as DHPG, does not produce outward current, but instead yields an inward current. A potential explanation for this inconsistency in receptor-mediated responses is because the outward current desensitizes in the presence of prolonged agonist exposure, at least partially due to the desensitization of the IP_3 receptor (Cui et al. 2007). Thus, in midbrain dopamine neurons, the mGlu receptor-mediated response depends on the particular method of receptor activation, with transient agonist

application resulting in a mixed response dominated by the outward current, but sustained bath perfusion resulting in an inward current (Diagram 4).

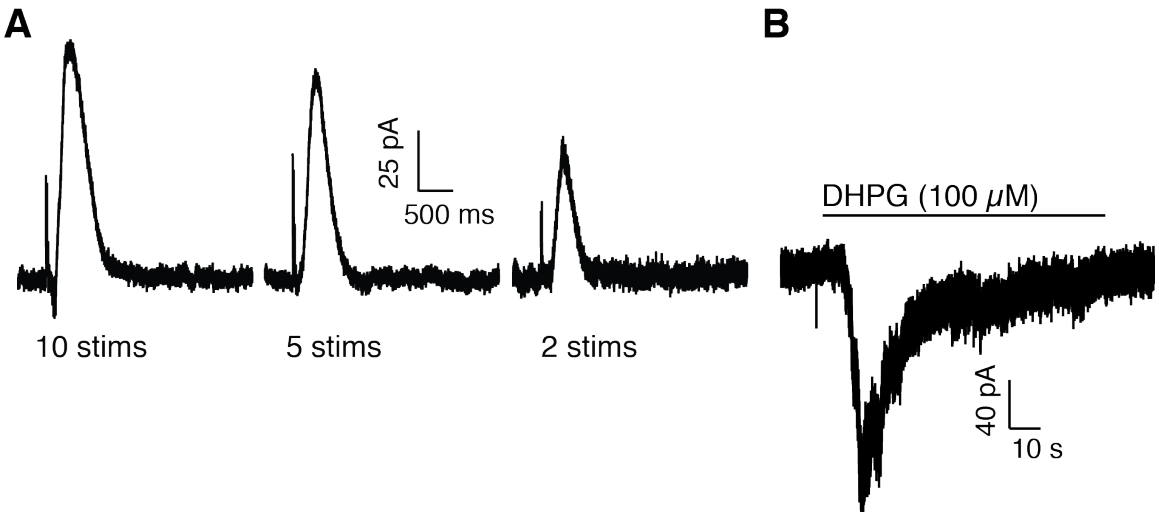

Diagram 4. Method of mGluR activation determines which current predominates.

A. Like with iontophoresis of L-aspartate, electrically stimulated mGluR IPSCs are predominately outward currents, mediated by SK.
B. Bath perfusion of the Group I mGluR agonist DHPG produces an inward current.

The presence of an electrically stimulated mGluR-dependent IPSC in dopaminergic neurons indicates that these receptors are likely located close to glutamatergic synapses. Indeed, structural studies have found evidence for mGluR1 and mGluR5 antibody labeling in the perisynaptic space on the postsynaptic membrane adjacent to asymmetric synapses. The majority of cell surface labeled receptors were mGluR1, with mGluR5 located primarily, but not exclusively, to intracellular membranes (Hubert, Paquet, and Smith 2001). However, mGluR5 located intracellularly can still functionally signal within the cell, and in the hippocampus intracellularly position mGluR5 plays a role in synaptic plasticity (Purgert et al. 2014; for a review see Jong et al. 2014).

Group I metabotropic glutamate receptors contribute to many different behavioral functions. Knockout mice have been generated for both mGlu1 and mGlu5 receptors, for a review of all the behaviors associated with these receptors see Niswender and Conn (2010). Mice lacking the mGlu1 receptor display ataxia, impaired motor learning, and deficits in context-specific associative fear learning; at the cellular levels these deficits are accompanied by impairment of cerebellar LTD and hippocampal LTP (Aiba, Kano, et al. 1994; Aiba, Chen, et al. 1994). Similarly, mice lacking the mGlu5 receptor display deficits in two learning tasks, a Morris water maze task to test spatial learning, as well as a context-specific fear association task; at the cellular level these mice have impaired LTP induction at CA1 and dentate gyrus synapses, but normal LTP at the mossy fiber to CA3 synapse (Lu et al. 1997). Together, these deficits indicate the Group I mGlu receptors are integral components of learning at the behavioral and cellular level.

One disease that is connected to changes in learning is addiction (Hyman, Malenka, and Nestler 2006). Perhaps the neurotransmitter most associated with addiction is dopamine (for a review see Koob and Nestler (1997). Briefly, dopamine is synthesized by dopamine neurons in the ventral tegmental area and the substantia nigra. Classically, the VTA mainly sends projects to the ventral striatum, also known as the nucleus accumbens, while the SNc mainly sends projects to the dorsal striatum.

Addiction has been studied in the context of many drugs of abuse; this review will focus on cocaine. Phasic increases in dopamine release in the nucleus accumbens promote cocaine seeking (Phillips et al. 2003); whereas lesions of the nucleus accumbens (Roberts et al. 1980) or ventral tegmental area (Roberts and Koob 1982) inhibit cocaine self-administration. Finally, when the dopamine transporter, one of the pharmacological targets of cocaine, was mutated to prevent the binding of the drug, the rewarding and reinforcing aspects of cocaine were eliminated (Chen et al. 2006). This work, and other studies examining different drugs, combined to lead to the dopamine theory of addiction (Nutt et al. 2015).

However, dopamine alone cannot account for the broad range of implicated mechanisms and observed consequences of drug addiction, nor the associated mechanisms and effects of non-contingent drug administration in an animal model. For example, a single injection of cocaine leads to a change in the AMPA receptor subunit composition in VTA dopamine neurons, as well as in striatal medium spiny neurons (Bellone and Luscher 2005; Mameli et al. 2009). This change can be reversed in the VTA by activating mGlu1 receptors (Bellone and Luscher 2006). This plasticity in glutamate signaling is similarly gated by mGlu receptors on medium spiny neurons in the ventral striatum, where an increase in calcium-permeable AMPA receptors is accompanied by a decrease in surface mGlu1 receptor expression, and can be enhanced by negatively modulating mGlu1 receptor activity (McCutcheon et al. 2011; Loweth et al. 2013).

Moreover, it has been shown that during the course of repeated drug exposure, this glutamate plasticity begins in the midbrain dopamine neurons and proceeds to the nucleus accumbens. However, this spread of cocaine-mediated plasticity can be prevented by increasing the activity at mGluR1 in the VTA (Mameli et al. 2009). These data indicate a key role for mGlu1 receptor activity within the dopamine network for gating cocaine-induced plasticity on both MSNs and dopamine neurons of the VTA. Specifically, it seems that mGlu1 receptor activity is protective against cocaine-induced cellular changes.

On the other hand, there is evidence that mGlu5 receptor activity is permissive or stimulatory for cocaine-related behaviors. Inhibiting mGlu5 with *in vivo* systemic administration of the specific negative allosteric modulator MPEP decreases priming-induced and cue-induced cocaine seeking in rats (Kumaresan et al. 2009). Systemic administration of MPEP also inhibits cocaine self-administration in rats and monkeys (Platt, Rowlett, and Spealman 2008; Kenny et al. 2005). Moreover, microinjection of MPEP into the nucleus accumbens core prevents cue-induced reinstatement of cocaine seeking, while injection of the mGlu5 receptor agonist CHPG simulates cocaine seeking (Wang et al. 2012).

Dopamine neurons act as reward prediction error generators, and are necessary for associative learning (Schultz 2016). Following this hypothesis, drug abuse pathologies are viewed as diseases of impaired learning that increases the value of drug rewards at the expense of naturalistic rewards, and disrupts normal plasticity mechanisms in the dopamine circuit (Kalivas 2009). From these

perspectives, addiction is not only a dopamine or glutamate related disease, but arises from disruptions in one that affect and reinforce the other. Indeed, it was found in one study that a decrease in D2 receptor-mediated signaling is required for the potentiation of glutamate EPSCs in VTA dopamine neurons.

The roles for Group I mGluRs in learning and memory, therefore, fit well with the involvement of these receptors in the development of drug-related pathologies. Yet, despite a wealth of evidence that Group I mGlu receptors on dopamine neurons can modulate the development of drug-induced pathologies, little is known about how the receptors are affected by these drugs. Drug-induced modulation of GPCRs has been shown for other receptors, such as $GABA_B$ receptors (Hearing et al. 2013; Arora et al. 2011), D2 receptors (Gantz, Robinson, et al. 2015; Dragicevic et al. 2014), and α_1 adrenoceptors (Paladini et al. 2004). Thus the hypothesis that cocaine treatment would affect mGluR signaling seemed reasonable.

The focus of this dissertation was to investigate first how mGlu receptors on dopamine neurons functionally interact with other receptors classically modulated by drugs of abuse, and second to test how a systemic cocaine injection affects mGluR signaling. Chapter 3 describes how calcium release from stores, mobilized by mGluR stimulation, disinhibits dopamine neurons by inhibiting GIRK currents. Chapter 4 describes the evidence for a single injection of cocaine decreasing mGluR1 functional signaling. Finally, Chapter 5 closes with a discussion on the interpretation of these results within the context of drug

abuse and intracellular network activity within dopamine neurons. The work presented in this dissertation provides a new appreciation for the role of Group I mGluR activation in dopamine neuron physiology and pathology.

Chapter 2 Materials and Methods

Animals

All animal experiments were performed in accordance with the National Institutes of Health guidelines and with approval from the Institutional Animal Care and Use Committee of the Oregon Health & Science University (Portland, OR). Mice (chapter 4) and rats (chapter 3) were both used for the following experiments, species will be specific where applicable. Mice were adult (5–10 week), male and female, wild-type C57 or C57/129. Rats were adult (6–10 week), male and female, Sprague-Dawley.

In vivo drug administration

Mice were injected with cocaine (20 mg/kg) or saline intraperitoneally (i.p.) and immediately replaced into their home cage. Some experiments consisted of naïve animals grouped with saline injected animals. There is no significant difference in the mGluR iontophoretic-induced current between these two conditions ($t(17)=1.4$, $p>0.05$).

Electrophysiology

Slices and solutions

Animals were anesthetized in a vapor chamber (isoflurane, OHSU pharmacy) and sacrificed. Brains were extracted and blocked, removing the cerebellum and frontal cortex rostral to the optic chiasm. The brain was then tilted onto the rostral face and the cortex was cut at a ~70 – 80º angle. The dorsal surface of the brain

was fixed onto the vibratome stage (Krazy Glue). Horizontal slices (220–230 μm) containing the substantia nigra were prepared. Slices were cut using a vibratome (Leica) in physiological ACSF containing (in mM): 126 NaCl, 2.5 KCl, 1.2 NaH_2PO_4, 1.2 $MgCl_2$, 2.4 $CaCl_2$, 11 glucose, 21.4 $NaHCO_3$, 5 MK801, saturated with 95% O_2 and 5% CO_2, pH 7.4, 300 mOsm/kg, and then incubated in the same solution warmed to 34°C for between 30 and 60 minutes. After incubation slices were transferred into physiological ACSF lacking MK801. Slices were placed in a recording chamber and superfused with warmed (35°C) physiological ACSF at 1.5 to 2 ml/min.

Whole-cell recording

All recordings were performed from dopamine neurons of the substantia nigra *pars compacta*, defined as a region lateral of the medial terminal nucleus of the accessory optic tract (MT). Dopamine neurons were identified by their large cell bodies, the characteristic pacemaker-like firing (1–5 Hz) observed in the cell-attached mode, and the presence of a large I_h current. Whole-cell pipettes had resistances of 1.5–1.8 MΩ. Unless otherwise noted, pipette solutions used for whole-cell recordings contained (in mM): 115 K-methanesulfonate, 20 NaCl, 1.5 $MgCl_2$, 5 HEPES, 0.1 EGTA, 2 Mg-ATP, 0.25 Na_2-GTP, and 10 Na_2phosphocreatine, pH 7.38–7.42, 280–285 mOsm/kg. Voltage-clamp recordings were made (holding potential -55 mV) using an Axopatch 200B amplifier (Axon Instruments, Foster City, CA). Series resistance was monitored using a square test pulse (collected at 50 kHz and filtered at 10 kHz). Recordings

were discarded if the series resistance exceeded 12 MΩ. Episodic data were obtained at 5 kHz and filtered at 2 or 5 kHz using AxoGraph X (Axon Instruments). Continuous recordings were obtained using Chart (version 5.5.6, AD Instruments, Colorado Springs, CO).

Techniques for Evoking Currents

mGlu receptor-mediated currents

As noted in the introduction, Group I mGlu receptor activation produces two simultaneous currents of opposing sign. Methodologically, this presents a problem for measuring either the SK or the inward current, since they occur simultaneously. To solve this issue, the inward current can be isolated through use of apamin, a selective and potent SK channel blocker. However, the reverse experiment cannot be performed, as blockers for TRP-like channels are non-selective. Therefore, isolating the SK component of the mGluR-mediated current is more difficult, but can be achieved through rapid application of a high concentration of agonist onto the neuron. This prevented desensitization of the mGluR-dependent outward current and minimally activated the inward current. Thus, rapid and short lasting application of agonists was required to obtain a steady reproducible responses mediated almost entirely by the outward SK current. For the following experiments, this was achieved either by iontophoresis of L-aspartate or local pressure ejection of agonist.

Iontophoresis. Iontophoretic currents were performed with an Axoclamp 2A amplifier (Axon Instruments) using pipettes containing L-aspartate (1 M, pH

7.4, 40–70 MΩ, -80–130 nA ejection and +1.5–3 nA backing current). Iontophoretic pipettes were placed within 5–10 µm of the soma.

PRESSURE EJECTION. DHPG (100 μM) was loaded into a patch pipette and connected to a Picospritzer II (Parker Hannifin Corporation, Cleveland, OH). The pipette was placed on the surface of the slice 30–50 µm from the cell body to minimize disturbance of the whole-cell patch by the pressure ejection artifact. DHPG was ejected with air pressure (10–100 ms, 8–10 psi, every 60 s).

CURRENT ISOLATION. For iontophoretic and pressure ejection experiments, the slices were pretreated with (5S,10R)-(+)-5-methyl-10,11-dihydro-5H-dibenzo[a,d]cyclohepten-5,10-imine (MK-801, 50–100 µM) for at least 30 min. Experiments in Chapter 4 were performed in the presence of 6,7-Dinitroquinoxaline-2,3-dione (DNQX, 10 µM), MK-801 (100 nM), picrotoxin (100 µM), CGP-55845 (100 nM), hexamethonium chloride (50 µM), atropine (100 nM), sulpiride (200 nM) and MNI-137 (200 nM) to block AMPA, NMDA, GABAA, GABAB, nicotinic, M1 muscarinic, dopamine D2, and Group II mGluR receptors. Experiments in Chapter 3 were performed only in NBQX (300 nM).

AGONIST PERFUSION. Concentration-response experiments to DHPG were done in the presence of apamin (200 nM) to block SK-mediated outward currents and to isolate mGluR-mediated inward currents. In some experiments, mGluR1 or mGluR5 receptors were blocked by bath perfusion of the negative allosteric modulators (NAMs) JNJ-16259685 (500 nM) or MPEP (300 nM), respectively.

D2 receptor-mediated currents

IONTOPHORESIS. Iontophoretic application was performed with an Axoclamp 2A amplifier (Axon Instruments) using pipettes containing dopamine (1 M, 40–60 MΩ, +30–100 nA ejection and -1.5–3 nA backing current. Iontophoretic pipettes were placed within 5–10 μm of the soma.

CURRENT ISOLATION. Prazosin (100 nM) was included in the superfusion solution to block α1-adrenoceptors, activation of which would desensitize the mGluR response (Paladini et al. 2001).

AGONIST PERFUSION. Quinpirole was added to the superfusion solution to evoke tonic D2 receptor-mediated currents.

$GABA_B$ receptor-mediated currents

IONTOPHORESIS. Iontophoretic application was performed with an Axoclamp 2A amplifier (Axon Instruments) using pipettes containing GABA (500 mM, pH 7.3, 30–50 MΩ, +100–190 nA ejection and -0.2–3 nA backing current). Iontophoretic pipettes were placed within 5–10 μm of the soma.

CURRENT ISOLATION. Picrotoxin (100 μM) and SR-95531 (300 nM) were included in the superfusion solution to block $GABA_A$ receptors.

AGONIST PERFUSION. Baclofen was added to the superfusion solution to evoke tonic $GABA_B$ receptor-mediated currents.

mGluR-independent SK channel activity

A voltage step protocol was used to analyze the SK conductance independent of mGluRs (Deignan et al. 2012). The membrane potential was held at -70 mV, stepped to 0 mV for 50 ms and stepped back -50 mV for 4 s. The SK-mediated current was measured at -50 mV and isolated after subtraction of the current that remained after application of the selective SK-channel blocker apamin (200 nM). Averages from 5 sweeps were analyzed.

Caged compound photolysis

Flash photolysis of caged-IP_3 (Walker, Feeney, and Trentham 1989) and caged-calcium (Ellis-Davies and Barsotti 2005) was performed on a separate experimental set-up. Whole-cell recordings were made with an Axopatch 1D amplifier (Molecular Devices, Sunnyvale, CA). Current was continuously recorded at 200 Hz with PowerLab (chart version 5.4.2; AD Instruments, Colorado Springs, CO). Episodic currents were recorded at 10 kHz for 1 minute using AxoGraphX (1.4.3; AxoGraphX, Berkeley, CA). All experiments were carried out in the dark.

All photolysis experiments were carried out with full-field illumination (365 or 405 nm LED, Thorlabs, Sterling, VA) coupled through a 60x objective (Olympus, 0.9 na). The LEDs were mounted on the epifluorescence port of the BX51 microscope (Olympus). The beam was reflected with a long-pass dichroic (387 nm, Chroma). A notch filter (365/20 nm, Chroma, Bellows Falls, VT) was placed in the light path from the 365 LED. A long-pass dichroic (488 nm,

Semrock, Rochester, NY) in the fluorescence turret was used to direct the beams to the objective.

CAGED-IP_3. A stock solution of caged-IP_3 (0.1 mM) was added to 0.1 mM EGTA containing KMS internal. The IP_3 generated SK currents were of similar size with 365 or 405 nm LED photolysis.

CAGED-CALCIUM. Photolysis of caged-calcium was performed by adding DMNPE-4 (1 mM) and $CaCl_2$ (0.9 mM) to 0.1 mM EGTA containing KMS internal. The 365 nM LED was used to release calcium from its cage by photolysis (10–30 ms pulse,

Alternating activation of $GABA_B$ or D2 and mGlu Receptors

In some experiments two iontophoretic pipettes were brought within close proximity to the cell (~10–20 μm), one filled with aspartate and one with dopamine or GABA. First L-aspartate was applied until the size and duration of the SK current was stable and reproducible, then apamin (100–300 nM) was applied. Then either GABA or dopamine was applied with iontophoresis until the current stabilized. Finally, the protocol illustrated in Figure 2.1A was used to test the effect of L-aspartate iontophoresis on the current elicited by GABA or dopamine.

Synaptic stimulation experiments

$GABA_B$ mediated IPSCs were evoked with a train (5 pulses at 100 Hz) using a monopolar electrode (filled with physiological ACSF, 2–2.5 MΩ) placed ~70-100 μm lateral and ~40-60 μm caudal from the patched neuron. Stimulation intensity

was adjusted to obtain a large (>20 pA) IPSC without evoking a direct action current in the recorded neuron. $GABA_B$ IPSCs were pharmacologically isolated by including NBQX (300 nM), picrotoxin (100 μM), sulpiride (300 nM), JNJ-16259685 (1 μM), and MPEP (300 nM), to block AMPA, $GABA_A$, D2, mGluR1 and mGluR5 receptors respectively. Slices had been pre-incubated in MK801 (50-100 μM) to block NMDA receptors. In most experiments CGP-55845 (300 nM) was applied after the experiment to verify that the IPSC resulted from $GABA_B$ receptors. Photolysis experiments of caged-IP_3 in combination with the $GABA_B$ IPSC included at least three trials per time point that were averaged. IPSCs were evoked at 1 min intervals and interleaved with experiments using the combination of photolysis and electrical stimulation.

DATA COMPUTATION

Construction of current-voltage plots

Current/voltage (*I*/V) plots were constructed using ramp protocols. Agonist-induced currents were isolated by subtracting the evoked current from its respective baseline. Averages of at least two ramps were combined before subtraction. The ramp protocol was used for steady state currents (Figure 2.2) and iontophoretically mediated currents (Figure 2.1B).

Calculating resting calcium levels

The Chelator web application, version 1.3 (maxchelator.stanford.edu), was used to calculate resting calcium levels using the values given for whole-cell voltage

clamp experiments, and 1.1 mM buffer with 900 μM added $CaCl_2$. Because there are two buffers in the internal that have slightly different affinities for calcium at pH = 7.4 (DMNPE-4: 19 nM and EGTA: 67 nM) a range for the possible resting calcium concentration was calculated. The upper estimate was based on the EGTA affinity, whereas the lower limit was based on DMNPE-4.

Data analysis

Activation of mGluRs causes both inward and outward currents resulting from a non-selective cation conductance and SK channels, respectively. To determine the total charge transfer induced by mGluR activation the area under the curve (AUC) was measured for both currents, the absolute value of the inward component was added to the outward component for a complete representation of the size of the mGluR-induced response and was expressed as pA*S. For many experiments while testing the inhibition of GIRK by mGluR activation, apamin was used to isolate inward currents. For these experiments current area was measured to account for the duration of GIRK inhibition. When the peak of the evoked current was measured, averaging 40 ms around a center point. To isolate the current induced by mGluR1 or mGluR5, selective receptor blockers were applied sequentially. Data are expressed as mean±SEM. For data in Figure 3.12, currents were summated using AxoGraph X. Statistical significance was determined with Student's t-test or one-way ANOVA followed by the Tukey's post-hoc test. The difference was considered significant at $p < 0.05$. When necessary a two-way ANOVA was performed followed by Bonferroni's post-hoc

test. Data were graphed using Igor Pro 6 (Wavemetrics, Portland, OR) and analyzed using Prism 6 (GraphPad, La Jolla, CA). At least three biological replicates were tested per condition. Figures were prepared using Illustrator CS5.1 (Adobe, San Jose, CA).

PHARMACOLOGY

- Cocaine was obtained from the National Institute on Drug Abuse Neuroscience Center (Bethesda, MD).
- Caged-IP_3 was a generous gift from Hitoshi Morikawa, PhD (University of Texas, Austin, TX), who obtained it from Kamran Khodakhah, PhD (Albert Einstein School of Medicine, Bronx, NY).
- DMNPE-4 caged calcium was a generous gift from Graham Ellis-Davies, PhD (GM053395, Ichan School of Medicine at Mount Sinai, NY, NY).
- CGP-55845, JNJ-16259685, MNI-137, VU-0357121, and MPEP were obtained from Tocris (Minneapolis, MN).
- Apamin was obtained from Calbiochem (San Diego, CA).
- NBQX, MK801, DHPG, and CHPG were obtained from Abcam (Cambridge, MA).
- SR-95531 was obtained from Hello Bio (Princeton, NJ).
- The remaining compounds were obtained from Sigma-Aldrich (St. Louis, MO).

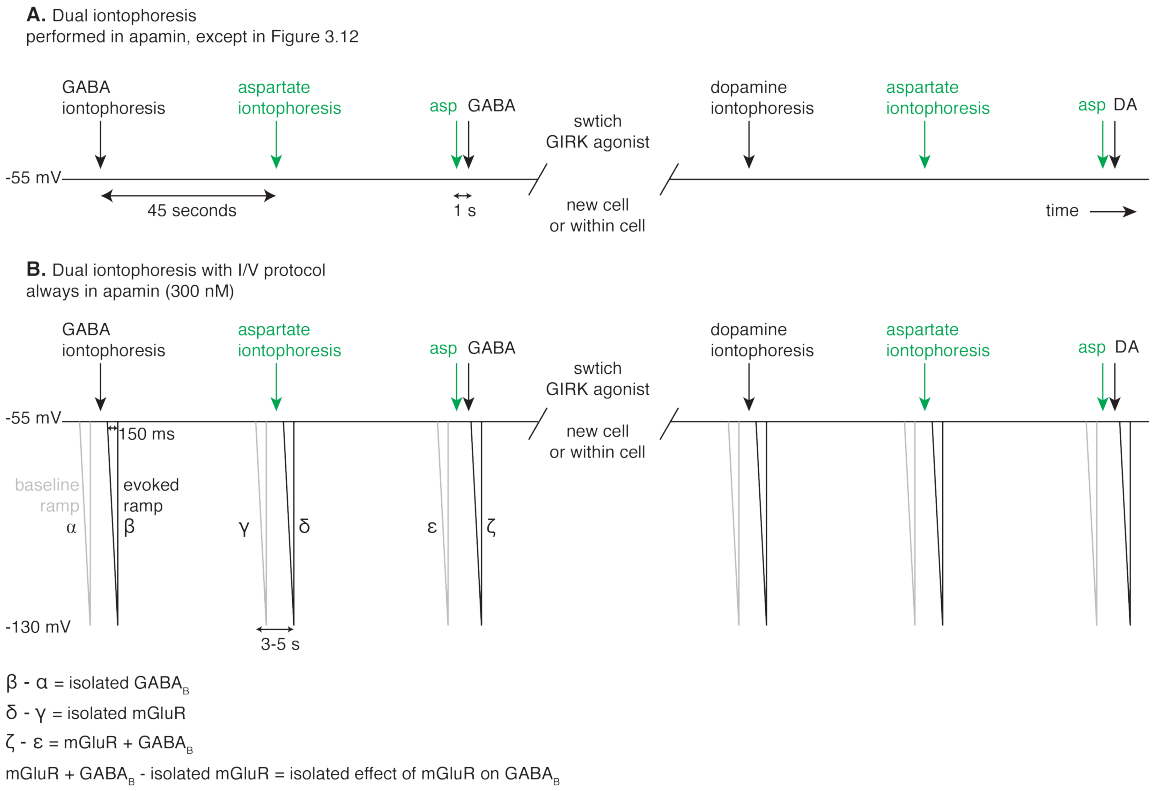

Figure 2.1 Protocol illustrations for sequential co-iontophoresis with and without voltage ramps.

A. On the first sweep GABA was applied 45 s prior to aspartate, on the next sweep GABA was applied 1s after the application of aspartate. This protocol was repeated periodically. After 3 complete repetitions, the iontophoretic pipette containing GABA was retracted and a pipette filled with dopamine was brought close to the neuron.
B. Same general protocol as in **A**, except voltage ramps were performed as illustrated. The current resulting from these ramps at the peak of the GABA current was then subtracted from the current in control, in the order to isolate the current induced by GABA before and following activation of mGluRs.

A. I/V protocol for steady-state $GABA_B$ activation

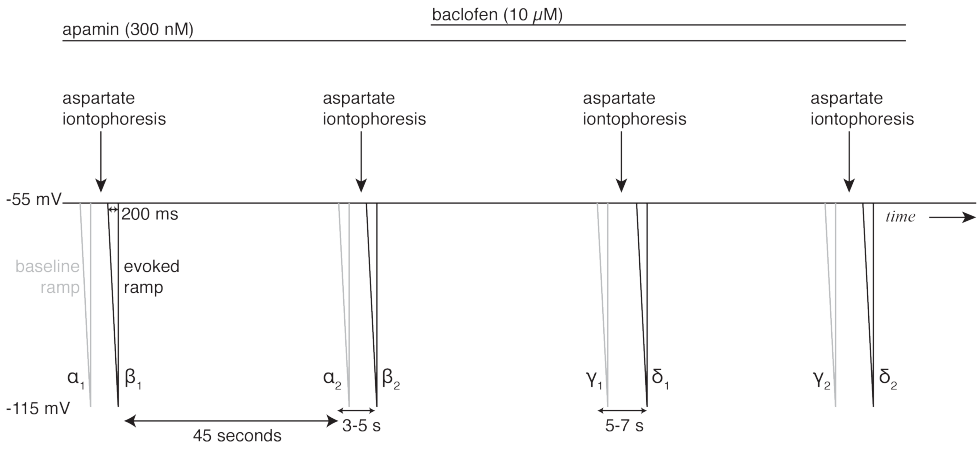

$((\beta_2 + \beta_1) / 2) - ((\alpha_2 + \alpha_1) / 2)$ = isolated mGluR inward

$((\delta_2 + \delta_1) / 2) - ((\gamma_2 + \gamma_1) / 2)$ = ΔGIRK

$((\gamma_2 + \gamma_1) / 2) - ((\alpha_2 + \alpha_1) / 2)$ = isolated baclofen I-GIRK

$((\delta_2 + \delta_1) / 2) - ((\beta_2 + \beta_1) / 2)$ = isolated effect of aspartate on baclofen *I*-GIRK

Figure 2.2 Construction of *I*-V plots for steady-state baclofen voltage ramps.

A. Aspartate was iontophoresed every 45 seconds. Voltage ramps were performed as illustrated in apamin, and again during baclofen (10 μM) application. The resulting currents were subtracted from their respective baselines to construct isolated *I*-V plots of interest.

Chapter 3 Calcium Release from Stores inhibits GIRK

Paul F. Kramer, BA[1] and John T. Williams, PhD[1,*]

[1]Vollum Institute, Oregon Health and Science University

*Correspondence to: John Williams, Oregon Health and Science University, Vollum Institute L474, 3181 SW Sam Jackson Park Rd., Portland, OR 97239 USA, Phone: 503-494-5465, fax: 503-494-4590, williamj@ohsu.edu

Support This work was supported by NIH DA04523 and the OHSU Brain Institute Neurobiology of Disease Lacroute Fellowship.

Acknowledgements We thank Dr. Hitoshi Morikawa for gifting us caged-IP_3 originally produced by Dr. Kamran Khodakhah, and Dr. Graham Ellis-Davies (GM053395) for creating and supplying the DMNPE-4 calcium cage. We also thank members of the Williams lab for comments on the work and manuscript.

Kramer, P.F. and Williams, J.T. (2016). “Calcium release from stores inhibits GIRK.” *Cell Reports* 17 (12): 3246–3255.

Summary

Synaptic transmission is mediated by ionotropic and metabotropic receptors that together regulate the rate and pattern of action potential firing. Metabotropic receptors can activate ion channels and modulate other receptors and channels. The present paper examines the interaction between group 1 mGluR-mediated calcium release from stores, and $GABA_B$/D2 mediated GIRK currents in rat dopamine neurons of the substantia nigra. Transient activation of mGluRs decreased the GIRK current evoked by $GABA_B$ and D2 receptors, though less efficaciously for D2. The mGluR-induced inhibition of GIRK current peaked in 1 second and recovered to baseline after 5 seconds. The inhibition was dependent on release of calcium from stores, was larger for transient than for tonic currents, and was unaffected by inhibitors of PLC, PKC, PLA_2, or calmodulin. This inhibition of $GABA_B$ IPSCs through release of calcium from stores is a postsynaptic mechanism that may broadly reduce GIRK-dependent inhibition of many central neurons.

Introduction

G protein-coupled receptors (GPCRs) can be separated into three major subclasses defined by their alpha G protein subunit: $G_{i/o}$, $G_{q/11}$, or G_s. These divisions confer the receptors with discrete signaling pathways. Dopamine neurons express a variety of GPCRs that activate different ion channels. For example, $G_{i/o}$ $GABA_B$ receptors ($GABA_BR$) and dopamine D2 receptors (D2R) increase a G protein-gated inwardly rectifying potassium (GIRK) conductance (Beckstead et al. 2004; Arora et al. 2010). By contrast, G_q group I metabotropic glutamate receptors (mGluR1 and mGluR5) activate the small conductance calcium gated potassium channel SK
(Fiorillo and Williams 1998; Kramer and Williams 2015). Thus, two signaling pathways activate distinct potassium conductances that hyperpolarize and pause action potential generation in dopamine neurons.

These signaling pathways do not always work in isolation. G_q receptor activation can inhibit GIRK currents generated by G_i receptors, although there are conflicting reports as to the mechanism underlying this interaction. The most commonly proposed mechanism(s) involve protein kinase C (PKC) (Mao et al. 2004). PKC-dependent inhibition has been reported to be either calcium-independent (Stevens et al. 1999; Leaney, Dekker, and Tinker 2001) or calcium-dependent (Hill and Peralta 2001; Xia, Margolis, and Hjelmstad 2010). The inhibition of GIRK by phospholipase C (PLC) has also been shown to be directly (Kobrinsky et al. 2000) and indirectly involved (Keselman et al. 2007). Finally, the

activation of phospholipase A_2 (PLA_2), a calcium and G protein activated phospholipase has also been shown to inhibit GIRK (Sohn, Lee, Cho, Lim, Shin, Lee, and Ho 2007a). Hence there are a variety of mechanisms underlying the G_q dependent inhibition of GIRK currents, depending on experimental conditions such as cell type, the particular GPCRs being studied, and agonist application protocols.

To date, the study of inhibition of GIRK by G_q signaling has relied on steady state application of agonists for both G_i and G_q receptors. It is known, however, that group I mGluRs signal differently depending on the method of activation. Steady state application of a selective agonist (DHPG) produced a tonic inward current, whereas transient activation via iontophoresis of aspartate or synaptic release of glutamate produced an outward current (Morikawa, Khodakhah, and Williams 2003; Kramer and Williams 2015). Thus distinct intracellular signaling pathways underlie the two methods of activation, and the question of how physiologically relevant receptor activation of group I mGluRs affects GIRK currents remains unexplored.

The present work shows that increases in cytosolic calcium transiently decreased a GIRK conductance that was activated by $GABA_BR$, D2R, or a non-hydrolyzable GTP analogue. Increases in cytosolic calcium were generated by transient mGluR activation, or by photolysis of caged-IP_3 or caged-Ca^{2+} loaded into the neuron. The inhibition of GIRK was not affected by inhibition of PLC, PKC, PLA_2, or calmodulin. In addition, the inhibition of transient GIRK currents

evoked by synaptic release or iontophoretic application of GABA was greater than steady state currents. The results demonstrate a dynamic role for calcium in the inhibition of GIRK currents in dopamine neurons on the timescale of synaptic transmission, a potential mechanism for inhibition of GIRK currents in other brain areas.

Results

GABA receptor-dependent decrease in SK current

To examine the mGluR-induced inhibition of GIRK current, voltage-clamp recordings were made from adult rat substantia nigra *pars compacta* dopamine neurons. Iontophoretic application of aspartate at 45s intervals activated an SK current mediated by mGlu receptors (mGluR1 and mGluR5 (Kramer and Williams 2015)). All experiments were carried out in the presence of ionotropic glutamate antagonists (see methods). Apamin (100-300 nM) was used to block SK (control 176 ± 21.4 pA*S, in apamin -5.97 ± 6.86 pA*S) in order to isolate the effect of the mGluR activation on the baclofen (10 μM) induced GIRK current. The small inward current that was induced by aspartate in the presence of apamin resembled the activation of a previously reported non-selective cation conductance (Figure 3.10E (Tozzi et al. 2003; Kim et al. 2003)).

Application of aspartate in the presence of baclofen and apamin resulted in a separate inward current (-212 ± 40 pA*S, Figure 3.1A) that was present only during the application of baclofen. That inward current declined as the outward current induced by baclofen reversed upon washing (-14.2 ± 5.3 pA*S, Figure 3.1A,B). The inward current induced by mGluR activation during GIRK activation could result from a breakdown in voltage control secondary to an increase in cell conductance. This mechanism accounted for an inhibition of the hyperpolarization-activated cation current I_h by the activation of $GABA_B$ receptors (Watts, Williams, and Henderson 1996). One test of this mechanism was to

increase the conductance of the cell with the $GABA_A$ agonist muscimol (10 μM). In the presence of muscimol (10 μM) aspartate iontophoresis did not induce a separate inward current (in apamin -0.99 ± 5.3 pA*S, +muscimol -6.97 ± 10.2 pA*S, Figure 3.1C, E). Thus the aspartate induced inward current seen in the presence of baclofen (referred to as ΔGIRK) was not the result of an increase in cell conductance.

When the $GABA_BR$ dependent current was reduced by the application of $BaCl_2$ (100 μM), the ΔGIRK current induced by aspartate also decreased (-206 ± 37 pA*S without $BaCl_2$ and -57.2 ± 5.1 pA*S with $BaCl_2$, Figure 3.8). Finally, when mGluR1 and mGluR5 were reversibly inhibited by the low affinity non-selective antagonist, MCPG (1 mM), there was a reduction in the inhibition of GIRK (baseline: 64.8% inhibition, in MCPG: 34.5%, Figure 3.8D). The high affinity negative allosteric modulators JNJ-16259685 (1 μM, mGluR1) and MPEP (1 μM, mGluR5) abolished the inhibition of GIRK (inhibition in control: 65.4%, in JNJ/MPEP: 0.9%, Figure 3.8D). These results suggest that the baclofen induced GIRK current is reduced by transient activation of mGluRs.

mGluR-dependent inhibition of GIRK conductance

The interaction between $GABA_B$ and mGlu receptors was next examined with iontophoretic co-application of GABA and aspartate. This technique allowed activation of $GABA_B$ and mGlu receptors that resembled synaptically stimulated transmitter release. All experiments were carried out in the presence of apamin (300 nM). When aspartate was applied one second before GABA, the peak

$GABA_B$ current was reduced to 43.3 ± 6.7% of control (from 137 ± 12.6 pA to 56.4 ± 9.9 pA; Figure 3.2C). The current induced by transient activation of $GABA_B$ receptors was inhibited significantly more than the steady state current induced by baclofen as measured from the peak of the baclofen current to the peak of the ΔGIRK current elicited by aspartate iontophoresis (inhibition of transient GIRK: 58.5 ± 5.8%, n = 9; inhibition of steady-state GIRK: 25.6 ± 3.0%, n = 30, $p < 0.001$, One-way ANOVA followed by Tukey test).

The voltage dependence of the decrease in the $GABA_BR$-induced current was examined using a voltage ramp protocol (Figure 3.2D). A hyperpolarizing ramp (-55 to -130 mV, 200 ms) was applied just before and at the peak of the $GABA_BR$ outward current (see Figure 2.1 for detailed protocol). The *I*-V plot for the $GABA_BR$ current without an mGluR pre-pulse had the characteristic inward rectification of a GIRK conductance and reversed near the potassium reversal potential (-93.7 ± 1.4 mV, calculated E_k = -103 mV, not corrected for junction potential; Figure 3.2D). When aspartate was applied one second prior to GABA the amplitude of the outward current was reduced but the rectification and reversal potential were unchanged (Figure 3.2D, reversal = -94.7 ± 1.2 mV, $p = 0.11$). The inhibition of GIRK was not voltage dependent; the scaled *I*-V plots with and without the mGluR pre-pulse were not different (Figure 3.10A-B).
Similar results were obtained in experiments using steady-state application of baclofen (Figure 3.10C-E).

Taken together, mGluR activation during, or immediately preceding, a $GABA_BR$-mediated GIRK current decreased the GIRK conductance. Both the SK current and the ΔGIRK current were mediated by mGluRs, however the kinetics of the two currents were different. The duration of the SK current was about half that of the inhibition of the GIRK conductance measured at 10% of the peak (SK: 2.38 ± 0.15 s; ΔGIRK: 4.56 ± 0.31 s; Figure 3.3A and B). But when the duration of each was compared within cells there was a significant positive correlation suggesting an association between the two signaling pathways (Figure 3.3C).

Calcium release from stores inhibits GIRK

The mGluR dependent SK current is activated by release of calcium from stores, and depletion of stores by inhibition of the smooth endoplasmic reticulum calcium pump with cyclopiazonic acid (CPA, 10 μM) blocks this current (Morikawa et al. 2000). CPA was therefore tested on the mGluR inhibition of the GIRK conductance. CPA eliminated the SK current and blocked the inhibition of GIRK (aspartate evoked SK in control: 160 ± 27.7 pA*S, after CPA: -18.7 ± 8.49 pA*S, in baclofen: -16.9 ± 11.3 pA*S, wash baclofen: -22 ± 17.4 pA*S; Figure 3.4A, B).

Strong calcium buffering also blocked the inhibition of GIRK. The control internal solution contained EGTA (100 μM) that minimally buffered calcium. The activation of mGluRs with this internal solution always resulted in the activation of SK and an inhibition GIRK (Figure 3.4C). When the concentration of EGTA was increased to 1 mM the SK current was inhibited in six of ten cells, and in those six cells the mGluR inhibition of GIRK was prevented. In the remaining four cells

where the SK current persisted, so did the mGluR induced GIRK inhibition (Figure 3.11). Increasing the concentration of EGTA to 10 mM blocked both the SK current and inhibition of GIRK after mGluR activation in every cell tested (Figure 3.4C, Figure 3.11A and 3.11C).

IP_3-mediated calcium release from stores inhibits GIRK

To test if bypassing G protein activation and directly releasing calcium from internal stores could inhibit GIRK, neurons were loaded with caged-IP_3 (100 μM) that was photolysed by blue light (100 ms, 405 nm). Photolytic release of IP_3 produced an SK current (183 ± 25.7 pA*S, time to 5% of peak: 81.5 ± 10.1 ms, 10–90% rise time: 49.4 ± 3.6 ms, width at 20% of peak: 677 ± 68.3 ms, Figure 3.5A), which was blocked by apamin (300 nM, 21.0 pA*S ± 4.3 pA*S; Figure 3.5B). When baclofen (10 μM, average peak: 425 ± 42.6 pA) was superfused, the photolytic release of IP_3 caused a ΔGIRK current (-177 ± 35.7 pA*S, time to 5% of peak: 143 ± 22.6 ms, 10–90% rise time: 324 ± 23.9 ms, width at 20% of peak: 2432 ± 181 ms, Figure 3.5A). The size of the ΔGIRK current induced by the release of IP_3 (-196 ± 37, Figure 3.5F) was similar to that induced by aspartate (-206 ± 37 pA*S). The IP_3-dependent inhibition of GIRK was eliminated by depleting calcium stores using CPA (inhibition after CPA: 14.8 ± 5.6 pA*S; in baclofen: -4.3 ± 1.2 pA*S; $p = 0.23$, $n = 4$ cells, one-way repeated measures ANOVA followed by a Tukey test).

Photolytic release of caged-Ca^{2+} inhibits GIRK

To test if the photolytic release of calcium alone is sufficient to inhibit GIRK, neurons were dialyzed with a calcium cage (DMNPE-4, see methods) loaded 90% with $CaCl_2$. Under these conditions, the upper limit of resting calcium levels in the cell was calculated to be 406 nM and the lower limit 115 nM (see methods). Calcium was released with UV light (10–100 ms, 365 nm) resulting in the activation of an apamin sensitive SK current (Figure 3.5C). Baclofen (10 μM, 305 ± 28.7 pA) was applied following treatment with apamin, and photolysis of caged-Ca^{2+} produced a ΔGIRK current during baclofen superfusion (calcium current at baseline: 178 ± 40 pA*S; in apamin: 19.7 ± 3.8 pA*S; in baclofen: -61 ± 8.9 pA*S; after wash: 9.4 ± 3.5 pA*S; Figure 3.5D). Thus, photolytic release of calcium alone results in the inhibition of the GIRK conductance.

To test if calcium could inhibit GIRK independently of receptor activation, neurons were loaded with a combination of DMNPE-4 caged-Ca^{2+} and GppNHp (500 μM), a non-hydrolyzable GTP analogue. Apamin (300 nM) was superfused immediately after the beginning of the recording, and experiments were performed in blockers of $GABA_B$, mGlu, and D2 receptors. GppNHp produced an outward current that was partially reversed with the GIRK channel inhibitor tertiapin-Q (TPN-Q, 300 nM). The GppNHp evoked GIRK current (230 ± 17.7 pA) was obtained by subtracting the TPN-Q sensitive current from the peak outward current. Calcium was photolytically released at the beginning of the recording, at the peak of the GppNHp current, and again after TPN-Q. There was an inward

current observed at the peak of the GppNHp current that was absent after TPN-Q treatment, representing a ΔGIRK current (Figure 3.5E). GIRK currents activated by GppNHp or by baclofen were similarly inhibited by photolytic release of caged-Ca^{2+} (Figure 3.5F). Thus, the calcium-mediated inhibition of GIRK does not depend on G_i-coupled receptor activation.

Inhibiting calcium-activated enzymes did not block the inhibition of GIRK

To test the possibility of downstream calcium-activated molecules being required for the inhibition of GIRK, known inhibitors of calcium-activated proteins were tested. Slices were incubated at least 10 minutes in staurosporine (1 μM) to inhibit PKC, but the mGluR inhibition of GIRK persisted (apamin: 11.6 ± 7.04 pA*s; baclofen: -179 ± 54.1 pA*s; wash: -14.3 ± 6.69 pA*s; Figure S4A). The PKC inhibitor calphostin-C was also tested, but did not block mGluR-mediated GIRK inhibition (apamin: 13.3 ± 14.8 pA*s; baclofen: -505 ± 155 pA*s; wash: -8.12 ± 13.5 pA*s; Figure 3.9B). Slices were incubated in OBAA (3–10 μM) to inhibit PLA_2, but the mGluR-mediated GIRK inhibition was not blocked (apamin: 6.35 ± 15.0 pA*s; baclofen: -397 ± 112 pA*s; wash: -46.9 ± 36.8 pA*s; Figure 3.9D). The PLC inhibitor U73122 (1 μM) was included in the pipette and allowed to dialyze into the neuron for at least 10 minutes, but the mGluR-mediated GIRK inhibition was not affected (peak *I*-GABA at 1 minute: - mGluR: 114 ± 19.8 pA, + mGluR: 36.1 ± 7.23 pA; at 7 min: - mGluR: 112 ± 18.7 pA, + mGluR: 31.5 ± 11.5 pA; Figure 3.9E). Finally, slices were incubated at least 10 minutes in the

calmodulin inhibitor, calmidazolium (10 μM), but this did not block the mGluR-mediated GIRK inhibition (apamin: -10.8 ± 32.6 pA*s; baclofen: -276 ± 25.9 pA*s; wash: -37.3 ± 32.4 pA*s; Figure 3.9C). The only consistent and robust block of the inhibition of GIRK by mGluR activation is through robust calcium buffering in the neuron, or prevention of calcium release from stores.

$GABA_B$ IPSCs are inhibited by calcium

The synaptic release of GABA results in a $GABA_B$R-dependent inhibitory postsynaptic current (IPSC) mediated by GIRK. To test if calcium inhibits this synaptic current, paired electrically activated $GABA_B$R IPSCs (5 pulses at 100 Hz, 10 seconds apart) were evoked once per minute. Blockers of mGluR1 and mGluR5 were included in the solution to block synaptic activation of mGluRs by glutamate release. Calcium was released from intracellular stores using photolysis of caged-IP_3 at various times before the second electrical stimulation (Figure 3.6A). The $GABA_B$R IPSC was maximally inhibited when calcium was released from stores 150 to 1000 ms prior to synaptic stimulation (inhibition after 1000 ms 30.3 ± 7.7%, after 500 ms 33.1 ± 6.8%, after 150 ms 37.8 ± 7.8 %; Figure 3.6B). Though, in three of five cells the IPSC was inhibited at last 10% by calcium release from stores two seconds prior to electrical stimulation, and in three of eight cells five seconds before stimulation. Thus a $GABA_B$ IPSC is sensitive to the release of calcium from stores.

Preferential inhibition of $GABA_B$ induced GIRK

Dopamine neurons also express the dopamine D2 receptor (D2R) that activates a GIRK conductance (Beckstead et al. 2004). The inhibition of D2R GIRK current by mGluR activation was examined next. The amplitude of the D2R GIRK currents was smaller than $GABA_B$ GIRK currents. A saturating concentration of quinpirole induced a current that was about the same as that induced by sub-saturating baclofen (baclofen, 1 μM: 109 ± 17.4 pA; quinpirole, 30 μM: 138 ± 12.6 pA). Using baclofen (1 μM) and quinpirole (30 μM), mGluR activation produced a significantly larger inhibition of the baclofen GIRK current than the quinpirole GIRK current (baclofen control: 2.89 ± 5.78 pA*S, baclofen: -101 ± 19.2 pA*S; quinpirole control: 7.85±6.72 pA*S, quinpirole: -27.9 ± 8.36 pA*S; Figure 7A,B)

This experiment was also carried out using iontophoretic application of dopamine, GABA and aspartate. The application of aspartate one second before dopamine significantly and repeatedly reduced the peak dopamine current (from 69.5 ± 7.3 pA to 61.7 ± 6.2 pA; Figure 3.7D). The percent inhibition of dopamine-mediated GIRK currents by mGluR activation (11.8 ± 1.3%) was significantly less than the inhibition of GABA-mediated GIRK currents (56.7 ± 3.8%; Figure 3.7E).

With the exception of experiments illustrated in Figure 3.1, all experiments were conducted in the presence of apamin to enable the characterization of the selective modulation of the GIRK conductance in the absence of the SK conductance. The interaction of currents induced by aspartate and dopamine or GABA applied using iontophoresis in the absence of apamin was examined next.

The currents induced by aspartate, dopamine, or GABA applied alone were measured. Aspartate was then applied one second before either dopamine or GABA (Figure 3.12A, B). The linear summation of the aspartate plus GABA or dopamine was compared with the observed current induced by iontophoretic application (GABA: figure 3.12A, C; dopamine: Figure 3.12B, D). The linear summation of the individual currents evoked by aspartate + GABA or dopamine was always larger than the observed co-application of agonists (GABA summated: 176 ± 27.9 pA, observed: 119 ± 23.7 pA; dopamine summated: 137 ± 20.3 pA, observed: 108 ± 18.2 pA). Furthermore, the inhibition of the peak $GABA_BR$ current was always significantly greater than for the D2R mediated GIRK current (Figure 3.12E).

Discussion

Transient mGluR activation evoked an IP_3-mediated increase in cytosolic calcium and a decrease GIRK conductance. The inhibition peaked in 1 s and lasted 2-5 s. The activation of mGluRs also inhibited $GABA_BR$ IPSCs. The calcium-mediated inhibition of GIRK was not prevented by pharmacological inhibition of PLC, PKC, PLA_2 or calmodulin, enzymes that had been previously implicated in the G_q-mediated inhibition of GIRK. The only manipulations that blocked the mGluR inhibition of GIRK were depletion of calcium stores and strong cytosolic calcium buffering. Furthermore, direct release of calcium from stores mimicked the GIRK inhibition produced by mGluR activation. While the precise mechanism remains unclear the results indicate that there is a functionally significant inhibition of GIRK by calcium released from stores.

Mechanism of GIRK inhibition by calcium release from stores

The inhibition of GIRK by mGluR activation and photolytic activation of IP_3-mediated calcium release from stores was indistinguishable, but photolytic release of calcium produced a significantly smaller inhibition. This could be because the GIRK was already partially inhibited by the resting level of calcium (between ~115 and ~406 nM), as has been reported (Gantz, Robinson, et al. 2015). On average, GIRK currents achieved with the same concentration of baclofen were ~30% smaller with caged-Ca^{2+} in the pipette than with caged-IP_3, likely occluding further calcium inhibition and minimizing the apparent effect of

photolytic release of calcium. However, despite this constraint, photolytic release of calcium was still able to inhibit GIRK currents whether they were mediated by $GABA_BR$ activation or from inclusion of GppNHp in the pipette.

The most direct interpretation of the present study is that calcium directly inhibits the GIRK channel. It has been reported that external calcium, as well as other divalent cations, can block IRK (including K_{ir} 3.1 and 3.4) channels (Owen et al. 1999). However there is no complete characterization of any direct inhibition of GIRK by intracellularly positioned calcium ions.

Given what is known about GIRK channel function, there are three potential sites for modulation by calcium. Calcium could act at the Gβγ site to inhibit binding, dissociate PIP_2 from the channel, or competitively bind to the sodium site. GIRK is an AND gate, meaning Gβγ and PIP_2 are both necessary for channel activation, so negative modulation of either of them would transiently close the channel until calcium was fully sequestered. Sodium, by contrast, enhances the activity of the channel but is not required for current flow, making it a less likely but still possible site of action of calcium (Whorton and MacKinnon 2011; Wang, Whorton, and MacKinnon 2014).

It is possible the inhibition of GIRK currents by calcium is not a direct action of calcium on the channel itself. While pharmacological inhibitors of PLC, PKC, PLA_2, and calmodulin failed to affect the calcium-mediated inhibition of GIRK, there could be some other unexpected calcium-activated protein responsible for the inhibition of GIRK currents.

IP_3-mediated SK currents and GIRK inhibition have different kinetics

It is of interest to note that, when photolytically releasing caged-IP_3, the SK current onset at 5% of peak was almost twice as fast as the inhibition of GIRK (82 vs 143 ms), the SK rise time from 10% to 90% of peak was about 6.5 times faster (49 ms vs 324 ms), and the SK width at 20% of peak was about 3.5 times shorter (677 ms vs 2432 ms). Both processes are calcium dependent, but SK channel activity has been better established and is known to depend solely on intracellular calcium levels and does not desensitize, making it a faithful sensor of intracellular calcium activity (Lancaster, Nicoll, and Perkel 1991). Therefore, the differing kinetics of current onset, time to peak, and width indicate a difference in underlying mechanisms. Without knowing the precise mechanism of calcium-mediated GIRK inhibition, only speculations can be offered to account for the differences in kinetics. For example, the difference in rise time could result from an inherit difference in SK versus GIRK activation or deactivation rates. It also remains possible that an intermediary step is responsible for the inhibition of GIRK.

Preferential $GABA_B$ GIRK inhibition by calcium release from stores

In the present study D2R GIRK currents were decreased by calcium release from stores to a significantly smaller degree than the inhibition of $GABA_BR$ GIRK currents. Previous work has shown that $GABA_B$ and D2 receptors have differential sensitivity to calcium. Resting cytosolic calcium levels play a central

role in the desensitization and long-term depression of the dopamine D2 receptor, but not the $GABA_B$ receptor (Beckstead and Williams 2007; Gantz, Robinson, et al. 2015). Increasing cytosolic calcium decreased peak $GABA_BR$-, but not peak D2R-, mediated GIRK currents (Gantz, Robinson, et al. 2015). It is known that D2 receptors associate with the neuronal calcium sensor-1 (NCS-1), which alters desensitization of the receptor (Kabbani et al. 2002). D2 receptors are also localized in close proximity to the calcium channel $Ca_v1.3$ (Dragicevic et al. 2014). Furthermore, depleting calcium stores or inhibiting calcium entry through the L-type voltage gated calcium channel increased the amplitude of a D2R-medaited GIRK current in wild type mice (Gantz, Robinson, et al. 2015). Given the results of the present study in light of these results, it is possible that D2 receptor mediated GIRK currents at baseline are nearly maximally inhibited by calcium entry through $Ca_v1.3$, IP_3 receptors, and/or resting calcium levels. Indeed, D2R-mediated currents in the present study were consistently smaller than $GABA_BR$-mediated currents. A second interpretation of the present results is that calcium release from stores was preferentially affecting $GABA_BR$ GIRK currents due to the close proximity of IP_3 receptors with the $GABA_B$ signaling complex, and separated compartmentalization of the D2R complex.

A general mechanism to decrease GIRK dependent synaptic inhibition

Glutamate release resulting in an mGluR-mediated IPSC could have an initial inhibitory SK-mediated component followed by a period lasting as long as 5 seconds during which GIRK-mediated inhibition could be decreased. Given that some VTA neurons have very little SK-mediated current (Wolfart et al. 2001), the activation of mGluRs would disinhibit cells through the calcium-mediated inhibition of GIRK-dependent synaptic currents. Furthermore, many neurons have functional GIRK currents and IP_3 receptors, such as hippocampal pyramidal cells (Nakamura et al. 2000; Degro et al. 2015) and 5-HT neurons of the dorsal raphe (Gantz, Levitt, et al. 2015; Pan, Grudt, and Williams 1994). Thus the interaction between calcium release from stores and GIRK channel currents described here may not be a dopamine neuron-specific effect.

Finally, calcium buffering and manipulations of the resting level of free calcium modulates the GIRK conductance activated by both D2 and $GABA_B$ receptors in that strong calcium buffering with BAPTA (10 mM) results in a larger GIRK currents (Beckstead and Williams 2007; Gantz, Robinson, et al. 2015). In addition the regulation of GIRK conductance by calcium is modulated following treatment of animals with psychostimulants. The calcium-dependent inhibition of GIRK is augmented following treatment of animals with cocaine (Gantz, Robinson, et al. 2015; Arora et al. 2011) and animals that self-administered methamphetamine (Sharpe et al. 2014).The mechanisms underlying these

observation may differ in that there was no receptor dependence in animals that self-administered methamphetamine (Sharpe et al. 2014) whereas the present results indicate that the $GABA_B$-induced currents are more susceptible to the calcium dependent regulation.

To close, GIRK channels are well known mediators of neuronal inhibition, and the modulation of this conductance has been studied extensively. Typically modulation has been studied on the order of minutes (Xia, Margolis, and Hjelmstad 2010) to days (Arora et al. 2011). The data presented here show that release of calcium from stores inhibits GIRK currents in milliseconds and reverses in seconds, a dynamic process that can modulate on the timescale of GIRK-dependent synaptic transmission. This demonstration of the direct effect of calcium on GIRK currents has broad implications for inhibition mediated by GIRK channels.

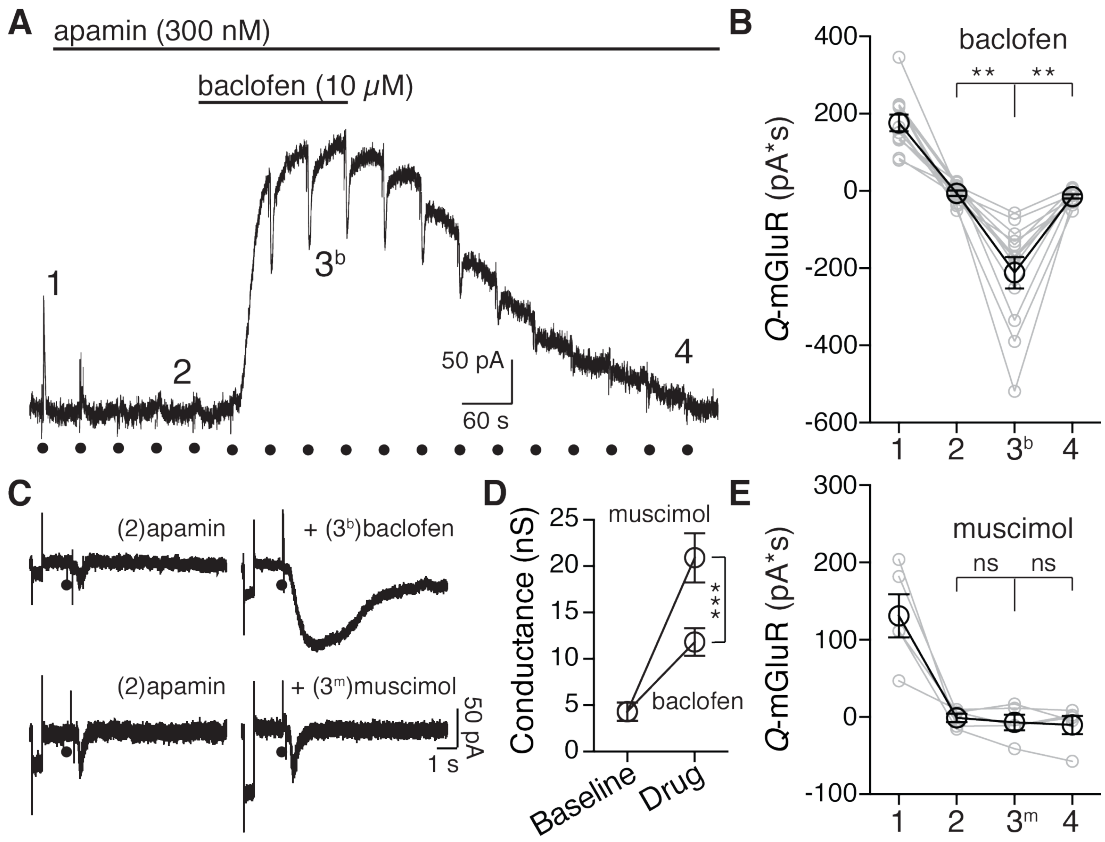

Figure 3.1 mGluR activation induced an inward current during $GABA_BR$ but not $GABA_AR$ currents.

A. Representative trace of a voltage clamp whole cell recording showing the block of the SK current by application of apamin (300 nM), followed by application of baclofen (10 μM). The numbers (1, 2, 3, and 4) correspond to time points plotted in B. Black circles represent the activation of mGluRs with aspartate iontophoresis.
B. Quantification across cells of the total charge transfer for the mGluR-activated current at baseline (1), after apamin (2) during baclofen (3^b) after washout (4). In the presence of baclofen aspartate resulted in a ΔGIRK inward current (one-way repeated measures ANOVA followed by Tukey test, n = 12 cells).
C. Representative episodic traces showing application of aspartate (indicated by the black circle), in apamin (left) showing the small non-selective cation conductance and during either baclofen (black, top) or muscimol (grey, bottom) treatment. Each episode begins with a 3 mV step to assay whole cell conductance (Figure 1C).
D. Quantification of the change in cell conductance. Both baclofen and muscimol caused a significant increase in the conductance (two-way repeated measure ANOVA followed by Bonferroni, n = 7 for muscimol, 11 for baclofen). The increase was significantly larger for muscimol than for baclofen (two-way repeated measure ANOVA followed by Bonferroni).
E. Comparison between cells of the aspartate induced current on baclofen or muscimol application. Muscimol and baclofen were not significantly different at baseline (1, p = .94), after apamin (2, $p > 0.99$), or after washout (4, $p > 0.99$). In muscimol the aspartate-induced current was not different from apamin or washout ($p > 0.99$). All statistics were conducted with a two-way repeated measures ANOVA followed by a Bonferroni. n = 5 (muscimol), n = 12 (baclofen), $^{**}p < 0.01$, $^{***}p < 0.001$, bars and summary data points represent means ± s.e.m. in B. each dot indicates a single cell.

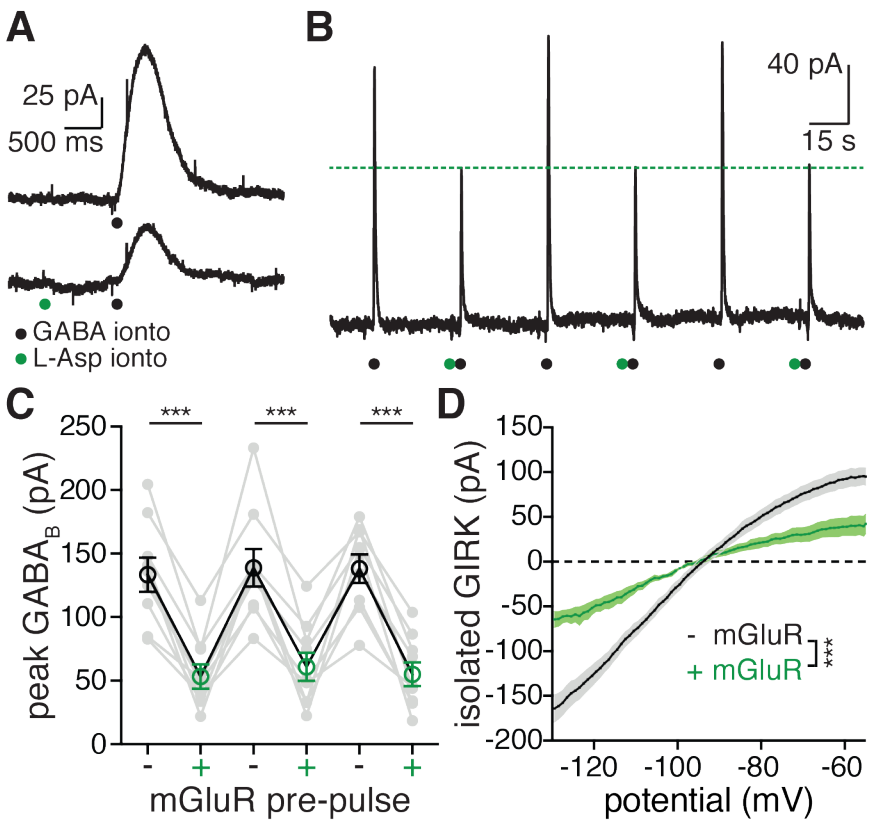

Figure 3.2 mGluR activation decreases GABA$_B$R GIRK currents by closing GIRK channels.

A. Representative traces (average of three raw traces for each condition) showing the effect of an mGluR pre-pulse (green dots) on the GIRK current mediated by GABA$_B$ receptor activation (black dots).

B. Representative chart record from a whole-cell recording showing iontophoresis of GABA (black circles) every 45 seconds. Aspartate (green circle) was applied by iontophoresis one second before every other application of GABA. These experiments were done in the presence of apamin (100–300 nM), as well as GABA$_A$ and AMPA receptor blockers (see methods).

C. Grouped data across cells showing the effect of an mGluR pre-pulse (green) one second before GABA on the peak GABA$_B$R GIRK current. In black are grouped traces where there was no mGluR pre-pulse. Each grey dot represents an individual cell, black and green circles are means ± s.e.m. Statistics were performed with a one-way repeated measures ANOVA followed by a Bonferroni test, n = 8 cells, ***$p \leq 0.001$.

D. *I*–V plots of the GABA$_B$ mediated GIRK current grouped across cells with (green) and without (black) pre-application of aspartate. Each dot on the *I*–V plot represents the mean, shaded area around the curves represents s.e.m. Statistics were performed with a one-way repeated measures ANOVA, n = 6 cells, ***$p < 0.001$ (interaction between voltage and mGluR pre-pulse).

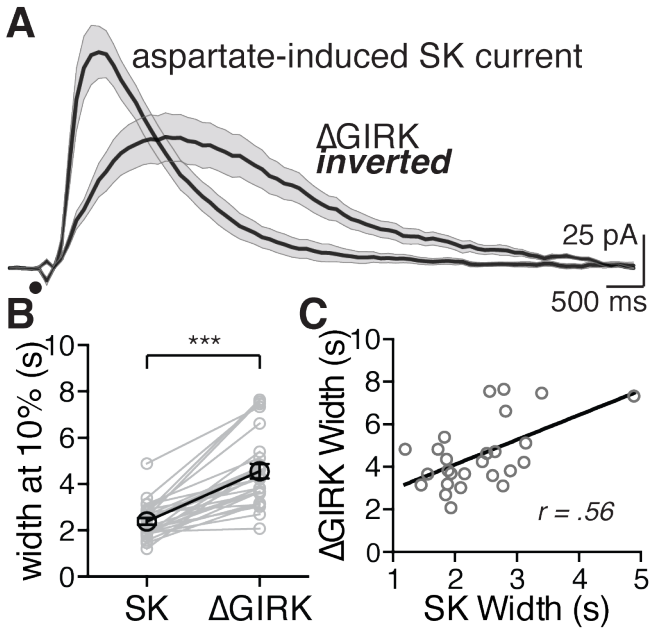

Figure 3.3 The mGluR-mediated SK current and ΔGIRK inward current have different kinetics and are correlated.

A. Averaged traces of currents (SK and ΔGIRK) following iontophoresis of aspartate (black circle). Each trace is an average of 12 cells, the shaded area around the mean value represents s.e.m. ΔGIRK current is inverted to compare the timescale to SK.
B. Within-cell comparison of the width at 10% of the peak for the SK current and the corresponding ΔGIRK current for that cell. ΔGIRK was significantly longer at 10% of the peak than SK. ***$p < 0.001$, statistics were performed with a two-tail paired t-test.
C. Comparing within-cell the width of the SK versus the width (both at 10%) of the ΔGIRK reveals a significant positive correlation, analyzed with a Pearson correlation test, $p < 0.01$, $r = 0.56$, $n = 26$ cells for B and C.

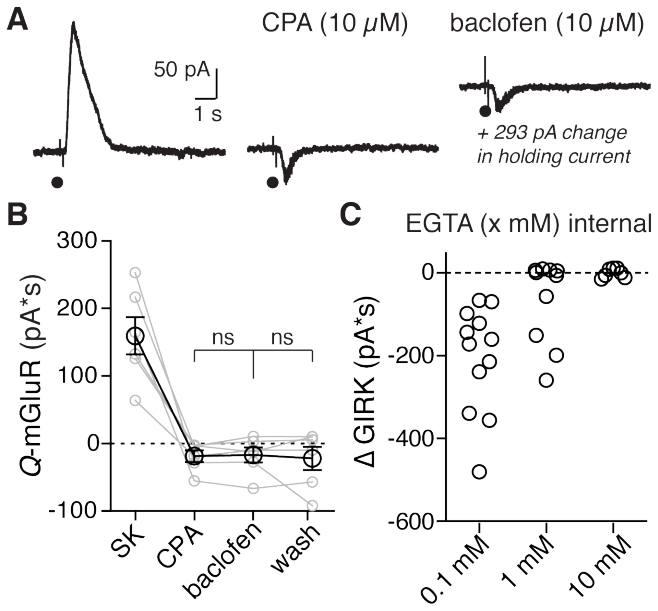

Figure 3.4 Inhibition of GIRK requires calcium release from stores.

A. Representative traces showing the currents elicited by aspartate iontophoresis at baseline (left), after CPA (10 μM, middle), and during baclofen (10 μM, right). In this example, baclofen elicited a standing outward current of 293 pA (not pictured to scale).
B. Grouped data showing the aspartate induced current at baseline, after CPA, during baclofen and after washout. Treatment with CPA blocked the aspartate induced a ΔGIRK inward current during baclofen. Each grey dot represents a single cell, lines connect treatments within a cell. Black circles are means ± s.e.m. Statistics were performed with a repeated measures two-way ANOVA followed by a Bonferroni test, ns = not significant ($p > 0.99$), n = 6 cells.
C. Comparison of the ΔGIRK charge during baclofen (10 μM) with different concentration of EGTA in the internal solution. In EGTA (0.1 mM) there is always a ΔGIRK current (12/12 cells). In 1 mM EGTA there is a ΔGIRK current in 4/10 cells. In 10 mM EGTA the ΔGIRK (0/7 cells) was completely blocked.

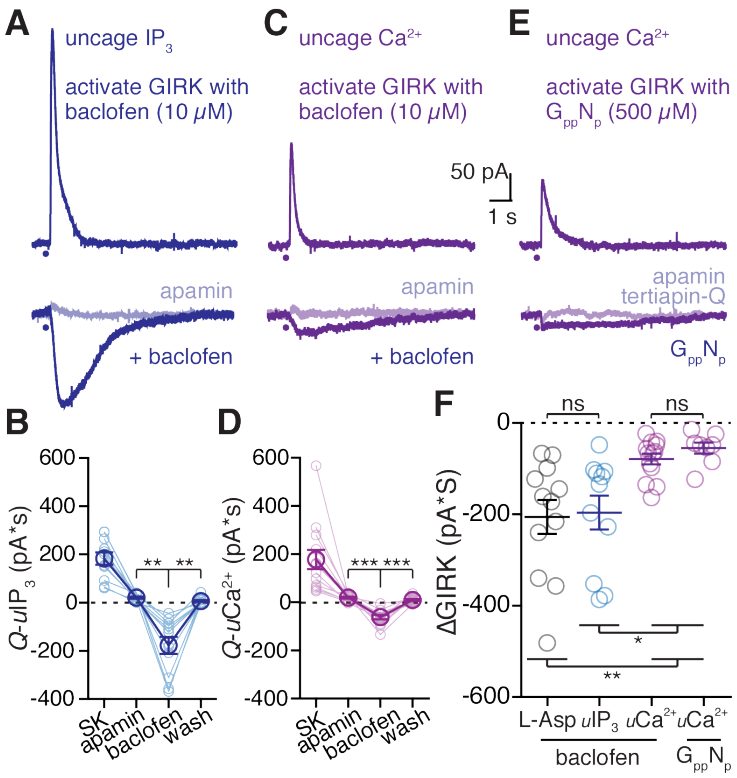

Figure 3.5 Receptor activation is not required for GIRK inhibition.

A. Representative traces from a whole cell voltage clamp recording using photolytic release (405 nM LED pulse) of caged IP_3 (100 μM) in control (top trace), after application of apamin (bottom light blue trace) and following superfusion of baclofen (10 μM, blue trace).
B. Quantified data across cells of all caged-IP_3 flash photolysis experiments. Light blue traces represent data from a single cells, dark blue represents mean data ± s.e.m. Statistics performed with a one-way repeated measures ANVOA followed by a Bonferroni, **$p < 0.01$, n = 11 cells.
C. Representative traces from a whole cell voltage clamp recording using photolytic release (365 nM LED pulse) of calcium with DMNPE-4 (1 mM). Top trace shows direct activation of SK, bottom trace (light purple) after apamin, and bottom trace (purple) following superfusion of baclofen (10 μM).
D. Quantified data across all caged-Ca^{2+} photolysis experiments. Light purple connected circles represent a data from a single cell, dark purple represents mean averaged data ± s.e.m. Statistics performed with a one-way repeated measures ANOVA followed by a Bonferroni test, ***$p < 0.001$, n = 13.
E. Representative traces from a whole cell voltage clamp recording using photolytic release of calcium with DMNPE-4. The internal solution also contained GppNHp (GppNp, 500 μM) that activated GIRK. Top trace is the SK current induced by photolysis of DMNPE-4. Bottom trace (light purple) is following treatment with apamin. Bottom trace is the decrease in GIRK induced by calcium at the peak of the outward current induced by GppNHp.
F. Comparing the ΔGIRK charge transfer (baseline subtracted) for GIRK currents activated with baclofen (10 μM) and calcium released via aspartate (black), photolysis of caged-IP_3 (blue) or photolysis of DMNPE-4 (purple, *left*), and for GIRK currents activated with GppNHp and calcium released by photolysis of DMNPE-4 (purple, *right*). Each circle represents a single cell, bars are the mean value ± s.e.m. ns = not significant. Statistics performed with a one-way ANOVA followed by a Tukey test. *$p<0.05$, **$p<0.01$, n = 12 (ionto), n = 11 (IP_3), n = 13 (DMNPE-4, baclofen), n = 8 (DMNPE-4, GppNHp) cells.

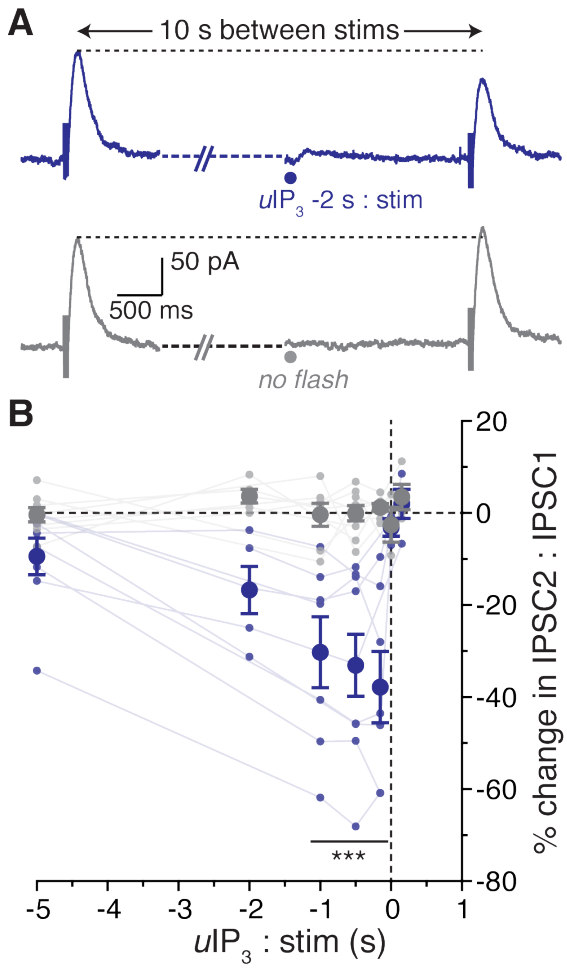

Figure 3.6 Calcium release from stores inhibits $GABA_B$ IPSCs.

A. Representative trace showing $GABA_BR$ IPSCs evoked with a monopolar stimulating electrode (100 Hz, 5 pulses) in pairs with a 10 second inter-stimulus interval. Photolysis of caged-IP_3 (blue dot, 405 nm, 30-100 ms) was applied at differing times between the pair of stimulations. Experiments were interleaved with traces where IP_3 was not applied (lower trace, grey).
B. Each small dot represents a data point from a single cell (average of three repetitions), connected by a line to show a within-cell data set. Points were averaged across cells (large dots). Pairs where IP_3 was released before the second stimulation are in blue, traces with no flash are in grey. Error bars represent s.e.m. Statistics were performed with a two-way repeated measures ANOVA followed by a Bonferroni test. ***$p < 0.001$, n = 3 – 9 cells per averaged data point.

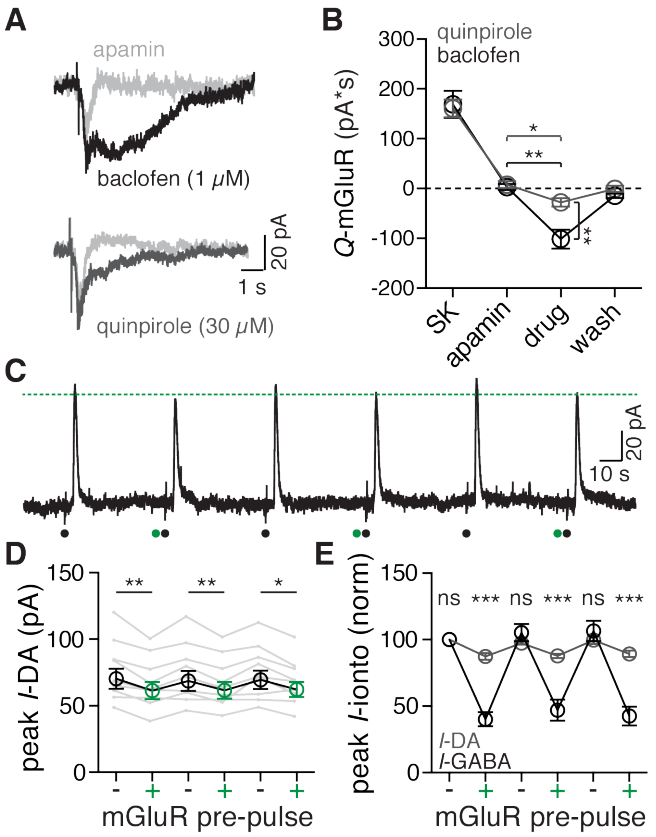

Figure 3.7 mGluR-induced calcium release inhibits D2R mediated GIRK currents less than $GABA_B$.

A. Representative traces of currents induced by iontophoresis of aspartate in the presence of apamin (300 nM, light gray), baclofen (1 μM, top trace, black), and quinpirole (30 μM, bottom trace, black).
B. Quantified data across cells comparing the aspartate induced mGluR currents at baseline (SK), after apamin (300 nM), in either quinpirole (30 μM, grey) or baclofen (1 μM, black), and upon washout or reversal of the agonist. Both quinpirole and baclofen resulted in a decrease in GIRK current relative to apamin. Statistics were performed with two one-way ANOVAs followed by a Bonferroni test. *$p < 0.05$, **$p < 0.01$, $n = 8$ (quinpirole), $n = 7$ (baclofen), points represent means ± s.e.m.
C. Representative trace from a dual iontophoresis protocol with dopamine (black dot) and aspartate (green dot) in the presence of apamin (300 nM). Dotted green line indicates the peak of the GIRK current induced by iontophoretic application of dopamine following application of aspartate. Aspartate iontophoresis caused a consistent decrease the D2R-mediated current.
D. Grouped data showing the peak amplitude of the dopamine D2 receptor-mediated GIRK current with (green) and without (black) iontophoretic application of aspartate one second before dopamine iontophoresis in the presence of apamin (300 nM). Statistics were performed with a one-way repeated measures ANOVA followed by a Bonferroni test, *$p < 0.05$, **$p < 0.01$, $n = 9$ cells. Grey traces indicate within-cell data for single neurons, circles (black and green) ± s.e.m.
E. Grouped data for all dopamine (grey) and GABA (black) dual iontophoresis experiments, normalized to the peak amplitude of the first pulse. Data points indicate means ± s.e.m. Statistics were performed with a two-way repeated measures ANOVA followed by a Bonferroni test, ***$p < 0.001$, ns = not significant ($p > 0.99$), $n = 9$ cells for both groups.

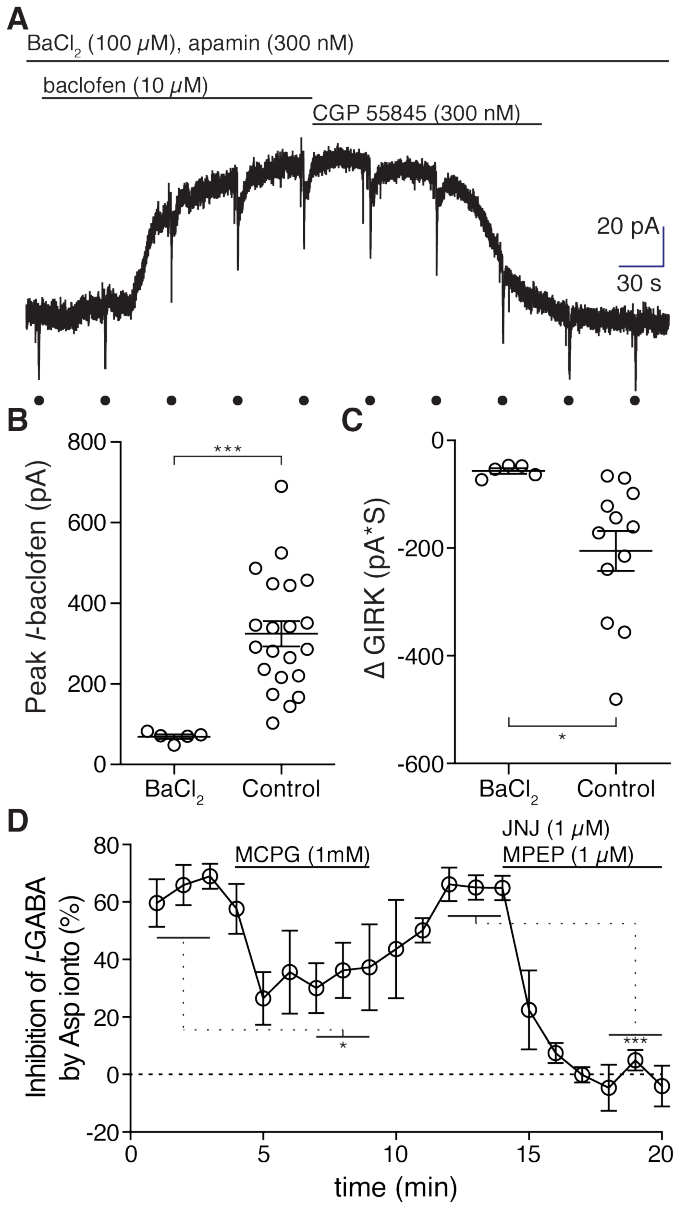

Figure 3.8 $BaCl_2$ decreased baclofen GIRK current and reduced the inward current induced by aspartate.

A. Representative trace from a whole-cell recording showing the reduced baclofen (10 μM) mediated GIRK current in the presence of $BaCl_2$ (100 μM) and apamin (300 nM), and the reduced size of the inward current mediated by aspartate iontophoresis during that current. The baclofen-mediated GIRK current was reversed by the specific $GABA_BR$ antagonist CGP-55845 (300 nM). Black circles represent the activation of mGluRs with aspartate iontophoresis.
B. Quantification across cells of the peak baclofen-mediated GIRK current. $BaCl_2$ significantly reduced the peak compared to controls.
C. Quantification across cells of the aspartate mediated ΔGIRK inward current during baclofen (10 μM) application. $BaCl_2$ significantly reduced the aspartate induced ΔGIRK. Statistics were performed with a 2-tailed unpaired t-test, n = 5 cells ($BaCl_2$) and 8 cells (control), *$p < 0.05$, ***$p < 0.001$, bars represent means and error bars s.e.m.

D. Percent inhibition of $GABA_BR$-mediated GIRK currents were calculated using the dual iontophoresis method. MCPG (1 mM) was applied after a baseline was achieved, and was the washed out. After a second baseline was achieved, JNJ and MPEP (1 μM each) were applied. Statistics were performed with a 2-way repeated measures ANOVA followed by a Bonferroni post-hoc test. n = 4 cells, *$p < 0.05$, ***$p < 0.001$, bars represent means and error bars s.e.m.

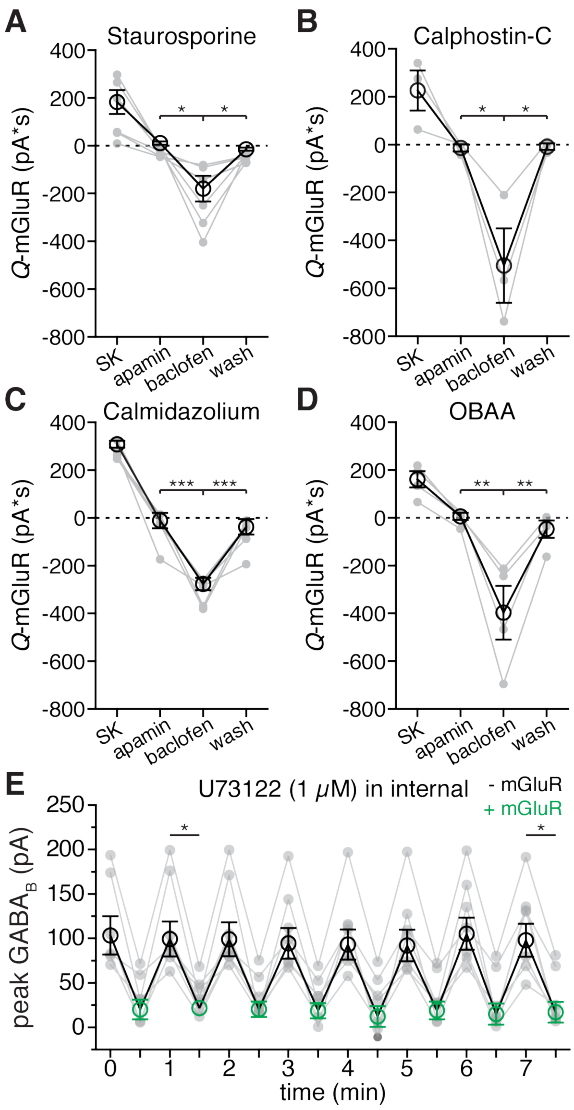

Figure 3.9 Pharmacological inhibition of calcium-activated lipases and other proteins has no effect on GIRK inhibition.

A. Slices were perfused with staurosporine (1 μM) for at least 10 minutes. In the presence of staurosporine, mGluR-mediated inhibition of GIRK was not impaired (apamin: 11.6 ± 7.04 pA*s; baclofen: -179 ± 54.1 pA*s; wash: -14.3 ± 6.69 pA*s; n = 6).
B. A second PKC inhibitor, calphostin-C (10 μM) was also examined. After incubating slices in the vial for an hour and keeping the slices in the drug during recordings, mGluR inhibition of GIRK was not impaired (apamin: 13.3 ± 14.8 pA*s; baclofen: -505 ± 155 pA*s; wash: -8.12 ± 13.5 pA*s; n = 3).
C. The PLA_2 inhibitor OBAA (Köhler et al. 1992) was tested on the mGluR-mediated inhibition of GIRK. Slices were treated with OBAA (3–10 μM, in the bath for 15 min), or incubated in OBAA (1 μM) for over an hour before transferring to the recording chamber. mGluR-mediated inhibition of GIRK was not impaired (apamin: 6.35 ± 15.0 pA*s; baclofen: -397 ± 112 pA*s; wash: -46.9 ± 36.8 pA*s; n = 4).
D. The effect of calmodulin was tested by using the inhibitor calmidazolium (10 μM). In the presence of calmidazolium, mGluR-mediated inhibition of GIRK was not impaired (apamin: -10.8 ± 32.6 pA*s; baclofen: -276 ± 25.9 pA*s; wash: -37.3 ± 32.4 pA*s; n = 5).

E. Neurons were loaded with the PLC inhibitor U73122 (1 μM) for at least 10 minutes before testing the inhibition of GIRK using the dual iontophoresis method. U73122 did not affect the mGluR-mediated inhibition of GIRK (At 1 minute: - mGluR: 114 ± 19.8 pA, + mGluR: 36.1 ± 7.23 pA; at 7 min: - mGluR: 112 ± 18.7 pA, + mGluR: 31.5 ± 11.5 pA; n = 7) *p<0.05, **p<0.01, ***p<0.001; all analyses performed with a repeated measures one-way ANOVA followed by a Bonferroni post-hoc test.

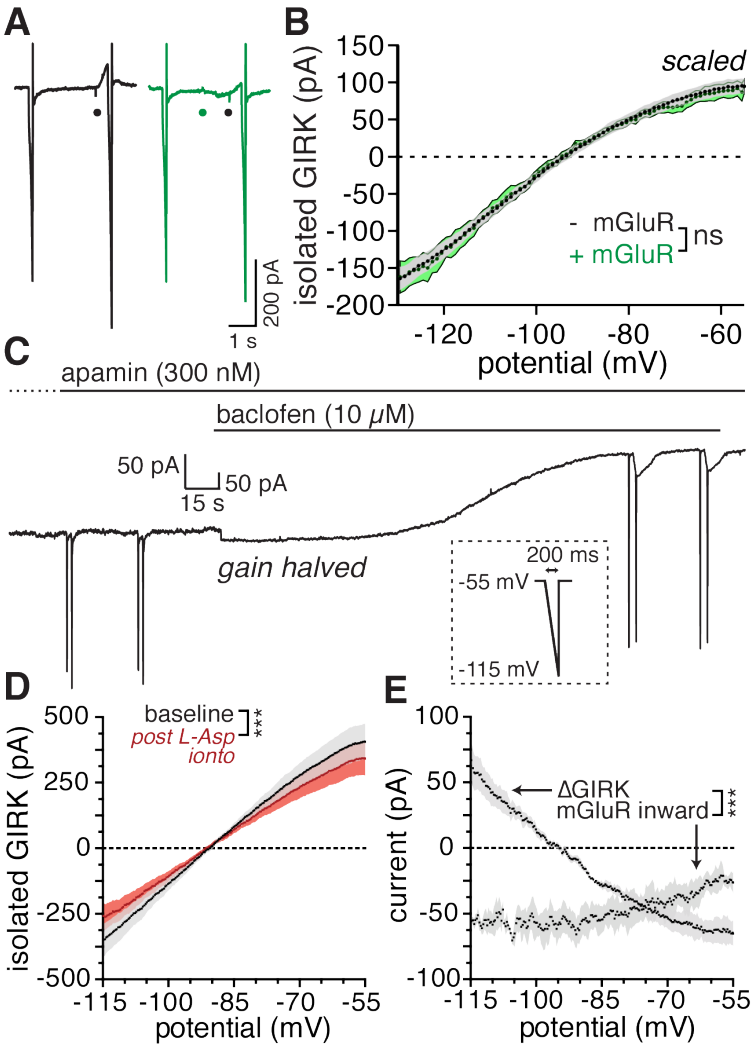

Figure 3.10 Block of steady state GIRK currents is similar to transient currents.

A. Representative traces showing the protocol for determining the current–voltage (*I*–V) relationship of the $GABA_BR$ current with (green) and without (black) an mGluR pre-pulse. See methods for a detailed protocol.
B. Mean isolated $GABA_BR$ GIRK *I*–V plots with mGluR pre-pulse curve (green) scaled to the curve lacking an mGluR pre-pulse (black). Scaling factor (no pre-pulse / pre-pulse amplitude) was determined for each cell at -55 mV and then applied across all voltages. After scaling, the two curves were no longer significantly different by a one-way repeated measures ANOVA, n = 6 cells, p = 0.94 (interaction between voltage and mGluR pre-pulse), ns = not significant.
C. Representative whole-cell voltage clamp trace showing generation of isolated *I*–V plots for the mGluR inward current in apamin, and the ΔGIRK current during baclofen application. *Inset* example voltage ramp used for determining *I*–V relationships. The amplifier gain (α) was halved from x10 to x5 upon application of baclofen to prevent saturation of the signal during voltage ramps. The scale bar reflects the two different vertical scales.
D. Isolated GIRK *I*–V curves before (black) and after (red) iontophoresis of aspartate, obtained by subtracting the ramp in baclofen from the corresponding ramp before baclofen application (see methods). The decrease in the *I*–V is significantly different from the control *I*–V, when using a two-way repeated measures (both factors) ANOVA n = 6 cells, ***p < 0.001 (interaction between voltage and current).

E. Isolated aspartate-induced decrease in GIRK and mGluR inward current *I*–V curves obtained by subtracting the baseline ramp from the ramp following aspartate iontophoresis, before and during baclofen treatment. The decrease in GIRK reverses near E_k, and the shape resembles what would be predicted for a decrease in GIRK conductance. The mGluR inward *I*–V ramps agrees with previous reports examining this current and resembles a non-selective cation conductance. These two *I*–V ramps were significantly different. Two-way repeated measures ANOVA (single factor), n = 3 (mGluR inward) n = 6 (ΔGIRK), ***$p < 0.001$ (main interaction between current and voltage) and $p < 0.01$ main effect of current.

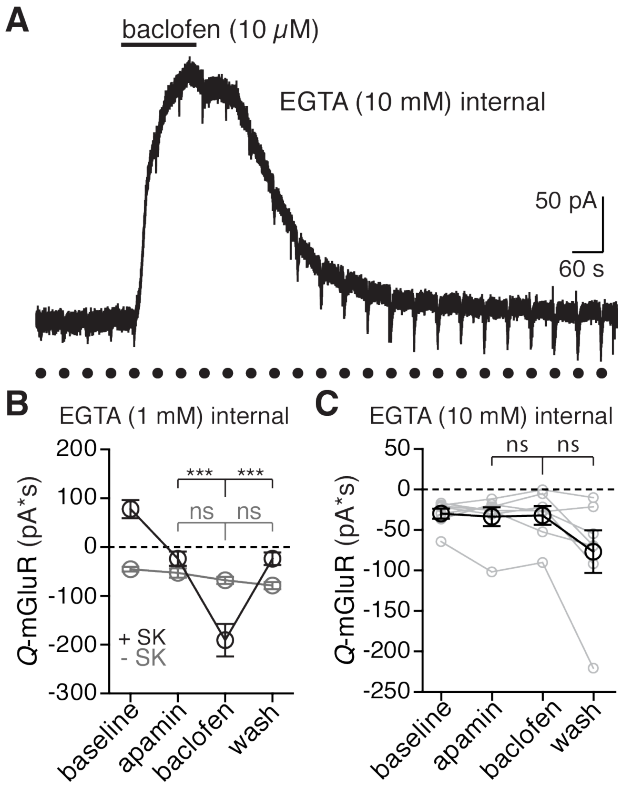

Figure 3.11 EGTA titration effects on calcium release from stores mediated currents.

A. Representative trace from a voltage clamp recording where the internal solution contained EGTA (10 mM). There was no baseline SK current, and application of baclofen (10 μM) did not change the current produced by aspartate iontophoresis. Black circles represent the activation of mGluRs with aspartate iontophoresis.
B. Data collected with EGTA (1 mM) in the internal solution, grouped according to the presence of absence of an SK current before apamin application. If there was an SK current (black) then mGluR activation inhibited the GIRK. If there was no SK current (grey) then mGluR activation did not inhibit the GIRK. Statistics were performed with a two-way repeated measures ANOVA followed by Bonferroni, ***$p < 0.001$, ns = not significant $p > 0.99$, n = 4 cells for + SK, 6 cells for - SK.
C. Grouped data (n = 8 cells) for experiments with EGTA (10 mM) in the internal solution. Statistics were performed with a repeated measures one-way ANOVA, ns = not significant $p = 0.98$ (apamin – baclofen), $p = 0.13$ (baclofen – wash).

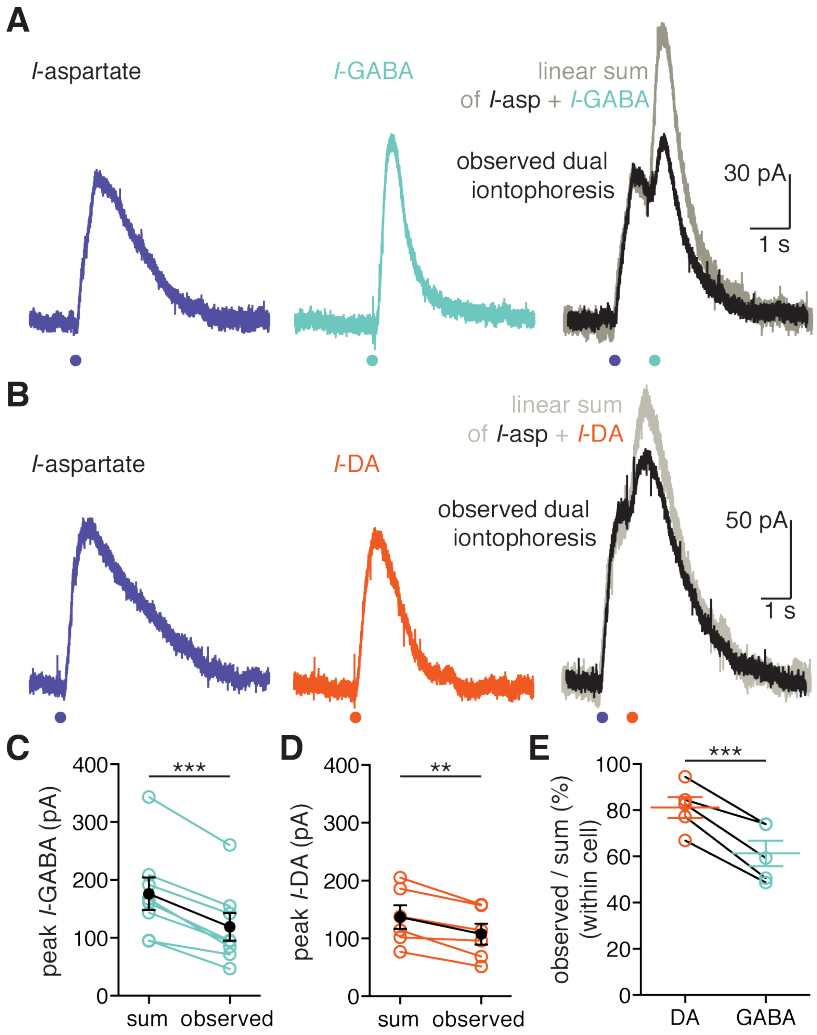

Figure 3.12 Blocking SK was not required for inhibition of GIRK by mGluR activation.

A. Representative traces from a whole-cell recording showing an example of the current mediated by iontophoresis of aspartate (purple, *left*), GABA (green, *middle*), and aspartate one second before GABA (black, *right*). Also shown is the summation of the currents produced by iontophoresis of aspartate and of GABA (grey, *right*).
B. Representative traces from a whole cell recording showing an example of the current mediated by iontophoresis of aspartate (purple, *left*), dopamine (orange, *middle*), and aspartate one second before dopamine (black, *right*). Also shown is the linear summation of the currents produced by iontophoresis of aspartate and of dopamine (grey, *right*).
C. Grouped data showing the difference between the peak of the $GABA_BR$ GIRK current expected by linear summation versus observed experimentally. Green circles and connecting lines represent data from single cells, black points represent means and error bars s.e.m. Statistics were performed with a paired two-tailed t-test, ***$p < 0.001$, $n = 8$ cells.
D. Grouped data showing the difference between the peak of the dopamine GIRK current expected by linear summation versus observed experimentally. Orange circles and connecting lines represent data from single cells, black points represent means and error bars s.e.m. Statistics were performed with a paired two-tailed t-test, **$p < 0.01$, $n = 6$ cells.

E. Grouped data showing the experimentally observed peak GIRK current / summated peak based on linear summation for dopamine (DA, orange) and GABA (green). Orange and green circles and connecting lines represent data from single cells, black points represent means and error bars s.e.m. Data for each pair were collected from single cells. Statistics were performed with a paired two-tailed t-test, $^{**}p < 0.01$, $n = 5$ cells.

3.1 Additional Experiments

Some experiments were not published with the above manuscript, but contribute to the principal interpretation of the results, that calcium inhibits GIRK currents. These unpublished experiments are presented below.

Main effect without apamin

As shown in Figure 3.12, blocking SK channels with apamin is not required to observe calcium-dependent block of GIRK by the dual iontophoresis method. Next, an experiment was performed to test the calcium-mediated inhibition of a standing GIRK current during bath perfusion of baclofen without blocking SK channels.

Results

$GABA_B$ and $GABA_A$ Receptor Activation Decrease mGluR SK Currents

L-aspartate was applied (once every 45 seconds) until the resulting SK current reached a steady baseline. Application of the $GABA_B$ agonist baclofen (10 μM) induced a GIRK mediated outward current (Figure 3.13A, 324 ± 31 pA). The charge transfer of the L-aspartate iontophoretic response was measured to account for the multiple components of the mGluR mediated current (inward and outward). The baseline mGluR current was reduced in the presence of baclofen (from 208 ± 38.5 pA*S to 46.4 ± 30.1 pA*S) and recovered following washout (214 ± 32.6 pA*S) (Figure 3.13B and C). This observation was surprising given

that different potassium conductances are evoked by the two receptors. Muscimol also decreased the mGluR-evoked current (from 254 ± 70.2 pA*S to 138 ± 49.2 pA*S) similar to the extent found with $GABA_B$ receptor activation (Figure 3.13C, D). Thus a conductance increase reduced the SK current induced by mGluR activation.

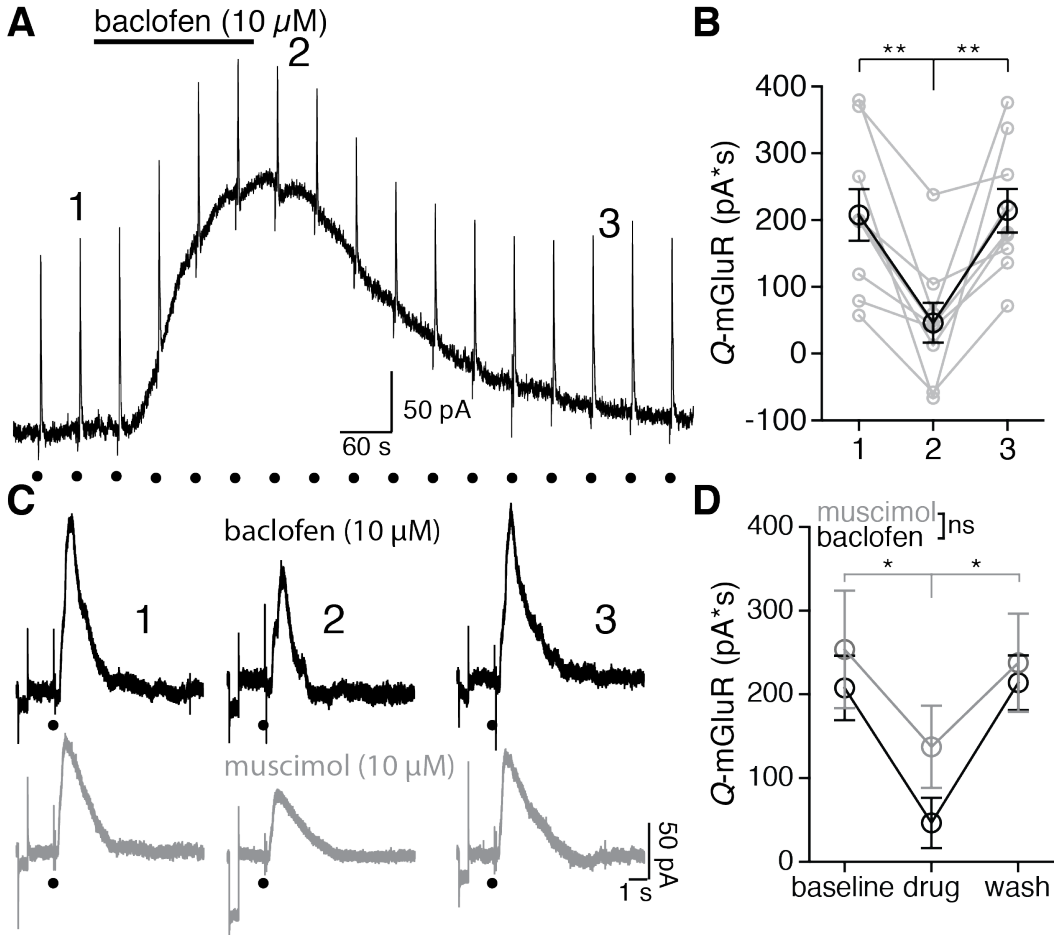

Figure 3.13 $GABA_B$ and $GABA_A$ receptor activation decrease mGluR-mediated SK currents.

A. Representative trace of a voltage clamp whole cell recording showing the change in holding current caused by application of baclofen (10 μM). Black circles represent the activation of mGluRs with L-aspartate iontophoresis. The numbers (1, 2, and 3) correspond to the individual acquisitions that were quantified for analysis in B.

B. Quantification across cells of the total charge transfer for the mGluR-activated current at baseline (1), during baclofen (2) and after washout (3). Baclofen significantly decreased the size of the SK current relative to both baseline and washout (one-way repeated measures ANOVA followed by a Tukey post-hoc analysis, n = 9 cells). Black open circles represent mean with error bars s.e.m., each set of grey dots connected by a line represents data from a single cell. **$p < 0.01$
C. Representative episodic traces showing iontophoresis of L-aspartate (indicated by the black circle), resulting in a transient outward current. On the left (1) is an example of a baseline current, in the middle (2) is a current in either baclofen (black, top) or muscimol (grey, bottom), and on the right (3) is the current after drug washout.
D. Group data quantifying the L-asp ionto evoked current charge transfer at baseline, during either baclofen (10 μM) or muscimol (10 μM) treatment, and after washout of the drug. Baclofen data are the same as in B. Muscimol caused a significant reduction in the SK charge transfer when compared to baseline and wash (two-way repeated measures ANVOA followed by a Bonferroni test, n = 5 cells) *$p < 0.05$. The difference between baclofen and muscimol was not significant at any point (two-way repeated measures ANOVA followed by a Bonferroni test comparing groups, $p > 0.99$ (baseline), $p = 0.48$ (drug), $p > 0.99$ (washout) ns = not significant.

DISCUSSION

Unlike with the dual iontophoresis method, there is a large increase in cellular conductance during bath perfusion of baclofen that decreased the SK current amplitude. Additionally, the effects of $GABA_B$ and $GABA_A$ receptor agonists appeared similar. However, there was the inward current seen after the SK current only during baclofen application, not muscimol. This inward current indicated an inhibition of the GIRK current. Yet it is clear that the presence of the SK current made an accurate measurement the inward current mediated by inhibition of GIRK during the standing current impossible, as the two current occluded each other.

Therefore, without apamin to block SK channels, it is difficult to isolate the effect of mGluR activation of the GIRK current. Instead this experiment reveals that tonic GIRK activation following agonism of the $GABA_B$ receptor will decrease the mGluR-mediated current measured in voltage-clamp. This effect is through a

combination of the inward current caused by calcium-mediated GIRK inhibition as well as the large increase in neuronal conductance.

Quantifying changes in cellular conductance

Neuronal conductance not only affects the measurement of currents in voltage-clamp, but is also an indicator of what is occurring during a current. A decrease in conductance indicates the closure of a channel, while an increase indicates the opposite. This basic principle was used to test two initial hypotheses for the identity of the large, slow inward current during baclofen that is mediated by mGluR activation. Either this slow inward current was an exaggeration of the non-selective cation conductance typically activated by Group I mGlu receptors, or it was closure of the GIRK channel. By measuring the change in neuronal conductance during this slow inward current, these two hypotheses can be tested, and one rejected.

The procedure was to apply repeated 10 mV square pulses and measure the amplitude of the resulting current to calculate cellular capacitance (using I = GV). This was performed before and following activation of mGlu receptors while at baseline, during GIRK activation.

Results

Voltage steps (10 mV every 300 ms) were run before and after the activation of mGluRs to test for changes in cellular conductance. Iontophoretic application of aspartate in the presence of apamin (300 nM) produced an inward current and an increase in the conductance (Figure 3.14E). This inward current did not reverse in the range of voltages tested and resembled the activation of a previously reported non-selective cation conductance. Iontophoretic application of aspartate

in the presence of baclofen, resulted in the inward current and caused a decrease in cellular conductance (Figure 3.14D and E).

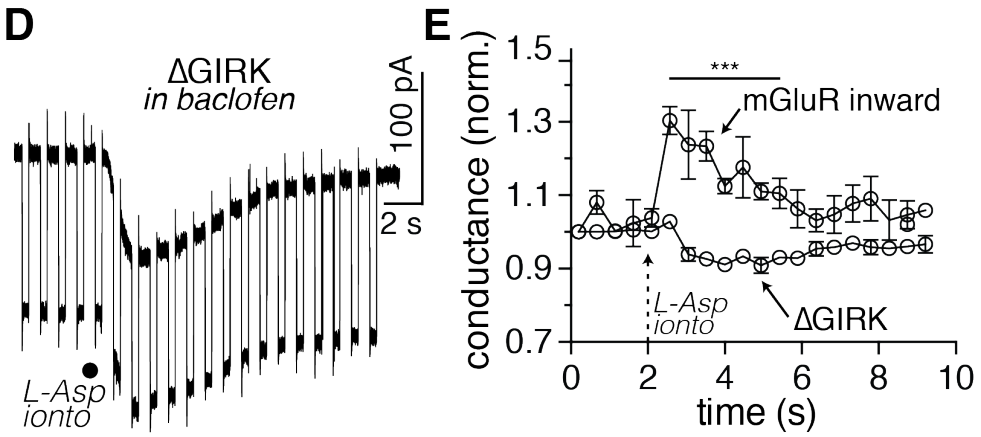

Figure 3.14 Inhibition of GIRK associated with a decrease in cellular conductance, mGluR-mediated cation current associated with an increase in conductance.

D. Example trace of a whole cell recording trace in baclofen (10 μM). Repeated voltages steps (10 mV, 200 ms) were conducted every 300 ms to measure the whole cell conductance. Iontophoresis of L-aspartate resulted in the ΔGIRK current, which corresponded with a decrease in cellular conductance.
E. Grouped data comparing changes in conductance relative to the value at 0 s before baclofen (mGluR inward) and during baclofen (ΔGIRK). At 2 s L-aspartate was applied using ionto. The conductance of the neuron went down in baclofen (ΔGIRK) and up before baclofen (mGluR inward). ***$p < 0.001$, $n = 3$ cells, statistics were performed with a repeated measures (both factors) two-way ANOVA followed by Bonferroni test. Each point represents the mean value, error bars are s.e.m.

DISCUSSION

These data show that the slow, inward ΔGIRK current is associated with a decrease in cellular conductance, which corresponds to a channel closing. While the inward non-selective cation current mediated by mGluR activation at baseline represents and increase in cellular conductance, and thus the opening of channels. These two opposing changes in cellular conductance indicate that the ΔGIRK current seen during baclofen perfusion, and the non-selective cation

current seen at baseline, are two separate inward currents mediated by mGluR activation. The ΔGIRK current is therefore not an exaggeration of the inward non-selective cation current.

Correlation of steady-state GIRK inhibition with amplitude of the GIRK current

In order to address the mechanism of how calcium release from stores inhibits GIRK currents, the properties of the GIRK inhibition were analyzed in many different respects to better understand the nature of the inhibition. Comparing the inhibition between cells for careful analysis required a normalization procedure, since both the size of the mGluR transient and the size of the GIRK current would affect the ΔGIRK current. In order to accomplish this normalization, the data generated from activation of mGlu receptors following iontophoresis of L-aspartate and measuring the peak of the inward ΔGIRK currents during baclofen (10 μM) perfusion were analyzed (Figure 3.15A). This form of analysis quantified the percent inhibition of the standing GIRK current.

Results

It was found that inhibition of GIRK was more sensitive for smaller amplitude GIRK currents. These data fit single exponential decay function (see below) with a goodness of fit of $R^2 = 0.52$ (Figure 3.15B).

$$Y = 55.1^{(-.01*X)} + 15.8$$

When separated at a 200 pA cutoff into “small” and “large” GIRK currents, the small group had significantly greater mGluR-mediated inhibition than the larger group (Figure 3.15C; small: 18.6 ± 2.2% n = 18; large: 36 ± 5.6% n = 12; $p < 0.01$, one-way ANOVA followed by a Tukey Test). Furthermore, inhibition of GIRK with Barium Chloride (100 μM) did not produce a significantly different

percent inhibition than without $BaCl_2$ (Figure 3.15C; $BaCl_2$: 23.1 ± 1.5% n = 5, p > 0.05, one-way ANOVA followed by a Tukey Test).

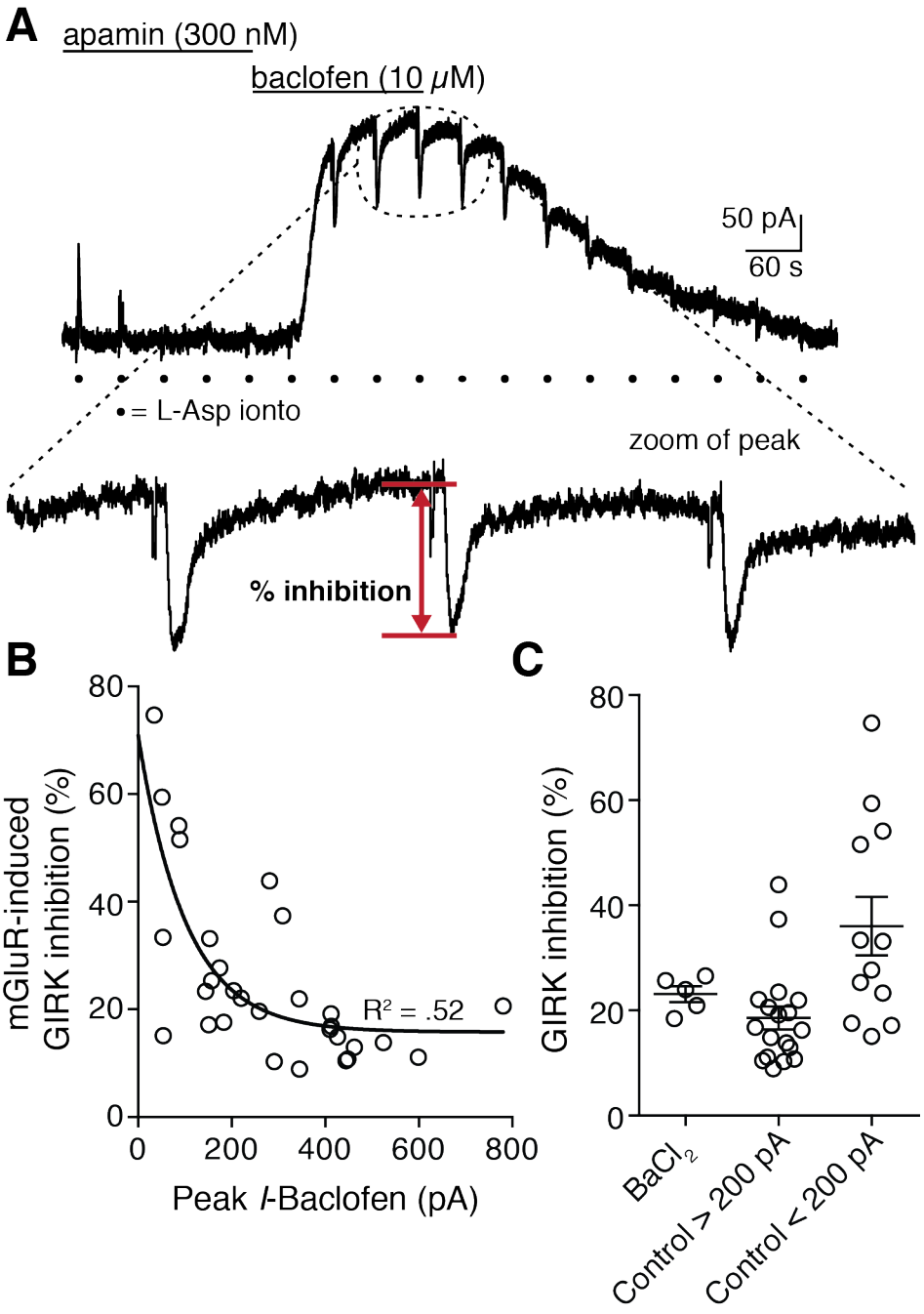

Figure 3.15 Smaller steady-state GIRK currents are more sensitive to calcium inhibition

A. Example trace depicting method of calculating GIRK inhibition percent for standing GIRK currents mediated by baclofen perfusion.

B. Relationship between the peak baclofen current and the amount of GIRK inhibition (% of peak). There is a negative relationship, with larger GIRK currents having less inhibition. This relationship is fitted best with a single exponential decay function.
C. Comparison of GIRK inhibition (% of peak) between $BaCl_2$, currents less than 200 pA, and currents greater than 200 pA. Currents greater than 200 pA had significantly less inhibition than those smaller than pA, but neither were different from in $BaCl_2$.

DISCUSSION

Since $BaCl_2$ does not affect the amount of inhibition, this indicates that calcium is most likely not acting at a charged divalent site, since one might expect $BaCl_2$ to compete with calcium at that site and reduce the efficacy of calcium-mediated GIRK inhibition, however the percent inhibition of GIRK was identical with and with $BaCl_2$. Interpretation of the single exponential decay relationship between GIRK amplitude and percent inhibition by mGluR activation is speculative without known the mechanism for GIRK inhibition. One potential hypothesis is that it could indicate that $GABA_B$ receptors compete with calcium to activate GIRK and that with more robust G protein turnover the calcium is out-competed. This could indicate that calcium is acting at the G protein binding site to decrease the affinity of G proteins for the channel, a hypothesis that has not yet been tested.

GIRK inhibition in mouse VTA and SNc

This study was performed by recording from dopamine neurons of the substantia nigra prepared from Sprague-Dawley adult rats. This left two obvious questions that needed to be tested. First: was this effect somehow specific to rats? Second: was this effect specific to SNc dopamine neurons? To test these questions, recordings were made from SNc and VTA dopamine neurons prepared from wild-type C57 bl6/j mice (adult males and females).

GIRK inhibition was quantified using the dual-iontophoresis protocol. At the end of each experiment, CPA (10 μM) was added to the perfusion solution to verify the observed inhibition was dependent on calcium release from intracellular stores. Additionally, the charge transfer mediated by SK channels following an escape spike was measured to look for species differences in relevant intrinsic properties of dopamine neurons.

Results

Activation of Group I mGluRs in mouse dopamine neurons inhibited $GABA_B$-mediated GIRK currents in both the SNc (59.5 ± 8.6%, n = 6) and the VTA (43.4 ± 5.8%, n = 6). This mGluR-mediated GIRK inhibition was abolished by inclusion of CPA in the perfusion solution in the SNc (after CPA: -2.1 ± 3.3%, $p < 0.001$ compared to pre-CPA) and in the VTA (after CPA: 3.6 ± 3.3%, $p < 0.01$ compared to pre-CPA, all statistics performed with a repeated-measures two-way ANOVA followed by Bonferroni test). There was no significant difference between the amount of baseline GIRK inhibition in the SNc or the VTA. The size of the SK

current generated by an escape spike in voltage clamp was not different between rats and mice (rats: 9.3 ± 1.2 pA*s, n = 18; mice: 10.6 ± 1.4 pA*s, n = 14; p > 0.05, unpaired t-test.

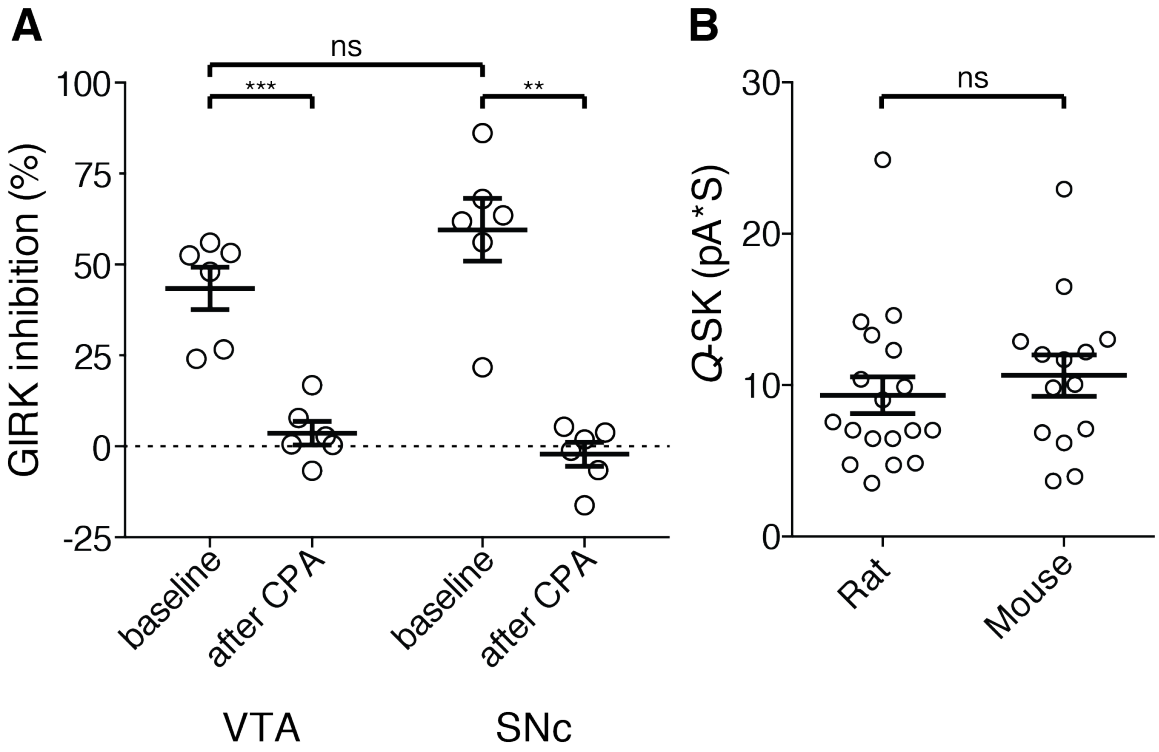

Figure 3.16 Comparison of currents in mouse dopamine neurons of the SNc and VTA

A. Percent inhibition of $GABA_B$ GIRK current from mGluR activation one second prior to $GABA_B$ receptor activation. Recordings were made from SNc (lateral to the MT) and frank VTA (very medial of the MT). In both VTA and SNc, mGluR activation inhibited GIRK, and this effect was reversed by depleting intracellular stores with CPA (10 μM).
B. The area under the curve was calculated for an SK current following an escape spike in voltage clamp evoked by a 60 mV depolarizing pulse for 3 ms. The charge was computed for 200 ms following the end of the step. There is no difference in *Q*-SK between rats and mice in SNc dopamine neurons.

DISCUSSION

These results convincingly show that mGluR activation inhibits GIRK in mouse dopamine neurons, like in rat dopamine neurons. This inhibition depends on calcium release from stores, and is not different between SNc and VTA neurons.

Moreover, rats and mice have similar amounts of SK channels that are activated by calcium entry during an action potential. This measure indicates that any differences in mGluR-evoked SK currents between rats and mice may depend on some other factor than SK channel expression.

BATH PERFUSION OF DHPG EFFECT ON PEAK $GABA_B$-MEDIATED CURRENT

One of the novel features of this study was examining how transient mGluR activation affects GIRK currents. This left open the question of what bath perfusion of DHPG, a Group I mGluR agonist, does to transient $GABA_B$ receptor activation. As has been reported before (Sohn, Lee, Cho, Lim, Shin, Lee, and Ho 2007b) bath perfusion of DHPG inhibits GIRK currents by depleting PIP_2 from the intracellular leaflet of the plasma membrane. These experiments were recapitulated in dopamine neurons.

RESULTS

Addition of DHPG (10 μM) to the perfusion solution reduced the peak $GABA_B$ mediated GIRK current by 49 ± 1.7%. This effect reversed with the washout of DHPG from the bath (Figure 3.17A). The GIRK current was isolated using the dual voltage ramp protocol, and subtracting the baseline ramp from the ramp at the peak of the GIRK current. Using this protocol, the current-voltage relationship of the GIRK current was measured. DHPG did not affect the GIRK *I*-V relationship and did not shift the reversal potential, indicating that mGluR activation decreased the GIRK conductance selectively (Figure 3.17B). Finally, in a pilot experiment, CPA was added to the perfusion solution before DHPG. If the DHPG-dependent decrease in the peak $GABA_B$ GIRK current was dependent on intracellular release of calcium from stores, this treatment should abolish the reduction in the peak GIRK current. However, while there are too few data points

to construct a data set, early experiments indicate that bath perfusion of DHPG inhibits GIRK in a calcium-independent fashion.

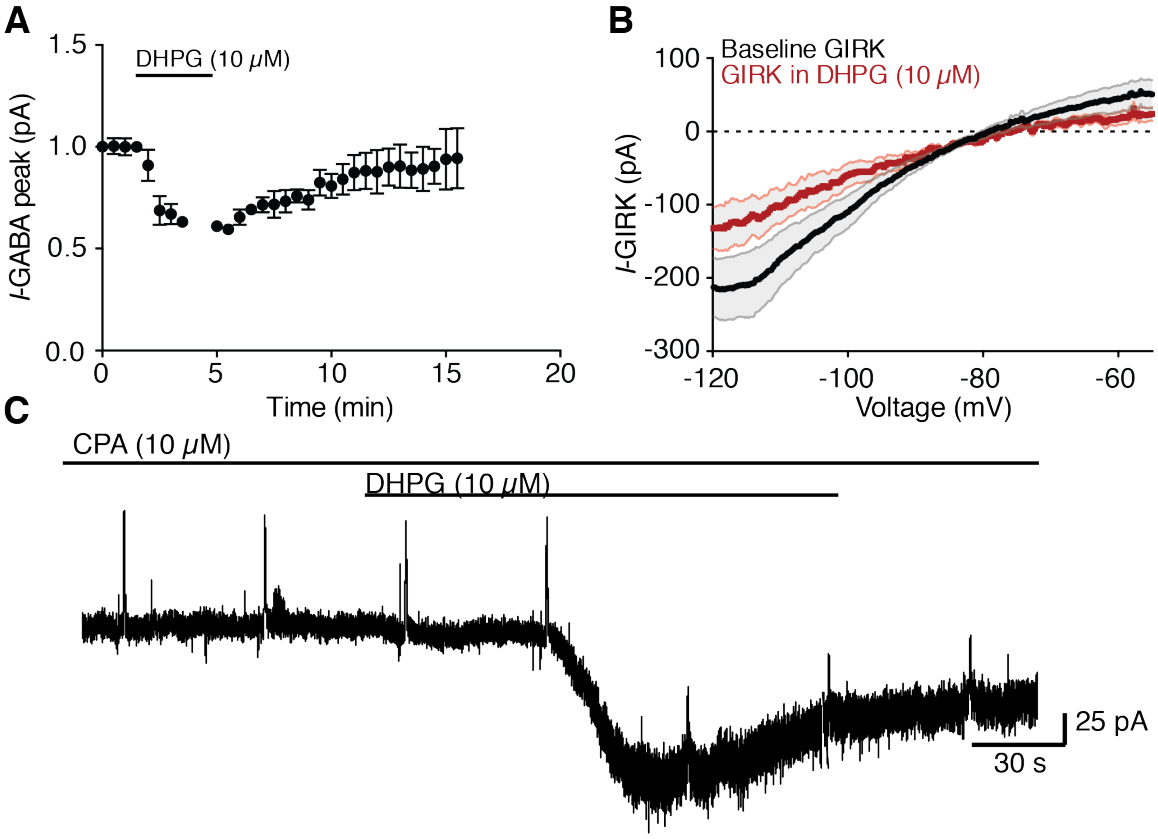

Figure 3.17 Tonic mGluR activation inhibits GABAB GIRK currents, but it may not depend on intracellular calcium

A. The effect of DHPG (10 μM) bath perfusion on the peak current generated by iontophoresis of GABA. DHPG inhibited the peak GIRK current, an effect that reversed following washout of DHPG.
B. *I*-V plots for the $GABA_B$ GIRK current in baseline conditions and during DHPG perfusion. DHPG decreased the conductance of the GIRK across the full range of voltages and did not shift the reversal potential.
C. Example trace from a recording where CPA (10 μM) was applied before DHPG. In this example, CPA did not prevent the DHPG-induced reduction in the peak GIRK current.

Discussion

These data add to the hypothesis that bath perfusion of DHPG and tonic activation of Group I mGlu receptors is functionally distinct from acute receptor activation. While both methods of mGluR activation inhibit GIRK currents, they do

so with different mechanisms. This could explain why the calcium-dependent inhibition of GIRK presented in this dissertation differs so much from previously published work examining G_q-dependent GIRK inhibition.

ISOLATED GIRK I-V PLOTS, CALCIUM UNCAGING EXPERIMENTS

Analyzing current-voltage relationships is a telling experiment for understanding the identity of a current, and for understanding how it is modulated. As shown in Figure 3.5, photolytic release of calcium alone is enough to inhibit GIRK currents, however the amount of inhibition by photolytic release of calcium was significantly less than for IP_3 or for mGlu receptor activation. This difference in the magnitude of GIRK inhibition led to the question of whether photolytic release of calcium was different from IP_3 or from receptor activation. To test this, *I*-V plots were constructed for the inhibition of GIRK by photolytic release of calcium.

RESULTS

I-V plots for isolated currents following photolysis of caged-Ca^{2+} in dopamine neurons in apamin (Figure 3.18, left panel, in red) and during the addition of baclofen to the perfusion solution (left panel, in black) are shown below. A control experiment was performed with no flash of UV light, which resulted in a flat curve near 0 pA (left panel, grey). The *I*-V plot in apamin most likely represents a calcium-mediated chloride conductance. Once this conductance was subtracted from the *I*-V plot in baclofen, an isolated effect of photolysis of caged calcium on the standing baclofen current was generated (right panel). This plot resembles the ΔGIRK *I*-V plot in Figure 3.10E, which was shown to be an inhibition of a steady GIRK current.

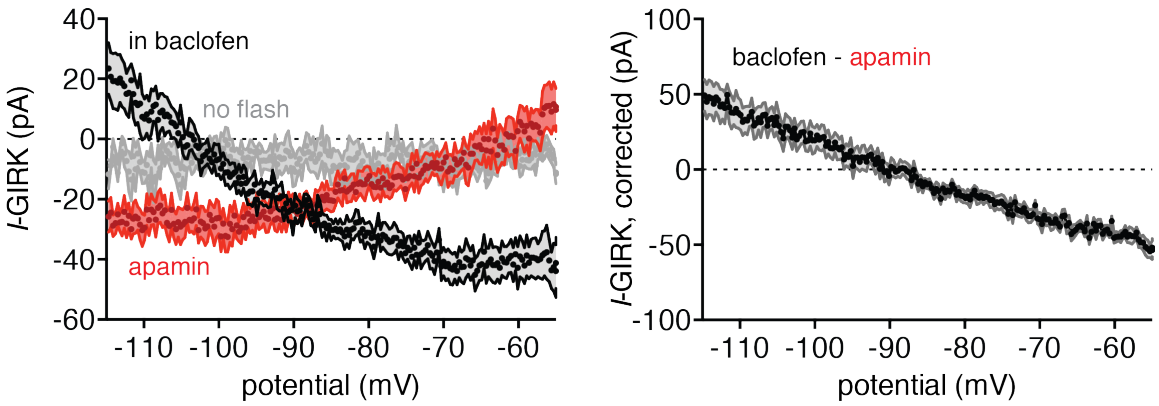

Figure 3.18 *I*-V plot for GIRK inhibition by uncaging of calcium

Left panel. Isolated *I*-V plots for currents generated by photolysis of caged-Ca^{2+} in apamin (300 nM) and in the presence of baclofen (10 μM). Also an isolated *I*-V plot using the same method as for the other currents without a UV flash, to show that the first ramp does not affect the second. **Right panel.** A calculated *I*-V plot, generated by subtracting the plot in apamin from the one in baclofen. This plot represents an isolated effect of photolysis of caged-Ca^{2+} on the GIRK current.

DISCUSSION

These experiments show that the nature of the inhibition of GIRK by photolytic release of caged-Ca^{2+} is similar to inhibition of GIRK by mGluR activation and release of caged-IP_3. This is despite the fact that the amplitude of inhibition is smaller. These results bolster the hypothesis that photolysis of caged-calcium also is sufficient to inhibit GIRK.

Comparison of Calcium and IP_3 uncaging kinetics

The photolytic release of caged-Ca^{2+} and caged-IP_3 are not identical biological processes, which could further explain why they vary so much in the efficacy of GIRK inhibition. This difference not only exists during calcium-mediated GIRK inhibition, but also at baseline, and is best exemplified by analyzing their kinetics of activating SK. Photolysis of caged-IP_3 resulted in an SK current with an onset that was significantly slower than for caged-Ca^{2+} (Figure 3.19; IP_3: 42.7 ± 3.3 ms, n = 17; Ca^{2+}: 16 ± 0.89 ms, n = 8; $p < 0.001$, unpaired t-test).

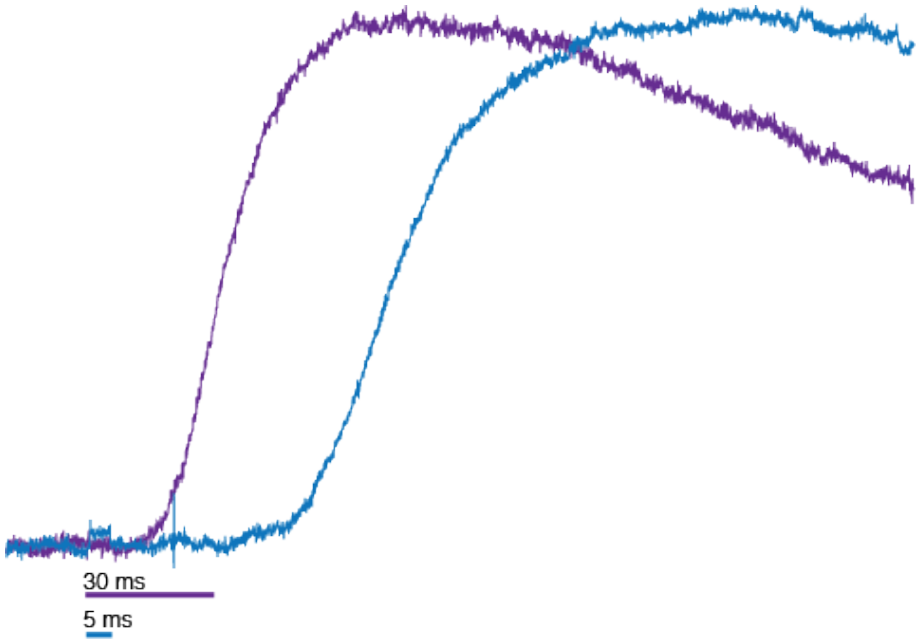

Figure 3.19 Example of different onset kinetics between SK currents mediated by calcium or IP_3 uncaging

Example of two SK currents mediated by photolysis of caged-IP_3 (blue) or caged-Ca^{2+} (purple).

Discussion

These data show that the photolysis of caged-Ca^{2+} leads to an increase in cytosolic calcium that is more rapid than the release of caged-IP_3, and is therefore not an identical biological process. This different in SK current onset could represent a possible quantification of the intermediate biological steps between liberation of IP_3 and activation of SK (IP_3 binding to the receptor, receptor gating, calcium diffusion to SK) that are not present when liberating calcium. Therefore the larger magnitude of GIRK inhibition by release of calcium through the IP_3 receptor as compared to global increase in cytosolic calcium, indicates that the more physiological release of calcium through the IP_3 receptor is better suited to inhibit GIRK. This is possibly because the concentration of calcium at the point of release from the receptor is higher than with photolytic release of caged-Ca^{2+}. Or it could be because the IP_3 receptor is positioned in a subcellular compartment to inhibit GIRK currents, and this compartment is only partially accessed by passive diffusion of the caged-Ca^{2+} into the neuron.

Chapter 4 Cocaine decreases metabotropic glutamate receptor mGluR1 currents in dopamine neurons by activating mGluR5

Paul F. Kramer, BA[1] and John T. Williams, PhD[1,*]

[1]Vollum Institute, Oregon Health and Science University

[*]Correspondence to: John Williams, Oregon Health and Science University, Vollum Institute L474, 3181 SW Sam Jackson Park Rd., Portland, OR 97239 USA, Phone: 503-494-5465, fax: 503-494-4590, williamj@ohsu.edu

Support This work was supported by NIH grant DA04523 (JTW) and the OHSU Brain Institute Neurobiology of Disease Lacroute Fellowship.

Acknowledgements We thank members of the Williams lab for their comments on the work and manuscript.

Kramer, P.F. and Williams, J.T. (2015). “Cocaine decreases metabotropic glutamate receptor mGluR1 currents in dopamine neurons by activating mGluR5.” *Neuropsychopharmacology* 40 (10): 2418–2424.

Summary

Midbrain dopamine neurons are important mediators of reward and movement and are sensitive to cocaine-induced plasticity. After even a single injection of cocaine there is in an increase in AMPA dependent synaptic transmission. The present study examines cocaine-induced plasticity of mGluR dependent currents in dopamine neurons in the substantia nigra. Activation of mGluR1 and mGluR5 resulted in a mixture of inward and outward currents mediated by a non-selective cation conductance and a calcium-activated potassium conductance (SK), respectively. A single injection of cocaine decreased the current activated by mGluR1 in dopamine neurons and had no effect on the size of the mGluR5-mediated current. When the injection of cocaine was preceded by treatment of the animals with a blocker of mGluR5 receptors (MPEP), cocaine no longer decreased the mGluR1 current. Thus, the activation of mGluR5 was required for the cocaine-mediated suppression of mGluR1-mediated currents in dopamine neurons. The results support the hypothesis that mGluR5 coordinates a reduction in mGluR1 functional activity after cocaine treatment.

Introduction

Group I metabotropic glutamate receptors (mGluR1 and mGluR5) are Gq-coupled receptors that modulate cocaine-induced plasticity (Yu et al. 2013; Bird et al. 2014). While mGluR1 and mGluR5 signal through the same class of G proteins (Hermans and Challiss 2001), selective activation of these receptors results in differing synaptic and behavioral outcomes induced by treatment of animals with cocaine. Increasing mGluR1 activity 24-hours after a single injection of cocaine reversed the well-described potentiation of AMPA receptor EPSCs in the ventral tegmental area (VTA, Ungless et al. (2001); Bellone and Luscher (2006)). The underlying mechanism involved an mGluR1-dependent long-term depression that removed calcium-permeable AMPA receptors (Bellone and Luscher 2006; Bellone and Luscher 2005). This observation raised the possibility that a decrease in basal mGluR1 signaling was necessary for cocaine-induced plasticity.

The role of mGluR5 in drug-induced plasticity is less well understood. Inhibition of mGluR5 by a variety of selective negative allosteric modulators or genetic knockout decreased cocaine self-administration (Kenny *et al*, 2005; Chiamulera, 2001), cue-induced reinstatement (Kumaresan et al. 2009), cocaine taking and seeking (Keck et al. 2013; Keck et al. 2014), and extinction in rats and monkeys (Bird et al. 2014; Keck et al. 2014; Keck et al. 2013; Kumaresan et al. 2009; Platt, Rowlett, and Spealman 2008). Thus blocking mGluR5 activity decreased behaviors associated with cocaine treatment and self-administration,

whereas blockade of mGluR1 facilitated cocaine dependent processes on AMPA receptor dependent EPSCs in the nucleus accumbens (Loweth et al. 2013). It remains unknown how cocaine treatment directly affects mGluRs on dopamine neurons.

The co-expression of mGluR1 and mGluR5 is found in a variety of areas, including pyramidal neurons, type II globus pallidus neurons and dopamine neurons of the olfactory bulb (Mannaioni et al. 2001; Poisik et al. 2003; Jian et al. 2010). Dopamine neurons of the ventral midbrain also co-express mGluR1 and mGluR5 as measured by immuno-gold EM and in situ hybridization studies (Hubert, Paquet, and Smith 2001; Testa et al. 1994). Functionally, it is know that mGluR1 evokes calcium release from intracellular stores, which activate SK channels in midbrain dopamine neurons resulting in a pause of firing (Chris D Fiorillo and Williams 1998; Morikawa, Khodakhah, and Williams 2003). The role of mGluR5 in dopamine neurons is not known.

This study examines the mechanisms that link the activation of mGluR1 and mGluR5 to cocaine-induced neuronal plasticity in dopamine neurons. Initial experiments demonstrate that both receptors active the same conductances. Following a single injection of cocaine the mGluR1-dependent currents were significantly decreased whereas mGluR5-dependent currents were unchanged. Finally, pharmacological blockade of mGluR5 *in vivo* prior to injection of cocaine blocked the cocaine induced decrease in mGluR1-dependent currents. Thus, activation of mGluR5 after cocaine coordinates the reduction in mGluR1.

Results

A single injection of cocaine decreased mGluR induced currents

Activation of group I mGluRs on dopamine neurons can elicit both an inward and outward current (Figure 4.1). The inward current is due to a Trp conductance (Tozzi et al. 2003) and the outward current is mediated by SK channels (Chris D Fiorillo and Williams 1998). Both the inward and outward currents were blocked by the combination of the negative allosteric modulators (NAMs, referred to subsequently as blockers) JNJ (500 nM) and MPEP (300 nM, Figure 4.2), which block mGluR1 and mGluR5 (respectively). Mice were injected i.p. with saline or cocaine (20 mg/kg) 24-hours prior to recording, and the sensitivity to iontophoretically applied L-aspartate and bath application of DHPG were examined. Bath application of DHPG was used to construct concentration-response curves for the inward current after block of SK with apamin (200 nM). The rapid and local application of aspartate by iontophoresis was used to isolate the outward current. With these two methods the inward and outward mGluR currents were examined independently in saline- and cocaine-injected animals.

In cocaine treated animals, the trend of the inward current induced by DHPG applied over a wide range of concentrations was toward a smaller maximum response ($p=0.13$). The only significant difference was at a near saturating concentration (100 μM, Figure 4.1A; control: 143±30 pA; cocaine: 54±10 pA; $t(41)=3.72$, $p<.05$, Bonferroni's posttest). At higher concentrations, the inward current peaked and declined during that period of application (see Figure

4.1A for an example). Thus accurate measurement of the peak current was blunted by the decline in current particularly at high concentrations during bath application of DHPG. The rapid decline in inward current prevented construction of an accurate concentration response curve in slices from both control and cocaine treated animals. To avoid this problem, aspartate was applied by iontophoresis. This method resulted in reproducible outward currents that could be compared in slices from saline and cocaine treated animals (Figure 4.1B). The average peak outward current in slices from control animals was 78.2±16.2 pA, whereas the current in slices from cocaine-injected animals was significantly smaller (32.9±5.3 pA, unpaired 2-way t-test, $t(17)=3.01$, $p<0.05$). These results indicate that following a single injection of cocaine there is a functional reduction in mGluRs signaling.

SK is unaffected in slices from cocaine-treated animals

One explanation for a reduced outward current in slices from cocaine-injected animals is that the SK-mediated currents are reduced. The SK conductance evoked by a voltage step protocol was used to test this possibility. Using a step depolarization to evoke calcium entry followed by the return to -50 mV an apamin-sensitive (SK) current was identified (Figure 4.1C). The SK current in control animals (107±12 pA*S) was not significantly different than in cocaine-injected animals (89.7±9.5 pA*S, $t(24)=1.1$, $p>0.05$, unpaired t-test, Figure 4.1D). Thus, the reduction in the current induced by activation of mGluRs does not

result from a decrease in channel expression, suggesting the change is due to an altered receptor function.

SNc dopamine neurons express both mGluR1 and mGluR5

In these experiments the mGluRs were activated using pressure ejection of DHPG (100 μM). This method of agonist application resulted in a combination of inward and outward currents that were reproducible with repeated applications. Selective blockade of DHPG-induced currents using the mGluR1 blocker, JNJ (500 nM) or the mGluR5 blocker, MPEP (300 nM) were examined using successive application of each blocker on individual cells. The order of blocker application was alternated between cells. In these experiments neither blocker alone completely eliminated the DHPG-induced currents. In general, each blocker inhibited about 50% of the current, and only after both blockers were applied was the current completely inhibited (JNJ first: baseline 77±24 pA*S, JNJ and MPEP 1.89±0.62, $q(8)=4.45$, $p<0.05$, Figure 4.2A; MPEP first: baseline 92±18 pA*S, MPEP and JNJ 2.56±0.83, $q(11)=7.30$ $p<0.05$, Figure 4.2B; post-hoc Tukey Test). The overall composition of the mGluR current varied between cells, with some cells expressing only mGluR1 (6/21), others with only mGluR5 (5/21), and most expressing both (10/21).

Cocaine treatment selectively decreased mGluR1 currents

Given that the mGluR current was reduced in slices from cocaine treated animals, the next experiment determined which receptor subtype was involved.

DHPG was applied by pressure application in slices taken from saline and cocaine treated animals. As in previous experiments, following the acquisition of a stable mGluR current, MPEP (300 nM) and JNJ (500 nM) were successively applied to the slice. The average current activated in the presence of the first blocker was then subtracted from the initial current to establish the size of the current activated by the other mGluR group I subtype. The charge transfer evoked by mGluR5 in control animals was not significantly different from cocaine-treated animals (control=28.9±7.6 pA*S; cocaine-treated=41.8±13.9 pA*S; $t(68)=0.85$ $p > 0.05$ Bonferroni post-test, Figure 4.3B). However, the mGluR1-induced current was significantly smaller in slices from cocaine treated animals (control: 53.0±12.4 pA*S; cocaine-treated: 7.8±3.5 pA*S; $t(68)=2.97$ $p<0.05$, Bonferroni post-test, Figure 4.3B). Therefore a single injection of cocaine selectively reduced the size of the mGluR1 current while not affecting the size of the mGluR5 current.

Acute activation of mGluR5 induces a long-lasting depression of mGluR1-induced current

In some neurons that express both mGluR1 and mGluR5, the activation of mGluR5 down-regulates mGluR1 receptor function (Poisik et al. 2003). The current induced by activation of mGluR1 was examined before and after activation of mGluR5. Unlike the DHPG pressure ejection, iontophoretic application of aspartate most often induced an outward current that was primarily mediated by mGluR1s as determined by the lack of inhibition of the peak current

by the mGluR5 selective blocker MPEP. The peak outward current induced by aspartate measured before and after the application of MPEP was not significantly different (difference is +1.6±7.8 pA, $t(5) = .45$, $p > 0.05$, Figure 4A). MPEP did however result in a significant decrease in the total charge transfer indicating that there was a small contribution of outward current that was dependent on mGluR5s ($t(5) = 3.29$ $p<0.05$; two-tailed t-test, mean difference: -37.1±11.3 pA*S, Figure 4.4A).

Selective activation of mGluR5 was achieved with the co-application of the orthosteric agonist CHPG (50 μM) and a positive allosteric modulator VU-0357121 (500 nM, 15 minutes). This combination of agonists did not consistently induce a change in the holding current. However, the outward current activated by iontophoretically applied aspartate was significantly reduced, and did not recover following washout of the mGluR5 agonists (Figure 4.4B; normalized baseline - wash: 53.5±13.9%, $t(14)=3.84$, $p<0.05$, 2-way ANOVA followed by Bonferroni's test). The reduction in the aspartate-induced mGluR current was prevented by the mGluR5 blocker MPEP (1 μM), indicating that the activation of mGluR5 induced a long-term reduction of mGluR1-dependent signaling.

In vivo injection of MPEP prevents cocaine-induced decline in mGluR1 signaling

The next experiment examined if the decrease in mGluR1 signaling induced by cocaine was dependent on the activation of mGluR5. Animals were treated with MPEP (30 mg/kg, i.p., (Gasparini et al. 1999)) 10 minutes before

treatment with cocaine (20 mg/kg) or saline (Figure 5A). There was no significant difference in the size of the mGluR charge transfer made up of both mGluR1 and mGluR5 induced by a pressure ejection of DHPG in any condition (MPEP+saline: 105±17.83 pA*S, MPEP+cocaine: 139.9±42.74 pA*S, control: 85.9±14.2 pA*S, cocaine: 50.98±12.8 pA*S; $F(3, 58)=1.75$, $p>0.05$, all post-hoc comparisons were not significant at the 0.05 level using a Tukey post-hoc test, Figure 4.5C). Only when the mGluR1 component of the current in each cell was calculated as a fraction of the total mGluR baseline charge transfer from saline and cocaine treated animals was it observed that a single injection of cocaine significantly reduced the mGluR1 component of the total (control=59.1±8.5%, cocaine=20.4±7.2% $q(58)=4.88$, $p<0.05$; MPEP+saline=62.0±9.7%, $q(58)=4.58$, $p<0.05$; and MPEP+cocaine=57.8±7.5%, $q(58)=4.30$, $p<0.05$, Figure 4.5D). There was no significant change in the size of the fractional mGluR1 charge transfer between the MPEP+saline and saline conditions ($q(58)=0.35$ $p>0.05$), indicating pretreatment with MPEP did not alter the fraction of the total mGluR currents made up by either receptor.

These results revealed that blocking mGluR5 *in vivo* prevented the cocaine-induced decrease of the mGluR1 component of the overall mGluR current in midbrain dopamine neurons.

Discussion

This study demonstrates the activation of currents made up by a combination of mGluR1- and mGluR5-dependent signaling in substantia nigra dopamine neurons. A single administration of cocaine selectively reduced mGluR1-dependent currents without changing the current induced by activation of mGluR5. The acute activation of mGluR5 in brain slices reduced the mGluR1-dependent current. Blockade of mGluR5 prior to administration of cocaine blocked the cocaine-induced decline in the mGluR1-dependent current. Thus treatment with cocaine results in the activation of mGluR5 that functionally down-regulates mGluR1.

The canonical reward pathway involves VTA neurons that project to the nucleus accumbens, and most literature that has examined changes in dopamine neurons in the VTA. There is, however, a growing body of literature implicating the substantia nigra dopamine neurons in the rewarding aspects of cocaine (Ilango et al. 2014; Ramayya et al. 2014; Rossi et al. 2013; Wise 2009). This study suggests that plasticity of dopamine neurons in the substantia nigra can contribute at a cellular level to cocaine-induced modulation. There is however a significant difference in expression of SK between neurons in the substantia nigra and VTA (Wolfart et al. 2001). Dopamine neurons found in the substantia nigra have substantially greater currents mediated by SK than neurons in the VTA, particularly medial aspects of the VTA. Thus the inward current induced by

activation of mGluR1 dominates in the VTA suggesting a qualitative difference between cells in the substantia nigra and VTA.

Presence of mGluR5

Previous studies in slices from rats found that mGluR-induced currents were not sensitive to mGluR5 blockers (Morikawa, Khodakhah, and Williams 2003; Guatteo et al. 1999; Cui et al. 2007). However, dopamine neurons in the rat express transcript and protein for both mGluR1 and mGluR5 isoforms (Testa et al. 1994; Hubert, Paquet, and Smith 2001). Technical differences between the way previous work and the present results were obtained most likely account of the different results. In the present study, as was found previously, the peak outward current induced by iontophoretically applied aspartate was not reduced by blocking mGluR5 with MPEP. Although the peak current was not sensitive to MPEP, the total charge transfer was reduced, indicating a subtle action of mGluR5 activation. Pressure application of DHPG used in the present study also most likely resulted in a more widespread and prolonged activation of receptors compared with local iontophoretic application of aspartate that is a transporter substrate.

Cocaine and mGluRs

Enhancing mGluR1 activity by a positive allosteric modulator reverses cocaine-induced plasticity in dopamine neurons (Bellone and Luscher 2006) and in medium spiny neurons of the nucleus accumbens (McCutcheon et al. 2011). Also

in medium spiny neurons, negative allosteric modulation of mGluR1s leads to an increase of cocaine-induced cellular plasticity (Bellone and Luscher 2006; Loweth et al. 2013). In multiple behavioral studies negative modulation of mGluR5 decreased the behavioral effects of cocaine, decreasing cocaine self administration, cocaine seeking and cue-induced reinstatement (Keck et al. 2014; Keck et al. 2013; Kumaresan et al. 2009; Platt, Rowlett, and Spealman 2008). This study provides a link between these behavioral studies and cellular studies by showing that negatively modulating mGluR5 *in vivo* can prevent a cocaine-induced decrease in mGluR1 signaling. This decrease in mGluR1 currents could result from internalization of receptors or a long-lasting desensitized state induced by the acute activation of mGluR5s after cocaine treatment. A number of mechanisms could be involved including direct phosphorylation of the receptor. Phosphorylation of mGluR1 following the activation of mGluR5 by a PKC-dependent mechanism has been reported (Poisik et al. 2003). Regardless of the precise mechanism responsible for mGluR5 coordinating the decrease in mGluR1 signaling, these results reveal a novel and immediate consequence of cocaine treatment on dopamine neuron cellular physiology.

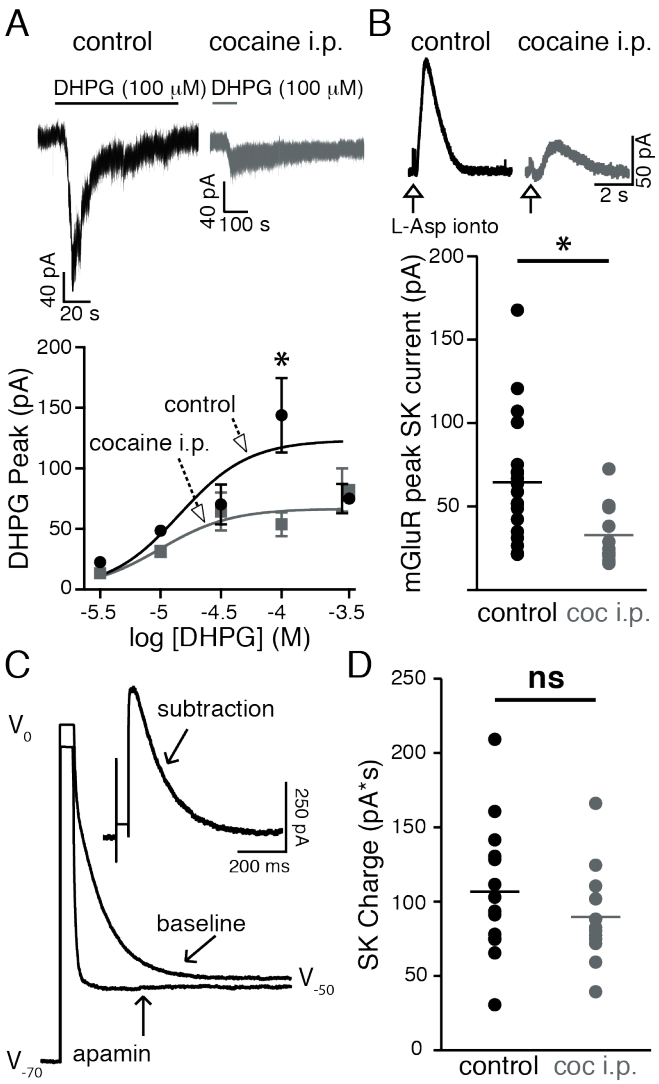

Figure 4.1 A single i.p. injection of cocaine decreased the maximum mGluR conductance.

A. A two-way ANOVA revealed no significant difference between the curves (n=3–10 cells for each data point). When the current induced by DHPG (100 μM) alone was tested, a post-hoc Bonferroni test indicated a significant difference between saline and cocaine-treated animals than in control.
B. The outward current isolated using iontophoresis of L-aspartate indicated that the current was significantly decreased in slices from cocaine treated animals (control n=19 cells; cocaine n=11 cells). The decrease in the mGluR outward current was not due to a decrease in SK conductance.
C. The voltage step-induced SK current (see methods) before and after apamin (200 nM). *Inset* subtracted SK current.
D. No significant difference between saline and cocaine-injected animals (control n=14 cells; cocaine n=12 cells). In **A** each point represents a mean±S.E.M. Each point in **B** and **D** represents and individual cell and bars indicate means, * indicates $p<0.05$, ns indicates not significant.

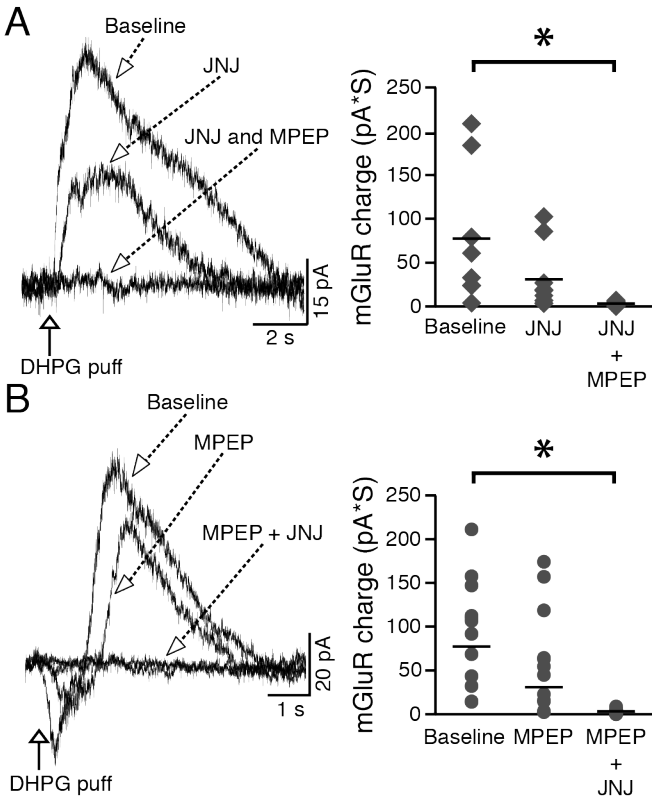

Figure 4.2 mGluR1 and mGluR5 contribute to DHPG-mediated currents.

JNJ-16259685 (500 nM) is an mGluR1-specific blocker, and MPEP (300 nM) is an mGluR5-specific blocker. The mGluR current was evoked by local puff application of DHPG (100 μM, 80 ms) and the area under the curve was measured.
A. JNJ is applied first and the average current is partially decreased, then MPEP is applied and the average response is totally inhibited (n=9 cells per condition).
B. MPEP is applied first and the average current is partially decreased, then JNJ is applied and the average response is totally inhibited (n=12 cells per condition). Each data point represents an individual cell, within subjects design across drug trials. * indicates $p<0.05$, bars indicate means.

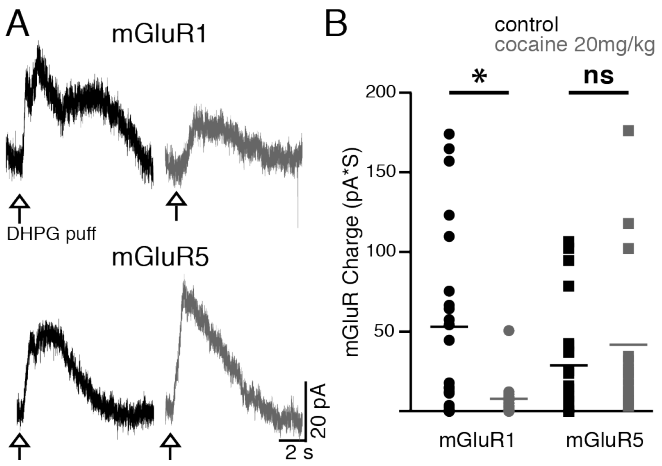

Figure 4.3 A single injection of cocaine significantly reduced mGluR1 currents while leaving mGluR5 unaffected.

DHPG-mediated pressure ejection currents were evoked from dopamine neurons and analyzed in control and cocaine-injected animals.
A. Example traces of isolated and subtracted mGluR1 and mGluR5 DHPG-evoked currents from control and cocaine-injected animals.
B. Group data showing a significant decrease in mGluR1 activity after a single injection of cocaine, with no significant change to mGluR5 (control n=22 cells; cocaine n=14 cells). * indicates $p<0.05$, ns indicates not significant.

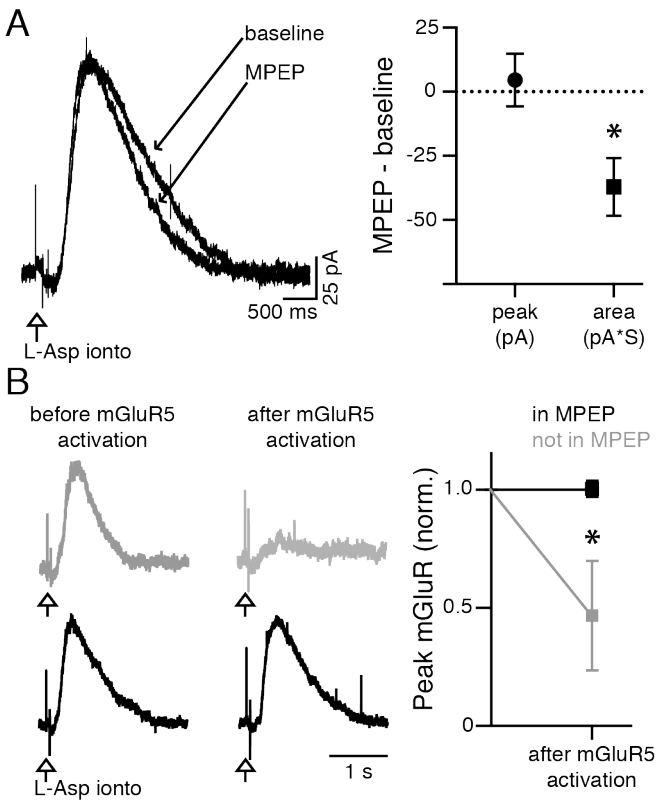

Figure 4.4 Acute activation of mGluR5 inhibits mGluR1 currents.

A. MPEP had no effect on the peak current but significantly decreased the area of the aspartate-induced mGluR current. *Left,* An example trace showing the average baseline current and the average current after MPEP (300 nM) in the same cell. *Right,* group data showing average MPEP - baseline values for the peak current (in pA, n=6 cells) and the area under the curve (in pA*S, n=6 cells).

B. *Left,* example traces of mGluR current induced by iontophoresis before (*left)* and after (*right)* mGluR5 activation, in MPEP to block mGluR5 (*black*) and not in MPEP (*grey*). *Right,* group data showing the normalized effect on the peak of the mGluR iontophoretic-induced current after bath applying CHPG (50 μM) and VU-0357121 (500 nM) to selectively active mGluR5 in the presence of MPEP (1μM, n=4 cells) and absence of MPEP (n=5 cells). Traces are normalized to baseline. * indicates $p<0.05$, markers and bars indicate means±S.E.M.

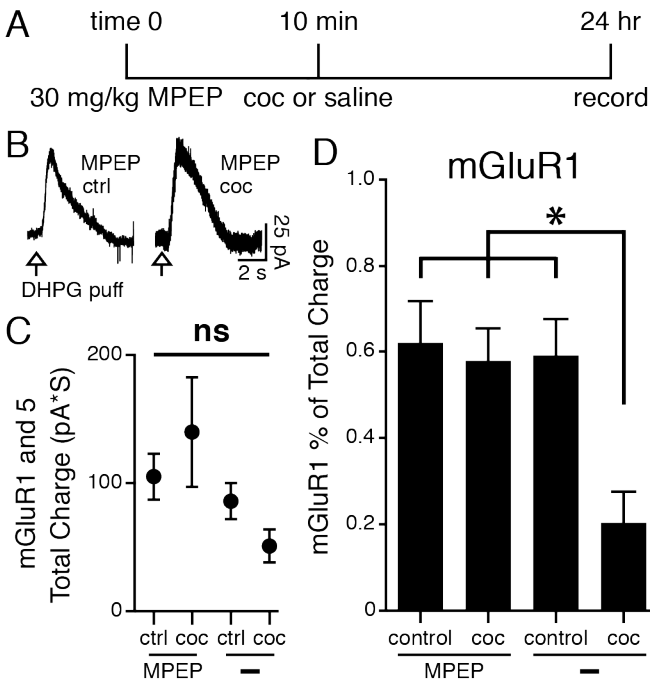

Figure 4.5 Blocking mGluR5 *in vivo* by i.p. injection of MPEP (30 mg/kg) prevented cocaine-induced inhibition of mGluR1 current.

A. Schematic showing the protocol where animals were treated with MPEP followed by treatment with cocaine or saline. Experiments were done 24 hours later.
B. Example traces from MPEP+saline and MPEP+cocaine of DHPG-evoked currents.
C. Group data showing no significant difference in the DHPG-induced mGluR current between MPEP+cocaine (n=14 cells), MPEP+saline (n=12 cells), control (n=21 cells) and cocaine (n=15 cells).
D. Group data comparing the percent of the total mGluR charge transfer that is accounted for by mGluR1. There was a significant decrease of the mGluR1 component only in mice treated with cocaine. There was no significant difference between the other three groups. * indicates $p<0.05$, ns indicates not significant, markers and bars indicate means±S.E.M.

4.1 Additional Experiments

Localization of mGluR1 and mGluR5

The receptor subtype makeup of electrically stimulated mGluR currents was interrogated using negative allosteric modulators specific to mGluR5 (MPEP, 300 nM) or mGluR1 (JNJ, 500 nM). The stimulated currents could be divided into two groups. Those currents that were susceptible to MPEP, and those that were resistant. The currents that were affected by MPEP decreased by ~60% relative to baseline, and were then completely inhibited by JNJ. By contrast, currents that were not affected by MPEP were totally inhibited by the mGluR1-specific NAM.

Furthermore, two assays were used to examine the rough subcellular distribution of mGluR1 and mGluR5. Pressure ejection of DHPG was performed roughly 50 – 100 μm from the soma, and covered a large area. By contrast, iontophoresis of L-aspartate was performed within 10 μm of the soma, and most likely represented a much more localized signal. The DHPG response was much more sensitive to mGluR5 negative modulation than the iontophoretic response. By contrast, the iontophoretic response was almost totally inhibited by the mGluR1 specific NAM.

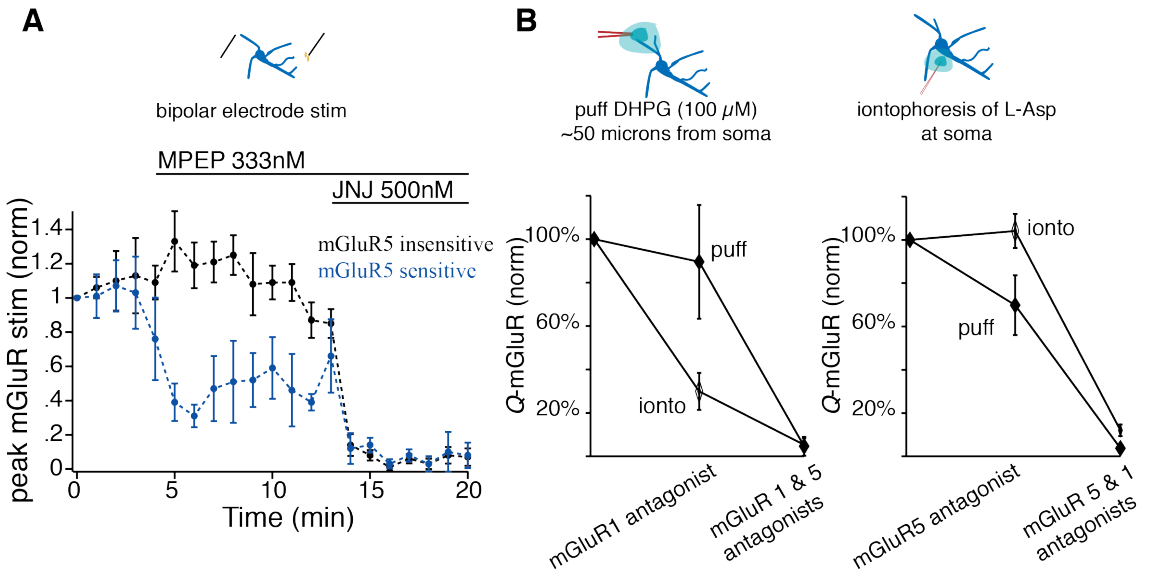

Figure 4.6 Evidence for differential sub-cellular distribution of mGluR1 and mGluR5.

A. Quantification of the peak of the stimulated mGluR IPSC, normalized to the first response. MPEP was applied after 5 minutes of baseline, and 7 minutes later JNJ was applied. The groups were separated based on sensitivity to the mGluR5-specific NAM, MPEP.
B. Quantification of the total charge transfer of the mGluR response following either pressure ejection of DHPG (puff) or iontophoresis of L-aspartate (ionto), and examining selective inhibition by either an mGluR1 or mGluR5 selective NAM; *left* application of JNJ preceded MPEP *right* application of MPEP preceded JNJ.

Discussion

While preliminary, these results support the hypothesis that mGluR1 and mGluR5 are in different subcellular locations, with mGluR5 located more distally relative to the soma and mGluR1 located more proximally. Furthermore, the experiment recording IPSCs indicates that only sometimes do post-synaptic currents include an mGluR5 component, while they always include an mGluR1 component. These experiments form the basis for further investigation into the selective roles for mGluR1 and mGluR5. Perhaps mGluR1 or mGluR5 are activated by distinct glutamatergic inputs. Or mGluR5 is only activated after robust glutamate release

that spills over into the extra-synaptic space. Qualitatively speaking, the IPSCs that were sensitive to the mGluR5 NAM required more robust stimulation.

Chapter 5 Discussion

Dopamine neurons are tonically active pacemaker neurons, making inhibition a critical modulator of activity. While the contribution of $GABA_A$ receptors is significant (Paladini and Tepper 1999), much of this inhibition comes from the synaptic activation of G protein-coupled receptors (Morikawa and Paladini 2011). Dopamine neurons functionally express an impressive array of G_i and G_q GPCRs that couple to plasma membrane bound ion channels, as well as other downstream signaling molecules. The activation of these GPCRs mostly leads to a robust inhibition in neuronal firing that often lasts hundreds of milliseconds. The data presented is this dissertation examines new roles for one of the GPCR classes expressed by dopamine neurons, Group I mGlu receptors.

These receptors are known mediate a mixture of inhibition and disinhibition in dopamine neurons, and are modulated by acute drug administration. Through the course of this dissertation it was further found that the calcium liberated from stores by mGluR1 and mGluR5 activation causes a rapid and transient decrease in the amplitude of GIRK currents. Pathologically, non-contingent administration of the psychostimulant cocaine leads to a reduction in mGluR1 signaling 24 hours following drug exposure. This plasticity of mGluR1 signaling requires the activation of mGluR5. These findings will be discussed within the broad contexts of intracellular signaling, drug abuse research, and dopamine neuron physiology.

Dopamine neurons are unique in many ways, but they also share many properties with other neurons throughout the brain. G protein-coupled signaling is one of the most ubiquitous and diverse mechanisms for converting extracellular chemical transmitter into intracellular molecular signaling cascades (Lagerström and Schiöth 2008). Consequently there are many areas where the findings of this dissertation might by broadly applicable. However, it is not known if there is a protein secondary to calcium release that is necessary for GIRK inhibition. The existence of this protein would limit generalizability of the findings in this dissertation to neurons that express that protein. In the section to come, many of the inferences are hypotheses that can be tested, and will be discussed in the *Future Directions* section.

Shared signaling pathways

OTHER G_Q RECEPTORS

Group I metabotropic glutamate receptors are one of many G protein-coupled receptors that activate G_q (Hubbard and Hepler 2006). Just in dopamine neurons, M1-type muscarinic receptors (Fiorillo and Williams 2000) and α_1 adrenoceptors (Paladini and Williams 2004) activate the calcium-dependent SK current through G_q receptor stimulation. Outside of dopamine neurons, histamine activates the H1 receptor (Hill et al. 1997) and serotonin activates the 5-HT2 receptor (Roth, Willins, and Kristiansen 1998), two more G_q-coupled receptors found throughout the brain. Therefore the liberation of calcium from stores and subsequent

inhibition of GIRK is not limited to glutamate alone. Acetylcholine, norepinephrine, histamine and serotonin all have the potential to inhibit GIRK currents through the release of calcium from stores.

However, it should be noted that there is the potential for more complex interactions occurring in neurons that express multiple G_q coupled GPCRs. For example, in dopamine neurons, activation of the α_1 adrenoceptor decreases mGluR mediated SK currents by either partially depleting calcium stores or desensitizing the IP_3 receptor. What's more, this activation of the α_1 can occur following high levels of extracellular dopamine, a weak α_1 agonist, during exposure to drugs like cocaine or amphetamine (Paladini et al. 2001). Thus, depending on the sequence of receptor activation, GIRK currents could be protected against inhibition by prior G_q-receptor activation mitigating the IP_3-generated currents for a few seconds.

OTHER FORMS OF CALCIUM RELEASE FROM STORES

The data in this dissertation indicate that receptor activation is not necessary for calcium release from stores to inhibit GIRK currents. Direct stimulation of release from stores by photolysis of caged-IP_3 inhibited GIRK to the same extent as mGlu receptor activation. This finding leads to the conclusion that, in a natural context, non receptor-dependent release of calcium from stores will also inhibit GIRK currents. While the activation of IP_3 receptors requires IP_3, which typically results from receptor activation (Patterson, Boehning, and Snyder

2004), ryanodine receptors also mediated calcium release from stores and are activated by calcium (Verkhratsky and Shmigol 1996).

Ryanodine receptors can mediate calcium release from stores following calcium channel activation, such as in dopamine neurons following spontaneous T-type channel openings (Cui, Okamoto, and Morikawa 2004), and during tonic firing in ventroposteriomedial / ventroposteriolateral thalamocortical neurons (Cheong et al. 2011). These findings indicate that calcium release from stores occurs, in certain situations, without G_q receptor activation. Therefore, in contexts where there is robust calcium-induced calcium release (CICR) together with GIRK mediated currents, it is possible that the level of CICR could modulate GIRK channel activity.

Finally, there is some evidence for the ability for IP_3 receptors to "leak" calcium in the absence of IP_3 (Szlufcik et al. 2012), though there is also much room for debate (Sammels et al. 2010). What is clear is that IP_3 receptors can become sensitized following protein modifications such as phosphorylation (Tang et al. 2003). In dopamine neurons, PKA-dependent phosphorylation increases calcium release following mGlu receptor activation (Riegel and Williams 2008). These IP_3 receptors with enhanced affinity for IP_3 will therefore lead to greater inhibition of GIRK following smaller or similar sized G_q receptor signals than before IP_3 receptor phosphorylation.

Other neurons with the necessary proteins

In addition to other intracellular signaling pathways, the inhibition of GIRK by calcium release from stores can be extended to other cell types. In the broadest sense, all that is known to be necessary for calcium-mediated GIRK inhibition is the GIRK channel and calcium, either released from stores or as a persistent tone. There are many neurons that express GIRK channels, opening the possibility for calcium-mediated GIRK inhibition outside of dopamine neurons. However, even if all that is required is calcium and GIRK, there are some unique properties of dopamine neurons that could make this GIRK inhibition more prominent.

For example, dopamine neurons express GIRK channels that are composed of Kir3.2 and 3.3 subunits, whereas many other neurons contain GIRK Kir3.1 (Beckstead et al. 2004; Arora et al. 2010; Munoz et al. 2016). Inwardly rectifying potassium channel consisting of different Kir subunits have differing affinities for PIP_2 (Du et al. 2004), so it's possible that they would also be differentially inhibited by calcium. Similarly, dopamine neurons are unique for their large G_q-mediated SK currents that overwhelm the non-selective inward cation current. Hippocampal pyramidal neurons, for example, also have synaptically activated group I mGlu receptors and SK channels, but synaptic stimulation produces only a modest SK current followed by a sustained depolarization (El-Hassar et al. 2011). This comparison indicates there could be a localization effect of IP_3 receptors in dopamine neurons that positions them

within a subcellular compartment to both activate SK and inhibit GIRK. Without experimentation, it is impossible to say if calcium inhibits GIRK outside of dopamine neurons, but the possibility is there.

Involvement in drug abuse pathologies

When examining the molecular and cellular components underlying drug abuse pathologies, there are two ways to consider the system: those components affected by the drug, and those that mediate the drug effects. These are not two exclusive groups, and often examining one leads to insights on the other. Often the effect seen in one part of the brain is mirrored in others, which could point to an underlying mechanism for drug abuse to affect a system by using certain effectors repeatedly. These drug affects and molecular effectors will be compared and contrasted between what has been shown in the dissertation and in the literature.

mGluR1 gates cocaine-induced synaptic plasticity

Cocaine is a psychostimulant with addictive properties. Pharmacologically, cocaine blocks biogenic amine reuptake transporters such as the dopamine transporter, the norepinephrine transporter and the serotonin transporter. However the main rewarding and addictive properties of the drug are through its actions at the dopamine transporter (Chen et al. 2006). Following a single injection of cocaine, dopamine neurons of the VTA exhibit an increase in the AMPA/NMDA ratio, resulting from a larger AMPA current (Ungless et al. 2001). This increase in the AMPA/NMDA ratio was also observed in animals treated with

morphine, ethanol, amphetamine, nicotine, and those that were exposed to an acute stressor protocol. Furthermore, when locomotor responses following cocaine administration were recorded, they positively correlated with the degree of the increase in the AMPA/NMDA ratio (Borgland 2004). This plasticity may therefore underlie a common synaptic response to salient positive or negative experiences for glutamatergic synapses onto dopamine neurons (Saal et al. 2003).

The underlying increase in AMPA current that mediates the change in the AMPA/NMDA ratio results from an insertion of calcium permeable AMPA receptors that have higher unitary conductance (Bellone and Luscher 2006). In this study, Bellone and Luscher found that the increase in AMPA conductance was reversed by mGluR1-dependent LTD. This LTD reversed the effects of cocaine in the slice *in vitro*, and also *in vivo* when an mGluR1 positive allosteric modulator was administered 24 hours following the injection of cocaine. The mGluR1-dependent LTD functioned by switching the subunit composition, removing calcium-permeable AMPA receptors from the synapse (Bellone and Luscher 2005).

In the nucleus accumbens there is a similar role for mGluR1 on medium spiny neurons, but unlike in the VTA, the changes to the NAc occur only after repeated injections of cocaine, for example for five days in a row (Kourrich et al. 2007). As opposed to the VTA, the plasticity in the NAc manifests as a depression of the AMPA/NMDA ratio. However, if mGluR1 activity in the VTA is

potentiated just after each of the five cocaine injections, the adaptations in synaptic plasticity in the NAc are prevented. Conversely, if mGluR1 signaling is blocked in the VTA, it only takes one injection of cocaine to see plasticity in the NAc (Mameli et al. 2009). These findings indicate that mGluR1 activity in dopamine neurons is protective against cocaine-induced synaptic plasticity in both the VTA and the NAc.

Furthermore, following prolonged withdrawal from cocaine after repeated administration, there is an insertion of calcium permeable AMPA receptors that leads to a potentiation of the AMPA/NMDA ratio and a phenomenon known as "incubation of craving" (Conrad et al. 2008). Behaviorally, incubation of craving is defined by an increased response rate for cues previously paired with a drug after 45 days of withdrawal over the response rate one day after. The cellular plasticity and behavioral effects of incubation of craving can be accelerated by decreasing mGluR1 activity in the NAc, can be prevented by potentiating mGluR1 activity, and were accompanied by a decrease in mGluR1 surface expression (McCutcheon et al. 2011; Loweth et al. 2013).

Together, these data indicate that cocaine-induced cellular plasticity begins in the dopamine neurons and is gated by mGluR1 activity. Following prolonged cocaine administration, medium spiny neurons in the NAc undergo synaptic plasticity (unless mGluR1 signaling is potentiated in the dopamine neurons). After NAc MSNs have undergone plasticity, potentiating mGluR1

activity in the NAc can return the synaptic properties to baseline levels, but if mGluR1 activity is blocked then the plasticity in the NAc is accelerated.

The data presented in this dissertation addressed the question of how Group I mGluRs in dopamine neurons are affected by cocaine exposure, rather than how they affect the change in ionotropic glutamate receptors. Non-specific activation of Group I mGluRs on dopamine neurons revealed a smaller overall current in cocaine treated animals than in control animals. Moreover, contrary to previous reports, dopamine neurons were found to functionally express both mGluR1 and mGluR5. Upon further investigation the cocaine-induced reduction in mGluR currents was discovered to be specific to mGluR1, while mGluR5 activity and the downstream channels activated by mGluRs were all unaffected by cocaine treatment.

Together, these data show that mGluR1 activity opposes the changes in synaptic plasticity induced by addictive drug administration. Possible roles for mGluR1 activity include preventing the insertion of calcium-permeable AMPA receptors, or tonically promoting the removal of calcium-permeable AMPA receptors. Additionally, the currents generated by mGlu1 receptor activation may be necessary for preventing the induction of LTP, perhaps by hyperpolarizing the neuron following large glutamate release, restoring the NMDA receptor magnesium block. Thus the results of a decrease in mGluR1 activity is not clear in terms of synaptic plasticity, but it is clear that this decrease is necessary.

Role for mGluR5 in drug-induced plasticity

The other Group I metabotropic receptor has received less attention in the study of how mGluRs contribute to drug-induced changes in synaptic plasticity. Most often studies find that at the cellular level blocking mGluR5 does not alter the plasticity of ionotropic receptors. However, at the behavioral level there is ample evidence that mGluR5 contributes to the effects of addictive drugs of abuse.

The first observation that mGluR5 is involved in mediating drug-induced changes came from a study examining cocaine self-administration in mice. It was found that in mGluR5 global knockout mice, cocaine self-administration was entirely prevented, along with the locomotor responses to non-contingent cocaine administration (Chiamulera et al. 2001). This dramatic result has not been entirely replicated in the literature, with one study showing the mGluR5 knockout mice still develop conditioned place preference to cocaine administration, but have altered drug extinction learning (Bird et al. 2014). Studies from global knockout animals are tricky to interpret due to possible strain differences and cellular compensation effect. Consequently, many groups have followed up using injection of mGluR5 NAMs to test what transiently inhibiting mGlu5 receptor activity does to drug-related behaviors.

In squirrel monkeys, systemic block of the mGlu5 receptor inhibited cocaine self-administration (Platt, Rowlett, and Spealman 2008), and cue-induced reinstatement of drug seeking (Lee et al. 2005). In rats, inhibition of mGlu5 receptors in the NAc core inhibits cocaine cue-induced reinstatement of

drug seeking, whereas activation of mGluR5 in the NAc core modestly promoted seeking without a cue, and dramatically promoted seeking in combination with a cue (X. Wang et al. 2012). Furthermore, a different mGluR5 NAM, fenobam, also inhibited cocaine seeking and self-administration in rats (Keck et al. 2013), and another mGluR5 NAM "MFZ 10-7," with greater selectivity for mGluR5 than MPEP or fenobam, had a similar effect on cocaine self-administration and seeking (Keck et al. 2013).

Together, these finding indicate the mGlu5 receptor activity promotes cocaine-induced behaviors such as drug self-administration and cue-induced reinstatement of seeking. While the cellular correlate of these behavioral findings is unclear, a possibility emerges from the findings presented in this dissertation. It was found that in dopamine neurons, like in other neurons, mGluR5 acts acutely in the slice to inhibit mGluR1 signaling (Poisik et al. 2003). To test if inhibition of mGluR5 affected the cocaine-induced reduction in mGluR1 signaling, systemic administration of the mGluR5 NAM, MPEP, was given 10 minute prior to cocaine. This treatment prevented the decrease in mGluR1 signaling following cocaine administration. These data indicate that, at the cellular level, mGluR5 might act to promote drug abuse by suppressing mGluR1 activity.

Calcium and drugs of abuse

Alterations in glutamate synaptic function are not the only cellular changes following cocaine treatment. In many studies examining the impact of drug administration on dopamine neurons, there is a decrease in GIRK function. This

effect often depends on calcium, or somehow involves calcium signaling. The effects of calcium are most often examined by using two different calcium chelators in the internal solution. Either a low concentration of EGTA to minimally buffer intracellular calcium, or a high concentration of BAPTA to maximally buffer calcium. EGTA and BAPTA have similar affinities for calcium, but EGTA has much slower association and dissociation kinetics than BAPTA and is more sensitive to pH (Tsien 1980). These studies now will be reviewed, and the findings presented in this dissertation will be evaluated in their context.

Mice that self-administered methamphetamine had reduced $GABA_B$ receptor- and D2 receptor-mediated GIRK currents in dopamine neurons of the VTA and SNc. This effect was normalized if an internal solution was used containing a high concentration of BAPTA. Therefore, methamphetamine's effects on the decrease in GIRK currents required sustained levels of calcium signaling in the neuron. Similarly, mice that were given non-contingent methamphetamine injections for 5 days systemically had reduced $GABA_B$ receptor-mediated GIRK currents. This reduction in current was not phosphorylation dependent, but depended on the presence of the GIRK3 subunit (Kir3.3). In GIRK3 KO mice, repeated methamphetamine administration had no effect on $GABA_B$ receptor-mediated currents. However, the calcium dependence of this effect was not examined, and 1.1 mM EGTA was used for all electrophysiological recordings.

In light of the data presented in this dissertation, it seems likely that repeated methamphetamine exposure, either through self-administration or non-contingent injections, increases tonic calcium levels in dopamine neurons and reduces GIRK activity. The fact that this effect depends on the GIRK3 subunit of GIRK channels is particularly intriguing. Perhaps it is GIRK3 that confers GIRK channels with susceptibility to calcium inhibition.

However, the evidence for GIRK3 subunit-containing channel in dopamine neurons is controversial. GIRK2 KO mice display complete loss of D2 and $GABA_B$ receptor-mediated currents, whereas GIRK1 and GIRK3 KO mice are equal to controls (Beckstead et al. 2004; Koyrakh 2005). Early characterization of the GIRK channel subunit composition in dopamine neurons indicated mainly homomeric channels of GIRK2 (Kir3.2) subunits, though there was detectable transcript for GIRK3, but the majority of proteins they analyzed were composed of GIRK2. This indicates that, if present, GIRK3-contianing channels are in the minority (Inanobe et al. 1999). This would agree with the present data where tonic bath perfusion of baclofen led to currents only inhibited about 20% by calcium, representing a minority of the total evoked current. This could explain why the effect could be occluded by increasing intracellular resting calcium levels, despite the presence of a GIRK current, since only a certain subpopulation of GIRK channels would be able to be inhibited.

Like methamphetamine, animals injected with a single injection of cocaine have diminished GIRK currents mediated by $GABA_B$ receptor activation (Arora et

al. 2011). This effect was specific for $GABA_B$ receptors and did not affect D2 receptor-coupled GIRK currents (Padgett et al. 2012). Both these studies used a concentration of EGTA (1.1 mM) that was found in the work presented here to produce an intermediate titration of intracellular calcium chelation, increasing the variability in the results. Furthermore, both these studies found decreases in $GABA_B$ and GIRK surface protein levels, which is unlikely to be the mechanism for calcium-mediated GIRK inhibition due to the millisecond timescales involved. In another study, mice injected with cocaine displayed smaller D2-mediated GIRK currents, which were normalized when intracellular calcium was buffered with only 100 μM of EGTA (Dragicevic et al. 2014). Therefore, the previous studies with cocaine may have missed a more robust inhibition of $GABA_B$ and / or D2 receptor-mediated GIRK currents by buffering internal calcium with 1.1 mM EGTA.

Finally, and somewhat paradoxically, mice that self-administered ethanol had increased D2 receptor-mediated GIRK currents, with less current desensitization (Perra et al. 2011), a process dependent on unbuffered internal calcium signaling (Beckstead and Williams 2007; Gantz, Robinson, et al. 2015). This effect was reversed with increased intracellular calcium buffering. These results suggest that after chronic ethanol consumption there is a calcium dependent process within dopamine neurons that enhances D2 receptor-mediated GIRK currents and decreases desensitization. These findings highlight

that not all abused drugs can be treated the same in terms of effects on cellular plasticity.

Heterogeneity of dopamine neurons

Dopamine neurons are defined by their primary function, the synthesis of dopamine. While all dopamine neurons share this trait, there are other areas where these neurons differ, forming a heterogeneous population (Roeper 2013). The majority of dopamine neurons are located in neighboring nuclei, the VTA and the SNc. However, there is no strict border between these two areas (Fuxe 1965). Instead, the dopamine neurons are grouped into major subclasses defined by their projection targets, either VTA neurons projecting to the ventral striatum and/or to cortical areas (mesolimbic / mesocortical), and SNc neurons that project to the dorsal striatum. However, these divisions are not strict, and there are many overlapping neurons between the two nuclei with varying projection targets. Some evidence further indicates that SNc dopamine neurons can be divided into two tiers, a dorsal tier and a ventral tier (Wise 2009). The ventral tier is the traditional, compact area that projects to the dorsal striatum, but the dorsal tier, and especially the most lateral zone of the dorsal tier, projects to the amygdala, a limbic structure. Thus the difference between the SNc and the VTA is not a strict distinction, but a mixed population of neurons with graded differences across the region. This background leads to questioning what role the SNc plays in reinforcement learning and reward.

Substantia nigra dopamine neurons and reward

The majority of drug abuse studies focus on VTA dopamine neurons and their projection areas. Canonically, VTA dopamine neurons, which project to the nucleus accumbens and areas in the cortex, are involved in reward, whereas SNc dopamine neurons, which mainly project to the dorsal striatum, are involved in movement (Koob and Nestler 1997). However, early studies by Wolfram Schultz and colleagues showed that almost all dopamine neurons respond to reward, and that there is a graded response across the ventral midbrain in intensity of response to rewarding stimuli, quantified by firing rate (Schultz 2002). These data indicated early on that the two regions might not be so strictly distinct.

Now, evidence is accumulating which indicates that dopamine neurons in the substantia nigra contribute to reward learning and processing (Wise 2009).In a study with human patients using deep-brain stimulation, SN dopamine neurons were shown to be important for strengthening action-reward associations (Ramayya et al. 2014). In the mouse, it has been shown that self-stimulation of dopamine neurons in the SNc drives operant learning, similar to self-stimulation of the VTA neurons (Rossi et al. 2013). Additionally, in a model of methamphetamine self-administration, cellular plasticity in response to the drug was found equally in VTA and SNc neurons (Sharpe et al. 2014). The data presented in this dissertation show another study using mice where drug administration (cocaine) led to a cellular change in SNc dopamine neurons.

These data are building a firm case for a role of the SNc in drug abuse and addiction that is similar to the VTA.

Internuclei heterogeneity

The heterogeneity of dopamine neurons does not only encompass their mixed role in reward learning. Dopamine neurons also vary in intrinsic properties, such as by expression of proteins like channels and calcium buffers. The SK channel is an important mediator of dopamine neuron firing rate, playing important roles in regulation of interspike interval and firing frequency (Deignan et al. 2012). Across the VTA and SNc, functional expression of SK channels varies between neurons, with more medial dopamine neurons tending to have smaller SK currents, leading to more irregular firing rates (Wolfart et al. 2001), There are also functional differences between neurons in expression and function of the hyperpolarization-activated cation channel I_h (Neuhoff et al. 2002), and the ATP-sensitive potassium channel K-ATP (Liss et al. 2005).

Dopamine neurons also differ in expression of the calcium buffer calbindin (Barrot et al. 2000). Recently, it was shown that the differences in calbindin-D28k expression lead to differences in control of calcium-mediated vesicular exocytosis and release of neurotransmitter (Pan and Ryan 2012). The data presented in this dissertation show that every dopamine neuron tested had a calcium-mediated inhibition of GIRK. However, the amount of inhibition varied across cells, perhaps indicating variability in intrinsic mechanisms for calcium buffering. In a calcium "challenge" experiment, with an intermediate concentration of EGTA (1 mM) in

the pipette, there was a clear separation between neurons, with half the neurons displaying mGluR-mediated SK currents and calcium-mediated GIRK inhibition, and the other half lacking either. It is tempting to hypothesize that these two populations represent calbindin negative and positive neurons, respectively.

Interspecies differences

There are differences between mice and rats when examining dopamine neurons. Long-term depression mediated by mGluR1 in dopamine neurons, which occurs through removal of calcium-permeable AMPA receptors, has been studied extensively. However, it is less often mentioned that this form of LTD is present in naïve rats (Bellone and Luscher 2005), whereas it is not present in naïve mice (Bellone and Luscher 2006). Furthermore, in naïve rats there is a basal rectification of the AMPA receptor current, where as in naïve mice there is not. It is only after acute drug exposure that there is rectification in the current of AMPA receptors in mice (Bellone and Luscher 2006). This species difference may reflect differences in basal expression of the GluA2 subunit, or in a difference in some other aspect that controls AMPA receptors subunit expression levels.

The data presented in this dissertation show that in both rats and mice, mGluR activation leads to the activation of a non-selective cation conductance and an SK current. However the relative sizes of these two currents is qualitatively different. In mice the current had a typical inward component

followed by the outward SK current. Whereas in rats the outward SK current dominated, typically obscuring the presence of an inward current.

However, there are more similarities than there are differences. The SK current generated by an unclamped action potential in voltage clamp was similar in area between the species (Figure 3.16B). And in both rats and mice, mGluR activation inhibited GIRK currents to a similar degree (Figure 3.16A).

Therefore, while there are differences in the relative ratio of inhibition and excitation following mGluR activation between rats and mice, both species have the necessary molecular components that underlie all acute effects of mGluR activation of channels. Whatever differences may exist between rats and mice in terms of activating those channels is not clear. This could be a difference in the expression level of the non-selective cation current protein, or in the coupling between the receptor and that channel. Relatively little is known about the identity of that inward current, making it a variable to control for, rather than one to include in a hypothesis.

Physiological relevance

Calcium release from stores inhibits $GABA_B$ mediated IPSCs by ~40% on average, but by as much as 70% in individual trials. This is a substantial disinhibitory signal that will increase excitatory drive in dopamine neurons, and in any other neuron that has both calcium release from stores and functional GIRK currents. This disinhibition occurs rapidly and reverses in seconds, making it a dynamic process that occurs on the timescale of synaptic transmission.

Therefore and synaptically driven release of calcium from stores will temporarily dampen the effect of GIRK channel activation.

Future Experiments

As illustrated by our lack of complete understanding about the identity and composition of the inward current following mGlu1 and mGlu5 receptor activation, there is still much to be answered regarding Group I mGluR activation in dopamine neurons. The data presented in this dissertation add new insights for understanding how these receptors modulate dopamine neuron activity. But, these data also present new questions that hadn't been appreciated before. The most relevant and approachable questions will now be addressed, along with ideas for experiments.

Mechanism of calcium-mediated GIRK inhibition

Prior to this study, it was known that strong chelation of calcium signals in dopamine neurons led to larger GIRK currents. The thinking was that there was some calcium and PKC-dependent mechanism that produced a tonic desensitization of the D2 receptor mediated current, as was shown to happen during prolonged exposure to a saturating concentration of an agonist. However the rapid inhibition of GIRK reported here does not depend on PKC, or on any tested calcium-dependent enzyme. Therefore, while PKC is important for D2 receptor-mediated desensitization, it is clear that there is a separated calcium-mediated process that affects the GIRK channel. Thus, the most pressing question raised by the work performed in the course of this dissertation is regarding the nature of the calcium-mediated GIRK inhibition: how does calcium inhibit GIRK?

This question was reviewed in the discussion section in Chapter 3. Briefly, the differences in SK channel kinetics and GIRK inhibition kinetics indicate that there is either specialized compartmentalization of the GIRK channel that has different calcium buffering from where SK channels are located, or there is an intermediate step between calcium and GIRK inhibition that alters the decay kinetics. This is because the inhibition of GIRK, while correlated with the duration of the SK current, significantly outlasts the SK current duration. Yet both processes are activated by release of calcium from stores (Diagram 5).

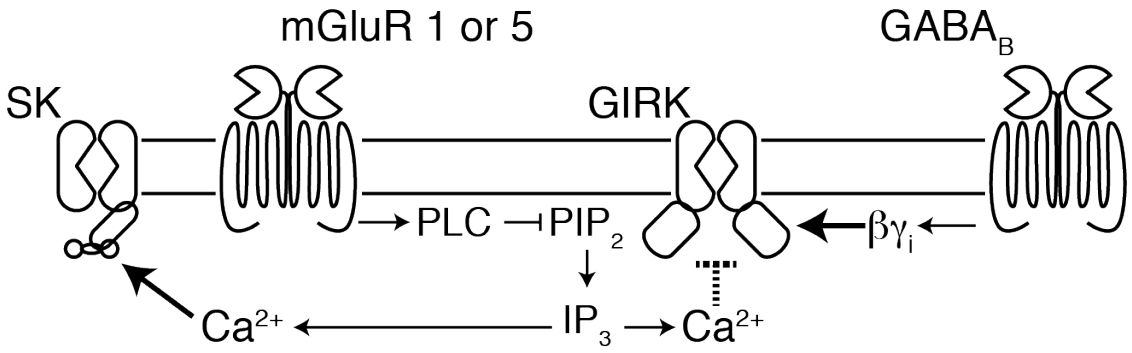

Diagram 5. Final schema for mGluR and $GABA_B$ actions and interactions in dopamine neurons

While calcium release from stores following Group I mGluR activation in dopamine neurons activates SK channels, it also inhibits GIRK currents activated by $GABA_B$ or D2 receptors.

An interesting hypothesis for the mechanism of calcium-medaited GIRK inhibition was summarized of page 117 of Chapter 5. Briefly, methamphetamine self-administration leads to reduced GIRK current amplitudes, and is rescued *in vitro* by dialyzing the neuron from the patch pipette with a high concentration of BAPTA. This indicates that there is a change in the tonic calcium signaling, perhaps an elevation in the tonic calcium levels within the cell, that inhibits GIRK

like what was reported here (Sharpe et al. 2014). In a separated study, it was reported that in GIRK3 KO mice, methamphetamine no longer affected GIRK currents in dopamine neurons (Munoz et al. 2016). Furthermore, it is believed that the GIRK3 subunit comprises a minority of the total GIRK subunit expression, and therefore is most likely found in a minority of the channels expressed on the plasma membrane (Koyrakh 2005), similar to the present results showing that calcium release from stores, during baclofen perfusion, only inhibited a minority of the overall current. Together, these data lead to the hypothesis that the GIRK3 subunit is calcium sensitive.

The most straightforward test of this hypothesis would be to obtain the GIRK3 KO mice. First, baseline evaluation of the GIRK currents in these mice would need to be tested to see if they are different from controls by examining current density (pA/pF). The second experiment would be to verify that these animals indeed lack the GIRK3 subunit through either genetic testing to confirm the knockout, and/or an *in situ* hybridization assay against the GIRK3 subunit mRNA. Third, it would be prudent to test the other basal properties of these transgenic mice such as capacitance, input resistance, gross morphology, and current density of other channels, and compare to littermate controls to verify that overall cell health and function are normal.

After building confidence in this transgenic knockout mouse model, the key experiment would be to test if the cells have calcium-mediated GIRK inhibition, and to compare to littermate controls. If indeed the only appreciable

difference between GIRK3 KO mice and littermate controls is a lack of calcium-mediated inhibition, it would be strong evidence that the GIRK3 subunit confers GIRK channels with calcium sensitivity. The final and most convincing test would be to inject virus that encodes the GIRK3 gene into the ventral midbrain of the GIRK3 KO mouse and rescue the calcium-mediated GIRK inhibition. However, even if the evidence indicates the GIRK3 subunit is required for the GIRK channel to be sensitive to calcium, the precise nature of the calcium interaction with the GIRK3 subunit would still be unresolved.

One way to begin to address this question is to ask whether GIRK the only Kir that can be inhibited by calcium? If it is not, then the Kir channels that are sensitive to calcium could be compared for sequence homology in areas that are likely to be sensitive to intracellular calcium (on the cytoplasmic surface of the protein, likely corresponding to charged amino acids). These sites could then be mutated to test if the sensitivity to calcium could be negated.

To test this question, caged calcium would be dialyzed into a cultured cell expression Kir channels of known composition. Negative voltage steps would be performed to increase conductance through the channel, and during the step inhibition would be tested by liberating calcium. Inhibition of the Kir would be seen as a transient current of opposing sign to the potassium current. Barium chloride (100 μM) would then be applied to block the Kir channel and see if the transient current observed by photolysis of Ca^{2+} was also blocked.

Another experiment to examine what gives the GIRK this calcium sensitivity could be performed in a set of very controlled reconstructed lipid bilayer system. This would eliminate the contribution of any unknown secondary protein, and could directly test the effect of calcium on GIRK activity. If, in this preparation, the calcium sensitivity remains intact then it is clear evidence for calcium directly affecting the channel. Then the channel could be mutated by converting likely calcium-sensitive sites to alanine to see which residues confer the channel with calcium sensitivity to better understand how calcium inhibits GIRK. However, if the calcium sensitivity is lost, then there is likely an intermediate protein that mediates the effect of calcium on GIRK.

How do drugs of abuse affect calcium-mediated GIRK inhibition?

Both cocaine and methamphetamine affect proteins necessary for calcium-mediated GIRK inhibition. Cocaine, as shown in Chapter 4, reduces mGluR1 signaling after a single injection. Methamphetamine, by contrast, inhibits GIRK through a calcium-dependent process. Therefore, it is reasonable to hypothesize that both cocaine and methamphetamine treatment will affect the calcium-mediated GIRK inhibition, though likely through two different mechanisms. Cocaine treatment would be hypothesized to decrease the amount of GIRK inhibition through a reduction in the amount of calcium released from stores; whereas methamphetamine treatment would be hypothesized to occlude further mGluR-induced, calcium-mediated, GIRK inhibition.

To test the effect of cocaine, animals would be injected with either 20 mg/kg cocaine or saline via an intra-peritoneal injection. The next day slices would be prepared containing midbrain dopamine neurons, and the mGluR-mediated inhibition of GIRK would be quantified using dual-iontophoresis. Because a single injection of cocaine selectively decreases mGluR1 activity, mGluR1 and mGluR5 would be isolated using selective negative allosteric modulators. These data would be compared against photolysis of IP_3 in order to test if the effect of cocaine was at the receptor level or downstream of receptor activation. Similarly, another G_q-coupled GPCR, like the M1-type muscarinic receptor, could be examined as a control.

Methamphetamine would be examined by performing 5 repeated injections of methamphetamine, and preparing slices 1-3 days following the last injection. Again, dopamine neurons from the VTA and SNc would be examined, and the calcium-mediated GIRK inhibition quantified using dual iontophoresis and photolysis of caged-IP_3 dialyzed into the neuron. Whereas it would be expected that, following cocaine treatment, there would be an mGluR1-specific reduction in calcium-mediated GIRK inhibition, following methamphetamine treatment the reduction in GIRK inhibition should be universal for all methods used to evoke calcium release from stores. These results would be consistent with the idea that the post-methamphetamine change in calcium handling in dopamine neurons occludes further calcium-mediated inhibition.

Other experiments to test the specificity of calcium-mediated GIRK inhibition

OTHER EFFECTORS

The identical calcium-mediated GIRK inhibition effect sizes from mGluR activation and from photolysis of caged-IP_3 strongly suggests that any G_q-coupled GPCR on dopamine neurons should mediate a similar inhibition of GIRK as mGluR. However, this experiment has not been performed. Using dual-iontophoresis, the pipette containing L-aspartate could be exchanged for norepinephrine to test the α_1 adrenoceptor, or acetylcholine to test the M1-type muscarinic receptor. At the end of each experiment, CPA (10 μM) would be added to the perfusion solution in order to verify that any observed inhibition of GIRK was equally calcium dependent. These experiments would test the selectivity of G_q-mediated GIRK inhibition.

CALCIUM-INDUCED CALCIUM RELEASE

It is clear that calcium release through IP_3 receptors inhibits GIRK currents, but what about calcium release through ryanodine receptors? The first way to test this in dopamine neurons would be to include heparin, an IP_3 receptor blocker, in the internal solution and test mGluR-mediated GIRK inhibition with dual iontophoresis. Heparin has been shown to completely block IP_3-mediated calcium release from stores, but not mGluR-mediated calcium release since Group I mGluRs on dopamine neurons act both through IP_3 and ryanodine receptors (Morikawa, Khodakhah, and Williams 2003). Next, caffeine (1 mM)

enhances release of calcium from stores through ryanodine receptors (McPherson et al. 1991). Therefore, if ryanodine-receptor mediated calcium release can inhibit GIRK, then caffeine should enhance the mGluR-mediated inhibition of GIRK when using mGluR activation to release calcium from stores.

Specific dopamine neuron subtypes

As noted previously, dopamine neurons are a heterogeneous population of cells. Therefore, it would be interesting to test mGluR-mediated GIRK inhibition in identified neurons. It would be most interesting, first off, to test the difference between calbindin negative and positive neurons. This could be achieved two ways. Either using a mouse-reporter line (after verifying the necessary controls), or filling neurons with a marker and post-fixing the cells after testing mGluR-mediated GIRK inhibition, looking for calbindin expression.

Similarly, it would be interesting to test specific neurons identified by projection area. This would be accomplished by injecting beads into discrete brain regions (nucleus accumbens, amygdala, prefrontal cortex, doral striatum) to test not only the mGluR-mediated GIRK inhibition but also the effect of cocaine on mGluR1 activity.

Testing GIRK inhibition outside of dopamine neurons

Does calcium release from stores inhibits GIRK in other neurons outside of the ventral midbrain? CA3 neurons of the hippocampus, for example, have $GABA_B$-mediated GIRK currents, and IP_3 receptor-dependent mGluR-mediated SK currents (Guerineau, Gähwiler, and Gerber 1994). Therefore, the hypothesis

would be that mGluR-mediated calcium release from stores should inhibit GIRK currents mediated by GABA. This could be tested, like in dopamine neurons, using dual iontophoresis and pharmacology to isolate the mGluR and $GABA_B$ receptors.

Endogenous mGluR5 activation

As shown in Figure 4.7, stimulated mGluR IPSCs mainly consist of mGluR1-mediated currents. But it was shown in Chapter 4 that dopamine neurons also functionally express mGluR5. The question therefore arises: under what conditions are these receptors activated? One hypothesis is that they are only active following robust stimulation and substantial release of glutamate. One method to achieve this level of glutamate release is through activation of presynaptic D1 receptors, which have been shown to enhance glutamate release in the VTA (Kalivas and Duffy 1995). Therefore, during cocaine exposure while dopamine levels are high, D1 receptor activation might lead to the post-synaptic activation of mGluR5 and inhibit mGluR1, leading to the cellular plasticity that has been shown to occur following cocaine exposure.

This hypothesis could be tested in slices. First, the percent of mGluR IPSCs mediated by mGluR1 versus mGluR5 would be quantified. Then, this experiment would be performed in the presence of a D1 receptor agonist. If this protocol enhanced the proportion of current mediated by mGluR5, the next experiment would be to test the effect of cocaine. If cocaine enhanced the proportion of mGluR5 IPSC current as well, the final experiment would be to

block that with a D1 receptor antagonist. This set of experiments could tie together cocaine, mGluR5, mGluR1 and the plasticity of AMPA receptors following cocaine administration.

Stimulated mGluR currents

Electrical stimulation of inputs onto dopamine neurons does not always produce an mGluR IPSC, even when robust AMPA currents are present. This leads to question of which inputs onto dopamine neurons activate Group I mGlu receptors? This experiment could be performed by infecting neurons with major glutamatergic projections to dopamine neurons with the light activated ion channel, channel rhodopsin (ChR). Each region would be evaluated to see if it stimulation of that region preferentially activated mGluRs over other regions. Major regions to test include the Subthalamic Nucleus, Prelimibic Cortex, Prefrontal Cortex, Median Raphe, and other structures (Geisler et al. 2007).

However, perhaps it isn't one region in particular that activates mGlu receptors. To test if multiple glutamate inputs need to be active simultaneously to activate mGluRs, ChR could be expressed in multiple regions simultaneously that send glutamate to dopamine neurons. This experiment would test the hypothesis that mGluRs act as coincidence detectors. Whatever the outcome from these experiments, something new would be learned about how glutamate regulates dopamine neuron activity through the activation of Group I mGlu receptors.

Summary and Conclusions

The study of neuroscience is interested in, ultimately, how the brain regulates behavior. Achieving complete understanding is a monumental task; the number of connections between neurons, and the complexity of how neurons process information, is multivariate, numerous and plastic. Yet, as shown by the seminal discovery of miniature end plate potentials (Fatt and Katz 1952), studying an isolated, model, system can lead to important revelations. Thus, the impetus to study the function of individual neurons in a model system remains strong. Neurons are the most basic unit of the brain, and any general theory of how the brain processes information must incorporate the function of these individual units.

Understanding how intracellular signaling within a neuron modulates the output of that cell is one step toward understanding how the neuron integrates signals generated at the plasma membrane. This dissertation has found two new roles for metabotropic glutamate receptor-mediated signaling in controlling and modulating dopamine neuron activity. First, calcium release from internal stores transiently and robustly inhibits GIRK currents, ubiquitous mediators of inhibition on dopamine neurons. Second, acute cocaine administration decreases the currents generated by mGlu1 receptor signaling. It has been shown in other brain areas that a reduction in mGluR1 activity is typically required, or precedes, an alteration in synaptic plasticity onto that cell. The data presented here further our understanding of how dopamine neurons integrate synaptic signals through

intracellular network activity, add to the glutamate hypothesis of addiction, and raise unanswered questions prompting new lines of research. Perhaps the most salient contribution of this dissertation is a new appreciation for the rapid role that calcium release from stores has in disinhibition of dopamine neurons, and the link that this effect could have to cellular changes induced by drugs of abuse. It seems the roles for calcium in controlling neuronal function are ever growing, and act on all time scales. Undoubtedly this is not the end of uncovering new roles for metabotropic glutamate receptor activation, and calcium signaling, in dopamine neuron physiology and pathology.

References

Aiba, A, C Chen, K Herrup, C Rosenmund, C F Stevens, and S Tonegawa. 1994. “Reduced Hippocampal Long-Term Potentiation and Context-Specific Deficit in Associative Learning in mGluR1 Mutant Mice.” *Cell* 79 (2): 365–75.

Aiba, A, M Kano, C Chen, M E Stanton, G D Fox, K Herrup, T A Zwingman, and S Tonegawa. 1994. “Deficient Cerebellar Long-Term Depression and Impaired Motor Learning in mGluR1 Mutant Mice.” *Cell* 79 (2): 377–88. doi:10.1016/0092-8674(94)90205-4.

Arora, Devinder, Desirae M Haluk, Saïd Kourrich, Marco Pravetoni, Laura Fernández-Alacid, Joel C Nicolau, Rafael Luján, and Kevin Wickman. 2010. “Altered Neurotransmission in the Mesolimbic Reward System of Girk–/– Mice.” *Journal of Neurochemistry* 114 (5). Blackwell Publishing Ltd: 1487–97. doi:10.1111/j.1471-4159.2010.06864.x.

Arora, Devinder, R Lujan, M Hearing, D M Haluk, K Mirkovic, A Fajardo-Serrano, M W Wessendorf, M Watanabe, and K Wickman. 2011. “Acute Cocaine Exposure Weakens GABAB Receptor-Dependent G-Protein-Gated Inwardly Rectifying K+ Signaling in Dopamine Neurons of the Ventral Tegmental Area.” *Journal of Neuroscience* 31 (34): 12251–57. doi:10.1523/JNEUROSCI.0494-11.2011.

Barrot, Michel, Laura Calza, Monica Pozza, Michel Le Moal, and Pier Vincenzo Piazza. 2000. “Differential Calbindin-Immunoreactivity in Dopamine Neurons Projecting to the Rat Striatal Complex.” *European Journal of Neuroscience* 12 (12). Blackwell Science Ltd: 4578–82. doi:10.1111/j.1460-9568.2000.01349.x.

Beckstead, Michael J, and John T Williams. 2007. “Long-Term Depression of a Dopamine IPSC.” *Journal of Neuroscience* 27 (8). Society for Neuroscience: 2074–80. doi:10.1523/JNEUROSCI.3251-06.2007.

Beckstead, Michael J, David K Grandy, Kevin Wickman, and John T Williams. 2004. “Vesicular Dopamine Release Elicits an Inhibitory Postsynaptic Current in Midbrain Dopamine Neurons.” *Neuron* 42 (6): 939–46. doi:10.1016/j.neuron.2004.05.019.

Bellone, Camilla, and Christian Luscher. 2005. “mGluRs Induce a Long-Term Depression in the Ventral Tegmental Area That Involves a Switch of the Subunit Composition of AMPA Receptors.” *European Journal of Neuroscience* 21 (5): 1280–88. doi:10.1111/j.1460-9568.2005.03979.x.

Bellone, Camilla, and Christian Luscher. 2006. “Cocaine Triggered AMPA Receptor Redistribution Is Reversed in Vivo by mGluR-Dependent Long-Term Depression.” *Nature Neuroscience* 9 (5): 636–41. doi:10.1038/nn1682.

Bird, Michael K, Peter Lohmann, Billy West, Robyn M Brown, Jeppe Kirchhoff, Clarke R Raymond, and Andrew J Lawrence. 2014. “The mGlu5 Receptor Regulates Extinction of Cocaine-Driven Behaviours.” *Drug and Alcohol Dependence* 137 (April): 83–89. doi:10.1016/j.drugalcdep.2014.01.017.

Borgland, S L. 2004. “Acute and Chronic Cocaine-Induced Potentiation of Synaptic Strength in the Ventral Tegmental Area: Electrophysiological and Behavioral Correlates

in Individual Rats." *The Journal of Neuroscience : the Official Journal of the Society for Neuroscience* 24 (34): 7482–90. doi:10.1523/JNEUROSCI.1312-04.2004.

Chen, Rong, Michael R Tilley, Hua Wei, Fuwen Zhou, Fu-Ming Zhou, San Ching, Ning Quan, et al. 2006. "Abolished Cocaine Reward in Mice with a Cocaine-Insensitive Dopamine Transporter." *Proceedings of the National Academy of Sciences of the United States of America* 103 (24): 9333–38. doi:10.1073/pnas.0600905103.

Cheong, E, C Kim, B J Choi, M Sun, and H S Shin. 2011. "Thalamic Ryanodine Receptors Are Involved in Controlling the Tonic Firing of Thalamocortical Neurons and Inflammatory Pain Signal Processing." *The Journal of Neuroscience : the Official Journal of the Society for Neuroscience* 31 (4): 1213–18. doi:10.1523/JNEUROSCI.3203-10.2011.

Chiamulera, C, M P Epping-Jordan, A Zocchi, C Marcon, C Cottiny, S Tacconi, M Corsi, F Orzi, and F Conquet. 2001. "Reinforcing and Locomotor Stimulant Effects of Cocaine Are Absent in mGluR5 Null Mutant Mice." *Nature Neuroscience* 4 (9): 873–74. doi:10.1038/nn0901-873.

Conrad, Kelly L, Kuei Y Tseng, Jamie L Uejima, Jeremy M Reimers, Li-Jun Heng, Yavin Shaham, Michela Marinelli, and Marina E Wolf. 2008. "Formation of Accumbens GluR2-Lacking AMPA Receptors Mediates Incubation of Cocaine Craving." *Nature* 454 (7200): 118–21. doi:10.1038/nature06995.

Cui, Guohong, Brian E Bernier, Mark T Harnett, and Hitoshi Morikawa. 2007. "Differential Regulation of Action Potential- and Metabotropic Glutamate Receptor-Induced Ca2+ Signals by Inositol 1,4,5-Trisphosphate in Dopaminergic Neurons." *Journal of Neuroscience* 27 (17): 4776–85. doi:10.1523/JNEUROSCI.0139-07.2007.

Cui, Guohong, Takashi Okamoto, and Hitoshi Morikawa. 2004. "Spontaneous Opening of T-Type Ca2+ Channels Contributes to the Irregular Firing of Dopamine Neurons in Neonatal Rats." *Journal of Neuroscience* 24 (49): 11079–87. doi:10.1523/JNEUROSCI.2713-04.2004.

Degro, Claudius E, Akos Kulik, Sam A Booker, and Imre Vida. 2015. "Compartmental Distribution of GABAB Receptor-Mediated Currents Along the Somatodendritic Axis of Hippocampal Principal Cells." *Frontiers in Synaptic Neuroscience* 7 (6): 1–15. doi:10.3389/fnsyn.2015.00006.

Deignan, J, R Lujan, C Bond, A Riegel, M Watanabe, John T Williams, J Maylie, and J P Adelman. 2012. "SK2 and SK3 Expression Differentially Affect Firing Frequency and Precision in Dopamine Neurons." *Neuroscience* 217 (C). IBRO: 67–76. doi:10.1016/j.neuroscience.2012.04.053.

Doumazane, E, P Scholler, J M Zwier, E Trinquet, P Rondard, and J P Pin. 2011. "A New Approach to Analyze Cell Surface Protein Complexes Reveals Specific Heterodimeric Metabotropic Glutamate Receptors." *The FASEB Journal* 25 (1): 66–77. doi:10.1096/fj.10-163147.

Dragicevic, Elena, Christina Poetschke, Johanna Duda, Falk Schlaudraff, Stephan Lammel, Julia Schiemann, Michael Fauler, et al. 2014. "Cav1.3 Channels Control D2-Autoreceptor Responses via NCS-1 in Substantia Nigra Dopamine Neurons." *Brain* 137 (June). Oxford University Press: 2287–2302. doi:10.1093/brain/awu131.

Du, Xiaona, Hailin Zhang, Coeli Lopes, Tooraj Mirshahi, Tibor Rohacs, and Diomedes E Logothetis. 2004. “Characteristic Interactions with Phosphatidylinositol 4,5-Bisphosphate Determine Regulation of Kir Channels by Diverse Modulators.” *The Journal of Biological Chemistry* 279 (36). American Society for Biochemistry and Molecular Biology: 37271–81. doi:10.1074/jbc.M403413200.

El-Hassar, L., Hagenston, A. M., D'Angelo, L. B., & Yeckel, M. F. 2011. "Metabotropic glutamate receptors regulate hippocampal CA1 pyramidal neuron excitability via Ca2+ wave-dependent activation of SK and TRPC channels." *The Journal of Physiology*, 589 (13): 3211–3229. http://doi.org/10.1113/jphysiol.2011.209783

Ellis-Davies, Graham C R, and Robert J Barsotti. 2005. “Tuning Caged Calcium: Photolabile Analogues of EGTA with Improved Optical and Chelation Properties.” *Cell Calcium* 39 (1): 75–83. doi:10.1016/j.ceca.2005.10.003.

Fatt, P, and B Katz. 1952. “Spontaneous Subthreshold Activity at Motor Nerve Endings..” *The Journal of Physiology* 117 (1). Wiley-Blackwell: 109–28. doi:10.1111/(ISSN)1469-7793.

Fiorillo, Chris D, and John T Williams. 1998. “Glutamate Mediates an Inhibitory Postsynaptic Potential in Dopamine Neurons.” *Nature* 394 (6688): 78–82. doi:10.1038/27919.

Fiorillo, Chris D, and John T Williams. 2000. “Cholinergic Inhibition of Ventral Midbrain Dopamine Neurons.” *Journal of Neuroscience* 20 (20): 7855–60.

Fuxe, K. 1965. “Evidence for the Existence of Monoamine Neurons in the Central Nervous System. 3. the Monoamine Nerve Terminal..” *Zeitschrift Für Zellforschung Und Mikroskopische Anatomie (Vienna, Austria : 1948)* 65 (February): 573–96.

Gantz, Stephanie C, Brooks G Robinson, David C Buck, James R Bunzow, Rachael L Neve, John T Williams, and Kim A Neve. 2015. “Distinct Regulation of Dopamine D2S and D2L Autoreceptor Signaling by Calcium.” *eLife*, August, eLife2015–4:e09358. doi:10.7554/eLife.09358.

Gantz, Stephanie C, Erica S Levitt, Nerea Llamosas, Kim A Neve, and John T Williams. 2015. “Depression of Serotonin Synaptic Transmission by the Dopamine Precursor L-DOPA..” *Cell Reports* 12 (6): 944–54. doi:10.1016/j.celrep.2015.07.005.

Gasparini, F, K Lingenhöhl, N Stoehr, P J Flor, M Heinrich, I Vranesic, M Biollaz, et al. 1999. “2-Methyl-6-(Phenylethynyl)-Pyridine (MPEP), a Potent, Selective and Systemically Active mGlu5 Receptor Antagonist..” *Neuropharmacology* 38 (10): 1493–1503.

Geisler, S, C Derst, R W Veh, and D S Zahm. 2007. “Glutamatergic Afferents of the Ventral Tegmental Area in the Rat.” *Journal of Neuroscience* 27 (21): 5730–43. doi:10.1523/JNEUROSCI.0012-07.2007.

Guatteo, E, N B Mercuri, G Bernardi, and T Knöpfel. 1999. “Group I Metabotropic Glutamate Receptors Mediate an Inward Current in Rat Substantia Nigra Dopamine Neurons That Is Independent From Calcium Mobilization.” *Journal of Neurophysiology* 82 (4): 1974–81.

Guerineau, N C, B H Gähwiler, and U Gerber. 1994. “Reduction of Resting K+ Current by Metabotropic Glutamate and Muscarinic Receptors in Rat CA3 Cells: Mediation by G-

Proteins.” *The Journal of Physiology* 474 (1): 27–33. doi:10.1113/jphysiol.1994.sp019999.

Hearing, Matthew, Lydia Kotecki, Ezequiel Marron Fernandez de Velasco, Ana Fajardo-Serrano, Hee Jung Chung, Rafael Luján, and Kevin Wickman. 2013. “Repeated Cocaine Weakens GABAB-Girk Signaling in Layer 5/6 Pyramidal Neurons in the Prelimbic Cortex.” *Neuron* 80 (1). Elsevier Inc.: 159–70. doi:10.1016/j.neuron.2013.07.019.

Hermans, E, and R A Challiss. 2001. “Structural, Signaling and Regulatory Properties of the Group I Metabotropic Glutamate Receptors: Prototypic Family C G-Protein-Coupled Receptors.” *The Biochemical Journal* 359 (Pt 3): 465–84.

Hill, Jennifer J, and Ernest G Peralta. 2001. “Inhibition of a Gi-Activated Potassium Channel (GIRK1/4) by the Gq-Coupled M1 Muscarinic Acetylcholine Receptor.” *The Journal of Biological Chemistry* 276 (8). American Society for Biochemistry and Molecular Biology: 5505–10. doi:10.1074/jbc.M008213200.

Hill, S J, C R Ganellin, H Timmerman, J C Schwartz, N P Shankley, J M Young, W Schunack, R Levi, and H L Haas. 1997. “International Union of Pharmacology. XIII. Classification of Histamine Receptors.” *Pharmacological Reviews* 49 (3): 253–78.

Huang, C. L., S Feng, and D W Hilgemann. 1998. "Direct activation of inward rectifier potassium channels by PIP2 and its stabilization by Gβγ." *Nature* 391 (6669):803–806. http://doi.org/10.1038/35882

Hubbard, Katherine B, and John R Hepler. 2006. “Cell Signaling Diversity of the Gqα Family of Heterotrimeric G Proteins.” *Cellular Signaling* 18 (2): 135–50. doi:10.1016/j.cellsig.2005.08.004.

Hubert, G W, M Paquet, and Y Smith. 2001. “Differential Subcellular Localization of mGluR1a and mGluR5 in the Rat and Monkey Substantia Nigra.” *Journal of Neuroscience* 21 (6): 1838–47.

Hyman, Steven E, Robert C Malenka, and Eric J Nestler. 2006. “Neural Mechanisms of Addiction: the Role of Reward-Related Learning and Memory.” *Annual Review of Neuroscience* 29 (1): 565–98. doi:10.1146/annurev.neuro.29.051605.113009.

Ilango, Anton, Andrew J Kesner, Kristine L Keller, Garret D Stuber, Antonello Bonci, and Satoshi Ikemoto. 2014. “Similar Roles of Substantia Nigra and Ventral Tegmental Dopamine Neurons in Reward and Aversion.” *Journal of Neuroscience* 34 (3): 817–22. doi:10.1523/JNEUROSCI.1703-13.2014.

Inanobe, A, Y Yoshimoto, Y Horio, K I Morishige, H Hibino, S Matsumoto, Y Tokunaga, et al. 1999. “Characterization of G-Protein-Gated K+ Channels Composed of Kir3.2 Subunits in Dopaminergic Neurons of the Substantia Nigra.” *The Journal of Neuroscience : the Official Journal of the Society for Neuroscience* 19 (3): 1006–17.

Jian, Kuihuan, Pierangelo Cifelli, Angela Pignatelli, Elena Frigato, and Ottorino Belluzzi. 2010. “Metabotropic Glutamate Receptors 1 and 5 Differentially Regulate Bulbar Dopaminergic Cell Function.” *Brain Research* 1354 (October): 47–63. doi:10.1016/j.brainres.2010.07.104.

Jong, Y J I, I Sergin, C A Purgert, and K L O'Malley. 2014. “Location-Dependent Signaling of the Group 1 Metabotropic Glutamate Receptor mGlu5.” *Molecular Pharmacology* 86 (6): 774–85. doi:10.1124/mol.114.094763.

Kabbani, Nadine, Laszlo Negyessy, Ridwan Lin, Patricia Goldman-Rakic, and Robert Levenson. 2002. “Interaction with Neuronal Calcium Sensor NCS-1 Mediates Desensitization of the D2 Dopamine Receptor.” *Journal of Neuroscience* 22 (19): 8476–86.

Kalivas, P W, and P Duffy. 1995. “D1 Receptors Modulate Glutamate Transmission in the Ventral Tegmental Area..” *The Journal of Neuroscience* 15 (7 Pt 2): 5379–88.

Kalivas, Peter W. 2009. “The Glutamate Homeostasis Hypothesis of Addiction.” *Nature Publishing Group* 10 (8). Nature Publishing Group: 561–72. doi:10.1038/nrn2515.

Keck, Thomas M, Hong-Ju Yang, Guo-Hua Bi, Yong Huang, Hai-Ying Zhang, Ratika Srivastava, Eliot L Gardner, Amy Hauck Newman, and Zheng-Xiong Xi. 2013. “Fenobam Sulfate Inhibits Cocaine-Taking and Cocaine-Seeking Behavior in Rats: Implications for Addiction Treatment in Humans.” *Psychopharmacology* 229 (2): 253–65. doi:10.1007/s00213-013-3106-9.

Keck, Thomas M, Mu-Fa Zou, Guo-Hua Bi, Hai-Ying Zhang, Xiao-Fei Wang, Hong-Ju Yang, Ratika Srivastava, Eliot L Gardner, Zheng-Xiong Xi, and Amy Hauck Newman. 2014. “A Novel mGluR5 Antagonist, MFZ 10-7, Inhibits Cocaine-Taking and Cocaine-Seeking Behavior in Rats..” *Addiction Biology* 19 (2): 195–209. doi:10.1111/adb.12086.

Kenny, Paul J, Benjamin Boutrel, Fabrizio Gasparini, George F Koob, and Athina Markou. 2005. “Metabotropic Glutamate 5 Receptor Blockade May Attenuate Cocaine Self-Administration by Decreasing Brain Reward Function in Rats.” *Psychopharmacology* 179 (1). Springer-Verlag: 247–54. doi:10.1007/s00213-004-2069-2.

Keselman, Inna, Miguel Fribourg, Dan P Felsenfeld, and Diomedes E Logothetis. 2007. “Mechanism of PLC-Mediated Kir3 Current Inhibition.” *Channels* 1 (2): 113–23. doi:10.4161/chan.4321.

Kim, Sang Jeong, Yu Shin Kim, Joseph P Yuan, Ronald S Petralia, Paul F Worley, and David J Linden. 2003. “Activation of the TRPC1 Cation Channel by Metabotropic Glutamate Receptor mGluR1.” *Nature* 426 (6964): 285–91. doi:10.1038/nature02162.

Kobrinsky, Evgeny, Tooraj Mirshahi, Hailin Zhang, Taihao Jin, and Diomedes E Logothetis. 2000. “Receptor-Mediated Hydrolysis of Plasma Membrane Messenger PIP2 Leads to K+-Current Desensitization.” *Nature Cell Biology* 2 (August): 507–14.

Koob, George F, and Eric J Nestler. 1997. “The Neurobiology of Drug Addiction.” *Journal of Neuropsychiatry and Clinical Neurosciences* 9 (3): 482–97. doi:10.1176/jnp.9.3.482.

Kourrich, Saïd, Patrick E Rothwell, Jason R Klug, and Mark J Thomas. 2007. “Cocaine Experience Controls Bidirectional Synaptic Plasticity in the Nucleus Accumbens.” *Journal of Neuroscience* 27 (30). Society for Neuroscience: 7921–28. doi:10.1523/JNEUROSCI.1859-07.2007.

Koyrakh, L. 2005. “Molecular and Cellular Diversity of Neuronal G-Protein-Gated Potassium Channels.” *The Journal of Neuroscience* 25 (49): 11468–78. doi:10.1523/JNEUROSCI.3484-05.2005.

Köhler, T, M Heinisch, M Kirchner, G Peinhardt, R Hirschelmann, and P Nuhn. 1992. “Phospholipase A2 Inhibition by Alkylbenzoylacrylic Acids.” *Biochemical Pharmacology* 44 (4): 805–13. doi:10.1016/0006-2952(92)90419-J.

Kramer, Paul F, and John T Williams. 2015. “Cocaine Decreases Metabotropic Glutamate Receptor mGluR1 Currents in Dopamine Neurons by Activating mGluR5.” *Neuropsychopharmacology* 40 (10). Nature Publishing Group: 2418–24. doi:10.1038/npp.2015.91.

Kumaresan, Vidhya, Menglu Yuan, Judy Yee, Katie R Famous, Sharon M Anderson, Heath D Schmidt, and R Christopher Pierce. 2009. “Metabotropic Glutamate Receptor 5 (mGluR5) Antagonists Attenuate Cocaine Priming- and Cue-Induced Reinstatement of Cocaine Seeking.” *Behavioural Brain Research* 202 (2): 238–44. doi:10.1016/j.bbr.2009.03.039.

Lagerström, Malin C, and Helgi B Schiöth. 2008. “Structural Diversity of G Protein-Coupled Receptors and Significance for Drug Discovery.” *Nature Reviews. Drug Discovery* 7 (4): 339–57. doi:10.1038/nrd2518.

Lancaster, B, R A Nicoll, and D J Perkel. 1991. “Calcium Activates Two Types of Potassium Channels in Rat Hippocampal Neurons in Culture.” *The Journal of Neuroscience* 11 (1): 23–30.

Leaney, Joanne L, Lodewijk V Dekker, and Andrew Tinker. 2001. “Regulation of a G Protein-Gated Inwardly Rectifying K+ Channel by a Ca2+ -Independent Protein Kinase C.” *Journal of Physiology* 534 (2): 367–79. doi:10.1111/j.1469-7793.2001.00367.x.

Lee, Buyean, Donna M Platt, James K Rowlett, Adepero S Adewale, and Roger D Spealman. 2005. “Attenuation of Behavioral Effects of Cocaine by the Metabotropic Glutamate Receptor 5 Antagonist 2-Methyl-6-(Phenylethynyl)-Pyridine in Squirrel Monkeys: Comparison with Dizocilpine.” *The Journal of Pharmacology and Experimental Therapeutics* 312 (3):1232–40. doi:10.1124/jpet.104.078733.

Liss, Birgit, Olga Haeckel, Johannes Wildmann, Takashi Miki, Susumu Seino, and Jochen Roeper. 2005. “K-ATP Channels Promote the Differential Degeneration of Dopaminergic Midbrain Neurons.” *Nature Neuroscience* 8 (12): 1742–51. doi:10.1038/nn1570.

Loweth, Jessica A, Andrew F Scheyer, Mike Milovanovic, Amber L LaCrosse, Eden Flores-Barrera, Craig T Werner, Xuan Li, et al. 2013. “Synaptic Depression via mGluR1 Positive Allosteric Modulation Suppresses Cue-Induced Cocaine Craving.” *Nature Neuroscience*, November. Nature Publishing Group, 1–10. doi:10.1038/nn.3590.

Lu, Y M, Z Jia, C Janus, J T Henderson, R Gerlai, J M Wojtowicz, and J C Roder. 1997. “Mice Lacking Metabotropic Glutamate Receptor 5 Show Impaired Learning and Reduced CA1 Long-Term Potentiation (LTP) but Normal CA3 LTP.” *The Journal of Neuroscience* 17 (13): 5196–5205.

Mameli, Manuel, Briac Halbout, Cyril Creton, David Engblom, Jan Rodriguez Parkitna, Rainer Spanagel, and Christian Luscher. 2009. “Cocaine-Evoked Synaptic Plasticity: Persistence in the VTA Triggers Adaptations in the NAc.” *Nature Neuroscience* 12 (8): 1036–41. doi:10.1038/nn.2367.

Mannaioni, G, M J Marino, O Valenti, S F Traynelis, and P J Conn. 2001. “Metabotropic Glutamate Receptors 1 and 5 Differentially Regulate CA1 Pyramidal Cell Function.” *Journal of Neuroscience* 21 (16): 5925–34.

Mao, Jinzhe, Xueren Wang, Fuxue Chen, Runping Wang, Asheebo Rojas, Yun Shi, Hailan Piao, and Chun Jiang. 2004. “Molecular Basis for the Inhibition of G Protein-

Coupled Inward Rectifier K(+) Channels by Protein Kinase C." *Proceedings of the National Academy of Sciences of the United States of America* 101 (4): 1087–92. doi:10.1073/pnas.0304827101.

Martorana, Alessandro, Carmela Giampà, Zena DeMarch, Maria Teresa Viscomi, Stefano Patassini, Giuseppe Sancesario, Giorgio Bernardi, and Francesca R Fusco. 2006. "Distribution of TRPC1 Receptors in Dendrites of Rat Substantia Nigra: a Confocal and Electron Microscopy Study." *The European Journal of Neuroscience* 24 (3): 732–38. doi:10.1111/j.1460-9568.2006.04932.x.

McCutcheon, J E, J A Loweth, K A Ford, M Marinelli, M E Wolf, and K Y Tseng. 2011. "Group I mGluR Activation Reverses Cocaine-Induced Accumulation of Calcium-Permeable AMPA Receptors in Nucleus Accumbens Synapses via a Protein Kinase C-Dependent Mechanism." *The Journal of Neuroscience* 31 (41): 14536–41. doi:10.1523/JNEUROSCI.3625-11.2011.

McPherson, P S, Y K Kim, H Valdivia, C M Knudson, H Takekura, C Franzini-Armstrong, R Coronado, and K P Campbell. 1991. "The Brain Ryanodine Receptor: a Caffeine-Sensitive Calcium Release Channel." *Neuron* 7 (1): 17–25.

Morikawa, H, F Imani, K Khodakhah, and John T Williams. 2000. "Inositol 1,4,5-Triphosphate-Evoked Responses in Midbrain Dopamine Neurons." *Journal of Neuroscience* 20 (20): RC103 1–5.

Morikawa, Hitoshi, Kamran Khodakhah, and John T Williams. 2003. "Two Intracellular Pathways Mediate Metabotropic Glutamate Receptor-Induced Ca2+ Mobilization in Dopamine Neurons.." *Journal of Neuroscience* 23 (1): 149–57.

Morikawa, H., and C. A. Paladini. 2011. "Dynamic regulation of midbrain dopamine neuron activity: intrinsic, synaptic, and plasticity mechanisms." *Neuroscience*, 198: 95–111. http://doi.org/10.1016/j.neuroscience.2011.08.023

Munoz, Michaelanne B, Claire L Padgett, Robert Rifkin, Miho Terunuma, Kevin Wickman, Candice Contet, Stephen J Moss, and Paul A Slesinger. 2016. "A Role for the GIRK3 Subunit in Methamphetamine-Induced Attenuation of GABAB Receptor-Activated GIRK Currents in VTA Dopamine Neurons." *Journal of Neuroscience* 36 (11): 3106–14. doi:10.1523/JNEUROSCI.1327-15.2016.

Nakamura, T, K Nakamura, N Lasser-Ross, J G Barbara, V M Sandler, and W N Ross. 2000. "Inositol 1,4,5-Trisphosphate (IP3)-Mediated Ca2+ Release Evoked by Metabotropic Agonists and Backpropagating Action Potentials in Hippocampal CA1 Pyramidal Neurons." *Journal of Neuroscience* 20 (22): 8365–76.

Neuhoff, Henrike, Axel Neu, Birgit Liss, and Jochen Roeper. 2002. "I(H) Channels Contribute to the Different Functional Properties of Identified Dopaminergic Subpopulations in the Midbrain." *Journal of Neuroscience* 22 (4): 1290–1302.

Niswender, Colleen M, and P Jeffrey Conn. 2010. "Metabotropic Glutamate Receptors: Physiology, Pharmacology, and Disease." *Annual Review of Pharmacology and Toxicology* 50 (1): 295–322. doi:10.1146/annurev.pharmtox.011008.145533.

Nutt, David J, Anne Lingford-Hughes, David Erritzoe, and Paul R A Stokes. 2015. "The Dopamine Theory of Addiction: 40 Years of Highs and Lows." *Nature Publishing Group* 16 (5). Nature Publishing Group: 305–12. doi:10.1038/nrn3939.

Owen, J M, C C Quinn, R Leach, J B C Findlay, and M R Boyett. 1999. “Effect of Extracellular Cations on the Inward Rectifying K+ Channels Kir2.1 and Kir3.1/Kir3.4.” *Experimental Physiology* 84 (3). Cambridge University Press: 471–88.

Padgett, Claire L, Arnaud L Lalive, Kelly R Tan, Miho Terunuma, Michaelanne B Munoz, Menelas N Pangalos, José Martínez-Hernández, et al. 2012. “Methamphetamine-Evoked Depression of GABAB Receptor Signaling in GABA Neurons of the VTA.” *Neuron* 73 (5). Elsevier Inc.: 978–89. doi:10.1016/j.neuron.2011.12.031.

Paladini, C A, Chris D Fiorillo, H Morikawa, and John T Williams. 2001. “Amphetamine Selectively Blocks Inhibitory Glutamate Transmission in Dopamine Neurons.” *Nature Neuroscience* 4 (3): 275–81. doi:10.1038/85124.

Paladini, Carlos A, and James M Tepper. 1999. “GABAA and GABAB Antagonists Differentially Affect the Firing Pattern of Substantia Nigra Dopaminergic Neurons in Vivo.” *Synapse* 32 (3): 165–76.

Paladini, Carlos A, and John T Williams. 2004. “Noradrenergic Inhibition of Midbrain Dopamine Neurons..” *Journal of Neuroscience* 24 (19): 4568–75. doi:10.1523/JNEUROSCI.5735-03.2004.

Paladini, Carlos A, Jennifer M Mitchell, John T Williams, and Gregory P Mark. 2004. “Cocaine Self-Administration Selectively Decreases Noradrenergic Regulation of Metabotropic Glutamate Receptor-Mediated Inhibition in Dopamine Neurons.” *Journal of Neuroscience* 24 (22): 5209–15. doi:10.1523/JNEUROSCI.1079-04.2004.

Pan, P.-Y., and T. A. Ryan. 2012. "Calbindin controls release probability in ventral tegmental area dopamine neurons." *Nature Neuroscience*, 15 (6): 813–815. http://doi.org/10.1038/nn.3099

Pan, Z Z, T J Grudt, and John T Williams. 1994. “Alpha 1-Adrenoceptors in Rat Dorsal Raphe Neurons: Regulation of Two Potassium Conductances..” *The Journal of Physiology* 478 (3). Wiley-Blackwell: 437–47.

Patterson, Randen L, Darren Boehning, and Solomon H Snyder. 2004. “Inositol 1,4,5-Trisphosphate Receptors as Signal Integrators.” *Annual Review of Biochemistry* 73 (1): 437–65. doi:10.1146/annurev.biochem.73.071403.161303.

Perra, Simona, Michael A Clements, Brian E Bernier, and Hitoshi Morikawa. 2011. “In Vivo Ethanol Experience Increases D(2) Autoinhibition in the Ventral Tegmental Area.” *Neuropsychopharmacology* 36 (5): 993–1002. doi:10.1038/npp.2010.237.

Phillips, Paul E M, Garret D Stuber, Michael L A V Heien, R Mark Wightman, and Regina M Carelli. 2003. “Subsecond Dopamine Release Promotes Cocaine Seeking.” *Nature* 422 (6932): 614–18. doi:10.1038/nature01476.

Platt, Donna M, James K Rowlett, and Roger D Spealman. 2008. “Attenuation of Cocaine Self-Administration in Squirrel Monkeys Following Repeated Administration of the mGluR5 Antagonist MPEP: Comparison with Dizocilpine.” *Psychopharmacology* 200 (2). Springer-Verlag: 167–76. doi:10.1007/s00213-008-1191-y.

Poisik, Olga V, Guido Mannaioni, Stephen Traynelis, Yoland Smith, and P Jeffrey Conn. 2003. “Distinct Functional Roles of the Metabotropic Glutamate Receptors 1 and 5 in the Rat Globus Pallidus..” *Journal of Neuroscience* 23 (1): 122–30.

Purgert, C A, Y Izumi, Y J I Jong, V Kumar, C F Zorumski, and K L O'Malley. 2014. “Intracellular mGluR5 Can Mediate Synaptic Plasticity in the Hippocampus.” *Journal of Neuroscience* 34 (13): 4589–98. doi:10.1523/JNEUROSCI.3451-13.2014.

Ramayya, A G, A Misra, G H Baltuch, and M J Kahana. 2014. “Microstimulation of the Human Substantia Nigra Alters Reinforcement Learning.” *Journal of Neuroscience* 34 (20): 6887–95. doi:10.1523/JNEUROSCI.5445-13.2014.

Riegel, Arthur C, and John T Williams. 2008. “CRF Facilitates Calcium Release From Intracellular Stores in Midbrain Dopamine Neurons.” *Neuron* 57 (4): 559–70. doi:10.1016/j.neuron.2007.12.029.

Roberts, D C S, G F Koob, P Klonoff, and H C Fibiger. 1980. “Extinction and Recovery of Cocaine Self-Administration Following 6-Hydroxydopamine Lesions of the Nucleus Accumbens.” *Pharmacology Biochemistry and Behavior* 12 (5): 781–87. doi:10.1016/0091-3057(80)90166-5.

Roberts, D, and G F Koob. 1982. “Disruption of Cocaine Self-Administration Following 6-Hydroxydopamine Lesions of the Ventral Tegmental Area in Rats.” *Pharmacology Biochemistry and Behavior*.

Roeper, Jochen. 2013. “Dissecting the Diversity of Midbrain Dopamine Neurons.” *TRENDS in Neurosciences*, April. Elsevier Ltd, 1–7. doi:10.1016/j.tins.2013.03.003.

Rossi, Mark A, Tatyana Sukharnikova, Volodya Y Hayrapetyan, Lucie Yang, and Henry H Yin. 2013. “Operant Self-Stimulation of Dopamine Neurons in the Substantia Nigra..” Edited by Xiaoxi Zhuang. *PloS One* 8 (6): e65799. doi:10.1371/journal.pone.0065799.

Roth, B L, D L Willins, and K Kristiansen. 1998. “5-Hydroxytryptamine 2-Family Receptors (5-Hydroxytryptamine 2A, 5-Hydroxytryptamine 2B, 5-Hydroxytryptamine 2C): Where Structure Meets Function.” *Pharmacology & Therapy* 79 (3): 231–57. doi:10.1016/S0163-7258(98)00019-9.

Saal, D, Y Dong, A Bonci, and R C Malenka. 2003. “Drugs of Abuse and Stress Trigger a Common Synaptic Adaptation in Dopamine Neurons in the Experimental Procedures Section, the Dose of Ethanol Administered.” *Neuron* 37: 577–582.

Sammels, Eva, Jan B Parys, Ludwig Missiaen, Humbert De Smedt, and Geert Bultynck. 2010. “Intracellular Ca2+ Storage in Health and Disease: a Dynamic Equilibrium.” *Cell Calcium* 47 (4). Elsevier Ltd: 297–314. doi:10.1016/j.ceca.2010.02.001.

Saugstad, J. A., T P Segerson, and G L Westbrook. 1996. "Metabotropic glutamate receptors activate G-protein-coupled inwardly rectifying potassium channels in Xenopus oocytes." *The Journal of Neuroscience* 16 (19):5979–5985.

Schultz, Wolfram. 2002. “Getting Formal with Dopamine and Reward.” *Neuron* 36 (2): 241–63.

Schultz, Wolfram. 2016. “Dopamine Reward Prediction-Error Signalling: a Two-Component Response.” *Nature Publishing Group* 17 (3). Nature Publishing Group: 183–95. doi:10.1038/nrn.2015.26.

Sharpe, Amanda L, Erika Varela, Lynne Bettinger, and Michael J Beckstead. 2014. “Methamphetamine Self-Administration in Mice Decreases GIRK Channel-Mediated Currents in Midbrain Dopamine Neurons.” *The International Journal of*

Neuropsychopharmacology 18 (5). The Oxford University Press: pyu073–pyu073. doi:10.1093/ijnp/pyu073.

Sohn, Jong-Woo, Doyun Lee, Hana Cho, Wonil Lim, Hee-Sup Shin, Suk-Ho Lee, and Won-Kyung Ho. 2007a. “Receptor-Specific Inhibition of GABAB-Activated K+ Currents by Muscarinic and Metabotropic Glutamate Receptors in Immature Rat Hippocampus..” *The Journal of Physiology* 580 (Pt. 2): 411–22. doi:10.1113/jphysiol.2006.125914.

Sohn, Jong-Woo, Doyun Lee, Hana Cho, Wonil Lim, Hee-Sup Shin, Suk-Ho Lee, and Won-Kyung Ho. 2007b. “Receptor-Specific Inhibition of GABAB-Activated K+ Currents by Muscarinic and Metabotropic Glutamate Receptors in Immature Rat Hippocampus..” *The Journal of Physiology* 580 (2). Blackwell Publishing Ltd: 411–22. doi:10.1113/jphysiol.2006.125914.

Stevens, E B, B S Shah, R D Pinnock, and K Lee. 1999. “Bombesin Receptors Inhibit G Protein-Coupled Inwardly Rectifying K+ Channels Expressed in Xenopus Oocytes Through a Protein Kinase C-Dependent Pathway.” *Molecular Pharmacology* 55 (6): 1020–27.

Szlufcik, Karolina, Ludwig Missiaen, Jan B Parys, Geert Callewaert, and Humbert Smedt. 2012. “Uncoupled IP3 Receptor Can Function as a Ca2+-Leak Channel: Cell Biological and Pathological Consequences.” *Biology of the Cell* 98 (1). Blackwell Publishing Ltd: 1–14. doi:10.1042/BC20050031.

Tang, Tie-Shan, Huiping Tu, Zhengnan Wang, and Ilya Bezprozvanny. 2003. “Modulation of Type 1 Inositol (1,4,5)-Trisphosphate Receptor Function by Protein Kinase a and Protein Phosphatase 1alpha.” *Journal of Neuroscience* 23 (2): 403–15.

Testa, C M, D G Standaert, A B Young, and J B Penney. 1994. “Metabotropic Glutamate Receptor mRNA Expression in the Basal Ganglia of the Rat.” *The Journal of Neuroscience* 14 (5 Pt 2): 3005–18.

Tozzi, Alessandro, C Peter Bengtson, Patrizia Longone, Corrado Carignani, Francesca R Fusco, Giorgio Bernardi, and Nicola B Mercuri. 2003. “Involvement of Transient Receptor Potential-Like Channels in Responses to mGluR-I Activation in Midbrain Dopamine Neurons.” *The European Journal of Neuroscience* 18 (8): 2133–45.

Tsien, R Y. 1980. “New Calcium Indicators and Buffers with High Selectivity Against Magnesium and Protons: Design, Synthesis, and Properties of Prototype Structures.” *Biochemistry* 19 (11): 2396–2404.

Ungless, M A, J L Whistler, R C Malenka, and A Bonci. 2001. “Single Cocaine Exposure in Vivo Induces Long-Term Potentiation in Dopamine Neurons.” *Nature* 411 (6837): 583–87. doi:10.1038/35079077.

Venkatachalam, Kartik, and Craig Montell. 2007. “TRP Channels.” *Annual Review of Biochemistry* 76 (1): 387–417. doi:10.1146/annurev.biochem.75.103004.142819.

Verkhratsky, A, and A Shmigol. 1996. “Calcium-Induced Calcium Release in Neurones.” *Cell Calcium* 19 (1): 1–14.

Walker, J W, J Feeney, and D R Trentham. 1989. “Photolabile Precursors of Inositol Phosphates. Preparation and Properties of 1-(2-Nitrophenyl)Ethyl Esters of Myo-Inositol 1,4,5-Trisphosphate.” *Biochemistry* 28 (8): 3272–80. doi:10.1021/jo020040g.

Wang, Lie, Stephen T Kitai, and Zixiu Xiang. 2005. “Modulation of Excitatory Synaptic Transmission by Endogenous Glutamate Acting on Presynaptic Group II mGluRs in Rat Substantia Nigra Compacta.” *Journal of Neuroscience Research* 82 (6): 778–87. doi:10.1002/jnr.20694.

Wang, Weiwei, Matthew R Whorton, and Roderick MacKinnon. 2014. “Quantitative Analysis of Mammalian GIRK2 Channel Regulation by G Proteins, the Signaling Lipid PIP2 and Na+ in a Reconstituted System.” *eLife*, eLife2014–3:e03671. doi:10.7554/eLife.03671.

Wang, Xiusong, Khaled Moussawi, Lori Knackstedt, Haowei Shen, and Peter W Kalivas. 2012. “Role of mGluR5 Neurotransmission in Reinstated Cocaine-Seeking.” *Addiction Biology* 18 (1): 40–49. doi:10.1111/j.1369-1600.2011.00432.x.

Watts, A E, John T Williams, and G Henderson. 1996. “Baclofen Inhibition of the Hyperpolarization-Activated Cation Current, Ih, in Rat Substantia Nigra Zona Compacta Neurons May Be Secondary to Potassium Current Activation.” *Journal of Neurophysiology* 76 (4): 2262–70.

Whorton, Matthew R, and Roderick MacKinnon. 2011. “Crystal Structure of the Mammalian GIRK2 K+ Channel and Gating Regulation by G Proteins, PIP2, and Sodium.” *Cell* 147 (1): 199–208. doi:10.1016/j.cell.2011.07.046.

Wise, Roy A. 2009. “Roles for Nigrostriatal--Not Just Mesocorticolimbic--Dopamine in Reward and Addiction.” *TRENDS in Neurosciences* 32 (10): 517–24. doi:10.1016/j.tins.2009.06.004.

Wolfart, Jakob, Henrike Neuhoff, Oliver Franz, and Jochen Roeper. 2001. “Differential Expression of the Small-Conductance, Calcium-Activated Potassium Channel SK3 Is Critical for Pacemaker Control in Dopaminergic Midbrain Neurons.” *Journal of Neuroscience* 21 (10): 3443–56.

Xia, Yan-Fang, Elyssa B Margolis, and Gregory O Hjelmstad. 2010. “Substance P Inhibits GABAB Receptor Signalling in the Ventral Tegmental Area.” *The Journal of Physiology* 588 (9): 1541–49. doi:10.1113/jphysiol.2010.188367.

Yu, Fei, Peng Zhong, Xiaojie Liu, Dalong Sun, Hai-Qing Gao, and Qing-Song Liu. 2013. “Metabotropic Glutamate Receptor I (mGluR1) Antagonism Impairs Cocaine-Induced Conditioned Place Preference via Inhibition of Protein Synthesis.” *Neuropsychopharmacology*: AOP 1–13 doi:10.1038/npp.2013.29.

Appendix A Two-color, one-photon uncaging of glutamate and GABA onto dopamine neurons in slice

Matthew T. Richers[1,3], Paul F. Kramer[2,3], Stefan Passlick[1,3], Joseph P. Amatrudo[1], John T. Williams[2] and Graham C.R. Ellis-Davies[1].

[1]Department of Neuroscience, Mount Sinai School of Medicine, New York, NY 10029, USA.

[2]Vollum Institute, Oregon Health and Sciences University, Portland, OR 97239, USA.

[3]Equal contributors.

Appendix A – Preface

The work presented here is from a collaboration with Graham Ellis-Davies and Matthew Richers. Drs. Richers and Ellis-Davies synthesized a new caged-GABA compound that had low UV-light absorption, and enhanced absorption in the blue light range. This made it possible to perform linear one-photon selective uncaging of a UV-caged glutamate and the blue light-caged GABA when present simultaneously in the perfusion solution. Our role was to test these compounds in brain slices, and to determine their potential for use.

Included here are only the experiments examining the utility and function of these two caged compounds in brain slices by recording from dopamine neurons of the substantia nigra *pars compacta*. The details on chemical synthesis of the new compound, and on the utility of the compounds in hippocampal CA1 slices, are not included. All the work presented here was performed by myself and John Williams, and all the ideas are our own.

Summary

The following experiments were performed on acutely prepared sections containing dopamine neurons of the SNc. It was found that the caged-GABA had minimal photolysis from UV light, but was liberated by blue light. When liberated, the caged-GABA led to an inhibition in dopamine neurons through activation of the $GABA_B$ receptor, and could also activate $GABA_A$. By contrast, the UV-caged glutamate was completely unaffected by blue light, and only liberated by UV light. Upon glutamate liberation there was activation of both ionotropic and metabotropic glutamate receptors, leading to an excitation and inhibition of the neuron.

Appendix A – Methods

PHYSIOLOGY

All experiments were approved by institutional IACUC.

Slice Preparations

Male and female adult Sprague-Dawley rats were anesthetized with isoflurane, killed and the brain removed. The brain was sliced at 230 μm in warm artificial cerebrospinal fluid ACSF containing (in mM): 126 NaCl, 2.5 KCl, 1.2 $MgCl_2$, 2.6 $CaCl_2$, 1.2 NaH_2PO_4, 11 D-glucose, 21.4 $NaHCO_3$, and 0.03 MK801 [(5*S*,10*R*)-(+)-5-methyl-10,11-dihydro-5*H*-dibenzo[a,d]cyclohepten-5,10-imine; Abcam, Cambridge, UK], equilibrated with 95% O_2/5% CO_2. Slices were allowed to recover at 34˚C for at least 30 minutes with oxygenated (95% O_2/ 5% CO_2) artificial cerebrospinal fluid containing (in mM): 126 NaCl, 2.5 KCl, 1.2 $MgCl_2$, 2.6 $CaCl_2$, 1.2 NaH_2PO_4, 11 D-glucose, and 21.4 $NaHCO_3$ and 0.40 MK801.

Electrophysiology recordings

After incubation, slices were hemisected and transferred to the recording chamber and superfused with ACSF (1.5 mL/minute, 34˚C). Dopamine neurons were identified by their location (rostrolateral of the MT). The identity of dopamine neurons was further validated by observing the characteristic pacemaker spiking of the neuron in cell-attached mode with an action potential duration of >2ms. Whole-cell recordings were made with an Axopatch 1D amplifier (Molecular Devices, Sunnyvale, CA, USA) in voltage-clamp mode (V_{hold} = –60 mV).

Recording pipettes (1.7–2.1 MΩ) were filled with internal solution containing (in mM): 60 potassium methanesulfonate, 55 KCl, 20 NaCl, 1.5 $MgCl_2$, 5 HEPES(K), 0.1 EGTA, 2 Mg-ATP, 0.25 Na-GTP, pH 7.4, 280-285 mOsM. Series resistance was monitored without compensation and was <15 MΩ. Current was continuously recorded at 200 Hz with PowerLab (chart version 5.4.2; AD Instruments, Colorado Springs, CO). Episodic currents were recorded at 10 kHz for 1 minute using AxoGraphX (1.4.3; AxographX, Berkeley, CA). Drugs were applied by bath superfusion. Cell-attached recordings were made with recording pipettes (2–2.5 MΩ) filled with ACSF.

Uncaging of DEAC454-GABA (25-30 μM) and dcPNPP-Glu (290-350 μM, or 160 μM in Fig. 3c) was carried out with full-field illumination (365 and 450 or 470 nm LED, Thorlabs, NJ, USA) coupled through a 60x objective (Olympus, 0.9 numerical aperture). The LEDs were mounted on the epifluorescence port of a BX51 or 61 microscope (Olympus). The beams were combined with a long-pass dichroic (387nm, Chroma). A notch filter (365/20nm, Chroma, Bellows Falls, VT, USA) was placed in the light path from the 365 LED (exccept for Fig. 3c). The 450 nm LED was filtered (455/20nm notch filter, Chroma). A long-pass dichroic (488 nm, Semrock, Rochester, NY, USA) in the fluorescence turret was used to direct the beams to the objective. Light power and duration was controlled via the LED driver (LEDD1B, Thorlabs) by external voltage modulation. The power was measured with a photometer (S120VC, Thorlabs) prior to the experiment.

Solutions containing either DEAC454-GABA, dcPNPP-Glu, or both (4 – 7 mL) were recirculated for at least 5 minutes before uncaging.

Experiments in Fig. A1 included GABA-B (CGP-55845a, 500 nM) and mGluR (JNJ-16259685, 1 μM and MPEP, 3 μM, Tocris, Minneapolis, MN, USA) antagonists. Experiments in Fig. A3 included GABA-A (picrotoxin, 10 μM, Tocris), NMDA (CPP, 10 μM, Tocris) and D2 (sulpiride, 2 μM, Sigma-Aldrich, St. Louis, MO) antagonists.

Appendix A – Results and Discussion

Functional cross-talk at ionotropic receptors of UV and blue-light caged compounds

The first test of the selectivity of either caged compounds was performed by analyzing ionotropic currents activated by these compounds. These experiments were performed in isolated conditions, with either dcPNPP-glutamate or DEAC454-GABA in the bath individually. A UV or blue LED was then used to deliver a light pulse to the slice of varying duration to test how much specific versus non-specific photolysis of the caged compounds there were, as measured by receptor activation.

Results

Like with the use of metabotropic receptors as a functional readout of caged compound photolysis, blue (450 nm) light was completely selective for activation of $GABA_A$ receptors, and only at the highest power and longest light pulse duration (10 mW, 1000 ms) was any current seen from AMPA receptors (Figure A6A). UV light (365 nm) was selective at liberating glutamate and activating only AMPA within a certain power window (5 mW power, below 30 ms, Figure A6D).

Discussion

Like with metabotropic receptors, with ionotropic receptors there is a window within which UV light is selective for activation of AMPA receptors over $GABA_A$. Thus these compounds, when used with appropriate photolysis conditions, can

be useful for one-photon selective activation of either glutamate or GABA ionotropic receptors with precise temporal control.

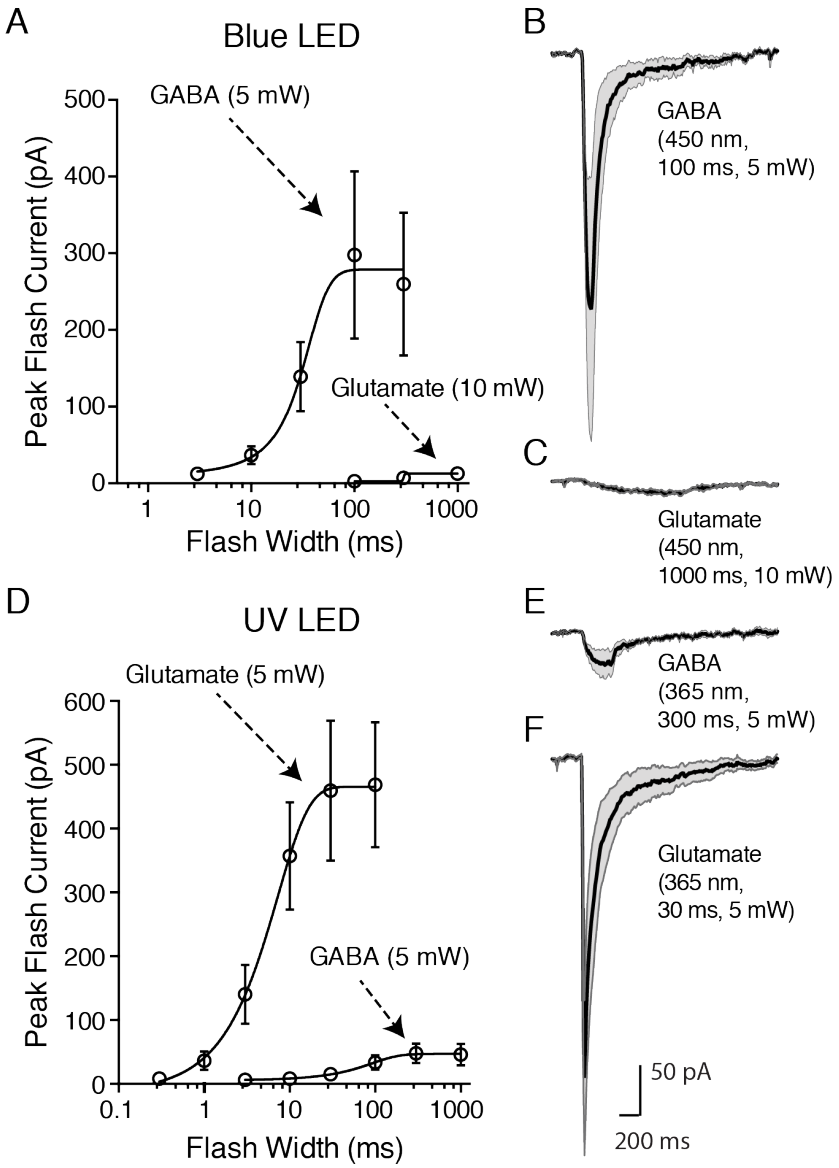

Figure A1 Crosstalk between UV and Blue light caged compound photolysis, assayed using ionotropic receptor readouts.

A. Summarized data showing the selectivity using 450 nm light when both compounds are in the bath. As can be appreciated, even maximum power light was unable to evoke appreciable currents. These currents are summarized in **B.** and **C.** as averaged examples across cells, with error bars representing sem.

D. Summarized data showing the selectivity using 365 nm light when both compounds are in the bath. There was less selectivity of liberating glutamate over GABA, but still an effective power window for selective activation of AMPA over $GABA_A$. These currents are summarized in **E.** and **F.** as averaged examples across cells, with error bars representing sem.

CAGED GLUTAMATE AND GABA ALSO ACTIVATE METABOTROPIC RECEPTORS

In addition to ionotropic glutamate and GABA receptors, dopamine neurons functionally express metabotropic receptors activated by these two neurotransmitters that couple to ion channels. Therefore, the efficacy of these two caged compounds on evoking currents mediated by $GABA_B$ and mGlu receptors was tested.

RESULTS

Photolysis of dcPNPP caged-glutamate and DEAC454 caged-GABA results in mGluR and $GABA_B$ mediated currents, respectively (Figure A2). These currents were inhibited by specific antagonists. Complete block of the outward current following photolysis of caged-glutamate required negative allosteric modulators against both the mGlu1 and mGlu5 receptors (Figure A4, top left). The $GABA_B$-specific antagonist CGP55845a completely blocked the outward current mediated by photolysis of caged-GABA (Figure A2 bottom left).

DISCUSSION

These experiments show that photolysis of caged glutamate and GABA activated metabotropic receptors as well as ionotropic receptors. These responses mimic endogenous receptor activation by synaptic release of neurotransmitter, and could be useful in future experiments.

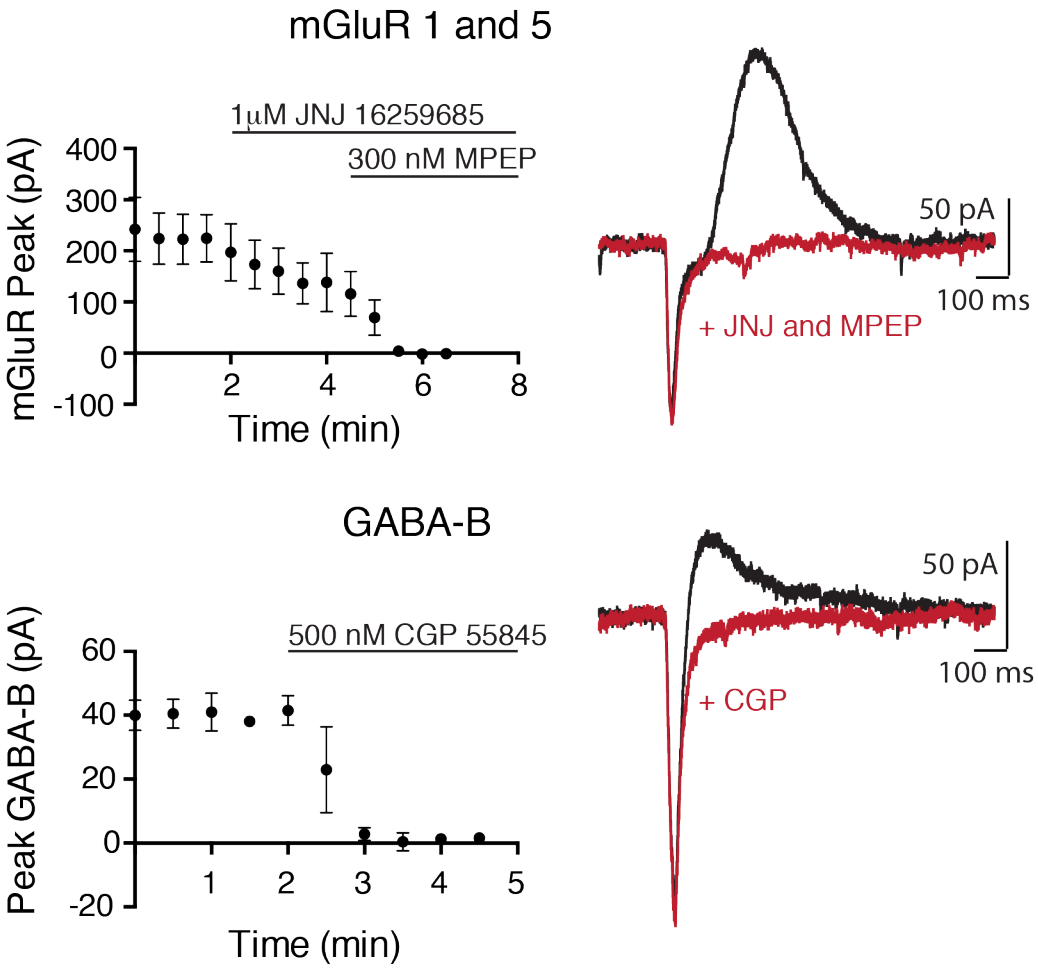

Figure A2 Metabotropic currents generated by photolysis of dcPNPP-Glu and DEAC454-GABA.

Top. *Left*, grouped data (averaged outward peak ± sem) of the outward current generated by photolysis using 365 nm LED light of dcPNPP caged-glutamate. The outward current was totally blocked by JNJ (1 μM) and MPEP (300 nM). *Right*, example trace of the outward current (black) by photolysis of caged-glutamate, and its block by mGluR NAMs (red).
Bottom. *Left*, grouped data (averaged outward peak ± sem) of the outward current generated by photolysis of DEAC454 caged-GABA using a 450 nm LED light pulse, and its block by the $GABA_B$-specific antagonist CGP-55845. *Right*, example trace of the outward current (black) and its block by the $GABA_B$ antagonist (red).

Non-selective activation of metabotropic receptors

Photolysis of caged glutamate and GABA produces metabotropic receptor-mediated currents. This assay was used to examine the specificity of photolysis of one compound or the other with both in the perfusion solution simultaneously. Ionotropic receptors might have different windows of selective compound photolysis than metabotropic receptors.

Results

Blue (450 nm) light was completely selective for activation of GAB_A receptors, and only at the highest power and longest light pulse duration (10 mW, 1000 ms) was any current seen from mGlu receptors (Figure A3A). By contrast, UV light (365 nm) was not very selective at liberating only glutamate. The range over which glutamate is preferentially liberated over GABA was when using 5 mW power with a 10 ms laser pulse (Figure A3D).

Discussion

These data show that the range over which UV light is specific for glutamate is narrower for metabotropic receptor activation than ionotropic receptors. This could be because of the receptor desensitization of ionotropic glutamate and GABAergic receptors, or because of the signal amplification inherent to GPCRs. However, this range (5 mW, 10 ms) is more than enough power to still get robust mGluR and AMPA receptor currents. So while the range is narrow, it is still effective for selective one-photon photolysis of the two caged compounds.

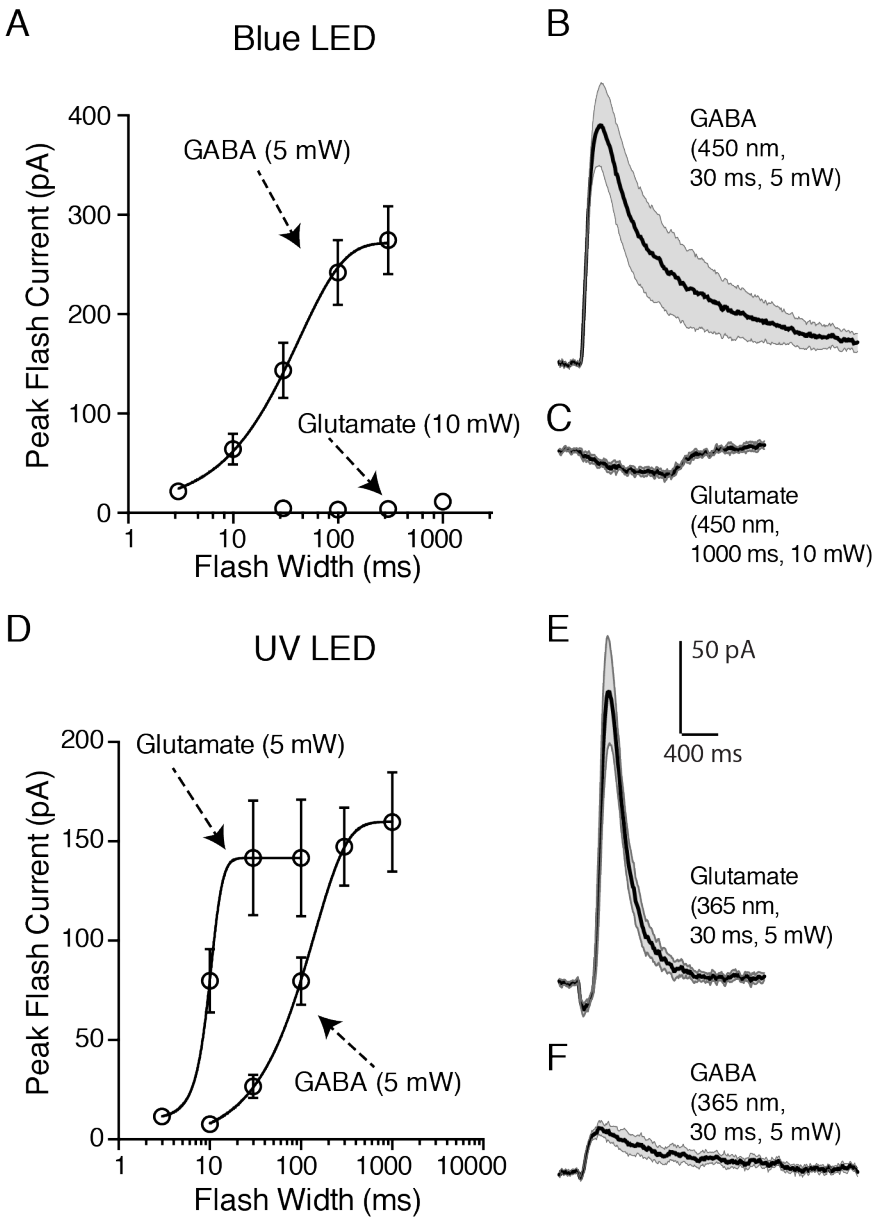

Figure A3 Crosstalk between UV and Blue light caged compound photolysis, assayed using metabotropic receptor readouts.

A. Summarized data showing the selectivity using 450 nm light when both compounds are in the bath. As can be appreciated, even maximum power light was unable to evoke appreciable currents. These currents are summarized in **B.** and **C.** as averaged examples across cells, with error bars representing sem.

D. Summarized data showing the selectivity using 365 nm light when both compounds are in the bath. There was much less selectivity of liberating glutamate over GABA. These currents are summarized in **E.** and **F.** as averaged examples across cells, with error bars representing sem.

Examples of using selective one-photon photolysis to modulate dopamine neuron output

Within an appropriate power range, 365 nm light can selectively activate AMPA receptors without activating $GABA_A$ or $GABA_B$ receptors when both dcPNPP caged-glutamate and DEAC454 caged-GABA are in the perfusion solution. 450 nm light always selectively activates GABA receptors. Now, to show a proof of principle that these compounds can be used to functionally modulate dopamine neuron activity, both increasing firing and inhibiting firing, recordings were made either in cell-attached mode or in whole cell current clamp mode. Both caged compounds were included in the perfusion solution, and the LEDs were tuned to the appropriate power outputs to ensure selective photolysis.

Results

Under these conditions, blue light caused a pause in firing and an associated hyperpolarization of the membrane (Figure A4A, left), UV light caused an increase in firing rate and evoked action potentials (Figure A4A, center), and blue light directly preceding UV light prevented the firing of the neuron (Figure A4A, right). The effect on firing rate was quantified by measuring the number of action potentials in a second following caged compound photolysis (Figure A4B). The robust effect of DEAC454-GABA, acting at $GABA_A$ receptors, to pause dopamine neuron firing is shown in Figure A4C.

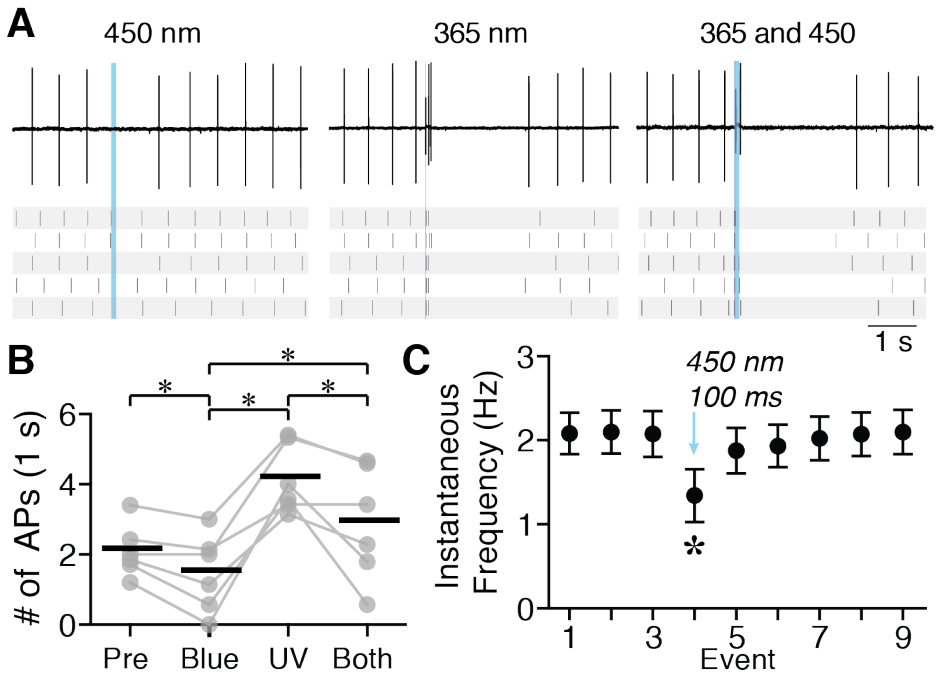

Figure A4 Using UV or Blue light to selectively excite or inhibit dopamine neuron firing when both compounds are in the bath simultaneously.

A. Example traces of action potential recordings for a single cell with raster plots below showing multiple trials. Left. Events where 450 nm LED was flashed for 100 ms. Center. Events where a 365 nm LED was flashed for 10 ms. Right. Events where both LEDs were flashed simultaneously.
B. The number of action potentials (APs) in one second quantified across trials. Each cell is displayed as one data point. Each grouping represents number of APs Pre: 1 s prior to 450 nm LED flash, Blue: 1 s after 450 nm LED, UV: 1s after 365 nm LED, and Both: 1 s after 450 and 365 nm LEDs flashed simultaneously. A repeated measures 2-way ANOVA was used with a tukey test to examine multiple comparisons. Bars indicatemeans. Each grey dot is an average of at least 5 trials for a single cell. All experiments were conducted within cell (signified with conecting lines).
C. Effect of a 100 ms, 450 nm LED pulse of the instantaneus firing frequency across cells (n = 6).
* indicates $p < 0.001$, error bars represent S.E.M.
$GABA_B$ and mGlu receptors were blocked the experiments in this figure.

Discussion

These results show in multiple forms that the caged compounds can be used, when both are included simultaneously in the bath, to selectively evoke or inhibit action potentials in dopamine neurons. With focal stimulation, it could be possible to inhibit or excite certain neurons in a single experiment and test output of the system.

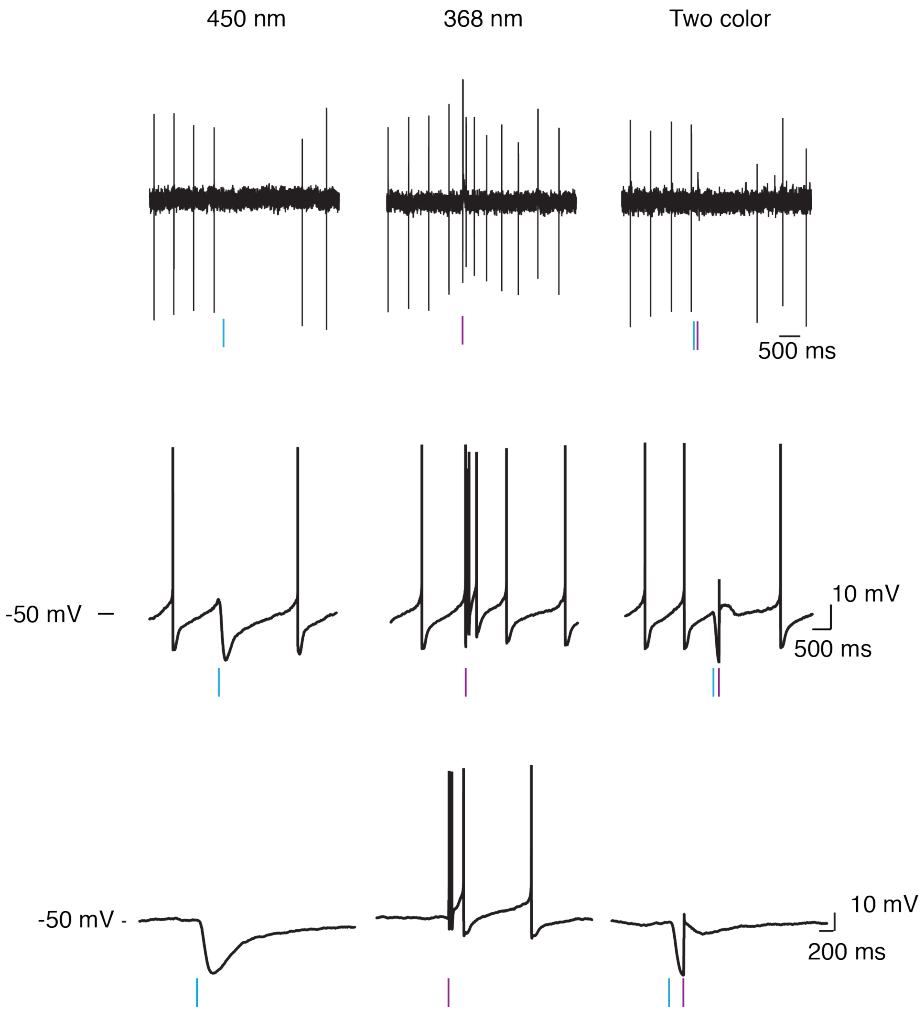

Figure A5 Examples showing $GABA_B$-mediated paused in firing of action potentials, and block of evoked firing from dcPNPP-Glu.

All experiments were performed in the presence of $GABA_A$ receptor and mGlu receptor blockers. dcPNPP-Glutamate and DEAC454-GABA were both included in the perfusion solution.
Top. Cell attached recording
Middle. Whole-cell current clamp recording where the neuron was spontaneously active
Bottom. Whole-cell current clamp recording where the neuron was not active
Left. Blue LED flash to liberate DEAC454-GABA
Center. UV LED flash to liberate dcPNPP-Glutamate
Right. Blue LED flash 100 ms prior to UV LED flash